Universidade de Lisboa

Faculdade de Farmácia

Investigation of two predicted calcium-binding sites located in the acylated segment of the adenylate cyclase toxin of *Bordetella pertussis*

Joana Filipa Tinoco Marçal

Dissertation supervised by Adriana Osickova, Ph.D., Institute of Microbiology of the Czech Academy of Sciences, v.v.i.
and co-supervised by Carlos de São José, Ph.D., Faculty of Pharmacy, University of Lisbon

Master in Biopharmaceutical Sciences

2020

Universidade de Lisboa

Faculdade de Farmácia

Investigation of two predicted calcium-binding sites located in the acylated segment of the adenylate cyclase toxin of *Bordetella pertussis*

Joana Filipa Tinoco Marçal

Dissertation supervised by Adriana Osickova, Ph.D., Institute of Microbiology of the Czech Academy of Sciences, v.v.i.
and co-supervised by Carlos de São José, Ph.D., Faculty of Pharmacy, University of Lisbon

Master in Biopharmaceutical Sciences

2020

“Imagination is more important than knowledge. Knowledge is limited. Imagination encircles the world.”

Albert Einstein

ABSTRACT

Pertussis, also known as whooping cough, has recently re-emerged as a major threat to the global health despite the existence of high levels of immunization against the causative agent, *Bordetella pertussis*. The Gram-negative bacterium colonizes ciliated respiratory epithelia of lower airways in humans and appears to excel in suppression of host immunity during early phases of infection.

The current acellular pertussis (aP) vaccines against pertussis consist only of a few selected antigens (pertussis toxin, filamentous hemagglutinin, pertactin and/or fimbriae). The absence of adenylate cyclase toxin (CyaA) in the current aP vaccine formulations likely accounts for the increasingly apparent failure of the aP vaccines to confer a long-term protection against whooping cough in highly vaccinated populations, as opposed to the efficient whole-cell pertussis vaccines that have been used for decades. This is because CyaA annihilates the bactericidal functions of the sentinel cells of innate immunity by paralyzing the opsonophagocytic bactericidal activities of phagocytes, such as neutrophils and macrophages. Due to the protective and immunosuppressive roles performed in *Bordetella* infections, CyaA toxoid is currently considered an ideal candidate for inclusion in the next generation of aP vaccines.

CyaA can enter eukaryotic cells and perform cytotoxic and hemolytic activities, both of which are calcium-dependent. CyaA harbours two different classes of calcium-binding sites, low affinity calcium-binding sites that appeared to be critical for the cytotoxic activity of the toxin, and high affinity calcium-binding sites important for the membrane binding capability and the hemolytic activity of CyaA. While the low affinity sites are located in the RTX (repeats in toxin) domain of the toxin, the location of the high affinity sites is still unknown. Analysis of the C-terminal part of the acylated segment of CyaA (residues 908-1008) revealed that there are two blocks of amino acid residues with a pattern similar to that of the highly conserved calcium-binding sites of the RTX domain, exhibiting a consensus sequence GGxGxD. Therefore, using site-directed mutagenesis, we intended to test the hypothesis that the two blocks of amino acid residues in the acylated segment of CyaA might form the high-affinity calcium-binding sites that could play a key role in CyaA membrane binding (membrane insertion) and pore-forming (hemolytic) activities. Therefore, the present work has two main objectives: (1) construction, isolation and purification of CyaA variants with substitutions in the predicted calcium-binding sites and their characterization by functional assays and by planar lipid bilayer electrophysiological measurements, and (2) construction, isolation and purification of the C-terminal part of the acylated segment of CyaA ($CyaA_{908-1008}$) and its variants, as well as their characterization by liquid chromatography-mass spectrometry and circular dichroism spectroscopy.

In this work, we have been able to express and purify CyaA-derived proteins carrying non-conservative mutations in blocks I and II of the acylated segment of the toxin and compare their activities (membrane binding, AC domain translocation, pore-forming activity) with the wild-type toxin. We observed that some of the introduced substitutions abolished the binding and invasive AC activities, as well as the pore-forming capacity of CyaA on both mammalian cell membranes and artificial planar lipid membranes. Furthermore, we have been able to express and purify a $CyaA_{908-1008}$ polypeptide, as well

as its mutant variants carrying mutations in the predicted calcium-binding sites. Results from circular dichroism spectroscopy on $CyaA_{908-1008}$ variants indicated the existence of two calcium-binding sites in CyaA, one located in block I and the other located in block II of its acylated region.

The obtained results are the basis for future investigation, especially for deeper structural characterization of the C-terminal part of the acylated domain of CyaA, namely X-ray crystallography and nuclear magnetic resonance studies.

Keywords: Whooping cough, *Bordetella pertussis*, CyaA, adenylate cyclase toxin, calcium-binding sites

RESUMO

A coqueluche ou pertússis, é uma doença respiratória infeciosa de alto contágio, sendo mais comumente conhecida como "tosse convulsa" por causa da tosse característica a ela associada. O agente etiológico principal é a bactéria Gram-negativa *Bordetella pertussis*, no entanto alguns casos estão associados ao microrganismo relacionado *B. parapertussis*. O agente pode ser transmitido por gotículas aerossolizadas sendo que, após a inalação, as bactérias colonizam os epitélios respiratórios ciliados das vias aéreas inferiores em humanos, onde exercem um papel na supressão da imunidade do hospedeiro durante as fases iniciais da infeção.

Apesar da disponibilidade e do uso mundial de vacinas contra a tosse convulsa, esta continua a ser a doença menos controlada entre as que dispõem de vacinação, mesmo em países com altas taxas de imunização, os quais têm experimentado um aumento nos casos de coqueluche nos últimos anos. Como esta doença pode ser fatal para os recém-nascidos não vacinados, a redução da disseminação da bactéria *Bordetella pertussis* por meio da compreensão dos seus mecanismos de ação biológica, associado ao desenvolvimento de vacinas mais eficazes contra a coqueluche, poderia ajudar a interromper o ciclo vicioso de colonização e transmissão. As vacinas acelulares ("acellular Pertussis", aP) atuais contra a tosse convulsa têm na sua composição apenas alguns antigénios selecionados de *B. pertussis* (toxina pertussis, hemaglutinina filamentosa, pertactina e/ou fímbrias). A ausência da toxina adenilato ciclase (CyaA) na atual formulação das vacinas aP é considerada uma das possíveis causas para a falha cada vez mais aparente no desenvolvimento de uma proteção de longo prazo contra a tosse convulsa em populações altamente vacinadas, em oposição à eficácia das vacinas celulares ("whole-cell Pertussis", wP) que têm sido usadas há décadas, mas que podem causar distúrbios neurológicos graves, entre outros efeitos colaterais. Isso ocorre porque CyaA aniquila as funções bactericidas das células sentinelas da imunidade inata, paralisando as atividades bactericidas opsonofagocíticas dos fagócitos, tais como neutrófilos e macrófagos. Devido ao seu papel protetor e imunossupressor desempenhado nas infeções por *Bordetella*, o toxóide CyaA é atualmente considerado um candidato ideal para a inclusão na próxima geração de vacinas aP.

B. pertussis produz uma série de fatores de virulência que a permitem superar as funções de defesa imune inatas e adaptativas da mucosa aérea do hospedeiro, tais como as toxinas pertussis e CyaA. CyaA é uma proteína (1706 resíduos aminoacídicos) formada por vários domínios, desempenhando um papel particular nas fases iniciais da infeção por *B. pertussis*. Possui um domínio catalítico adenilato ciclase (AC) localizado nos ~400 resíduos N-terminais, o qual depende de calmodulina eucariótica (CaM) para a sua atividade enzimática, e uma porção C-terminal (~1300 resíduos) responsável pela translocação deste domínio AC, bem como para o fenótipo hemolítico de *B. pertussis*. A presença de um segmento de ~100 resíduos ligando os domínios enzimáticos e hidrofóbicos de CyaA (resíduos 400-500) é crucial para a translocação do domínio AC através da membrana plasmática e para a regulação da atividade de formação de poros da toxina. O domínio hidrofóbico, que abrange os resíduos 500 a 700, contém pares de resíduos de glutamato carregados negativamente localizados nos segmentos hidrofóbicos que estão envolvidos no controle da taxa de formação, seletividade catiónica e tamanho dos poros formados por CyaA. Após a acilação específica de resíduos de lisina internos

(K860 e K983) por uma aciltransferase (CyaC), a toxina é convertida a partir de um precursor inativo, proCyaA, na sua forma ativa. Estes resíduos de lisina estão localizados na região acilada compreendida entre os resíduos 800 a 1000, e a sua modificação pós-traducional é necessária para as atividades citotóxicas (translocação do domínio AC) e hemolíticas (formação de poros) de CyaA, bem como para a conversão da toxina numa holo-proteína monomérica. A metade C-terminal de CyaA (resíduos 1006 a 1706) compõe o domínio de ligação ao recetor celular e exibe várias características comuns a todas as proteínas pertencentes à família RTX (repeats in toxin), tal como as repetições nonapeptídicas de glicina e aspartato do protótipo GGxGxD (onde x representa qualquer aminoácido). Estas repetições formam os numerosos (~45) locais de ligação a cálcio de CyaA. Os motivos RTX são intrinsecamente desordenados e são caracterizados por uma carga global média negativa na ausência de cálcio, que é parcialmente neutralizada com a ligação do mesmo, favorecendo uma transição de estrutura desordenada para ordenada. Assim, CyaA é uma proteína de ligação a cálcio que sofre alterações conformacionais após se ligar a este catião. A secreção de CyaA através do invólucro bacteriano envolve um sistema de secreção do tipo I (T1SS), constituído pelas proteínas CyaB, CyaD e CyaE, o qual exibe o mesmo mecanismo de translocação de HlyA, a α-hemolisina da família RTX de *E. coli*, que usa o aparelho HlyBD/TolC. Após a secreção, a ligação a cálcio presente no meio extracelular leva a alterações conformacionais do domínio de ligação ao recetor celular de CyaA, tornando-se numa estrutura estável. Esta conversão induzida pelo cálcio no domínio de ligação ao recetor é necessária para a atividade biológica de CyaA. Uma vez secretado, este domínio liga-se à subunidade CD11b do recetor CD11b/CD18, que é expresso em células mieloides como macrófagos, células dendríticas, neutrófilos e células NK ("natural killer cells"), e que são os alvos primários de CyaA *in vivo*. No entanto, CyaA pode-se ligar com eficácia reduzida a uma variedade de outros tipos celulares que não expressam a integrina CD11b/CD18, como eritrócitos ou células epiteliais. Após penetração da membrana da célula eucariótica (contendo ou não o recetor CD11b/CD18), a proteína CyaA liberta o seu domínio AC no citosol da célula alvo. Neste compartimento, a enzima adenilato ciclase é ativada pela ligação da calmodulina citosólica e catalisa uma conversão extremamente rápida (k_{cat}~2000 s^{-1}) e descontrolada de ATP em cAMP. A acumulação desta molécula de sinalização subverte a fisiologia celular e suprime rapidamente as funções bactericidas dos fagócitos. Paralelamente, a porção hemolisina oligomeriza em poros seletivos para catiões e permeabiliza as células para o efluxo de iões potássio citosólicos.

A toxina CyaA é capaz de penetrar as células eucarióticas e realizar atividades citotóxicas e hemolíticas, ambas dependentes de cálcio. CyaA possui duas classes diferentes de locais de ligação ao cálcio, locais de ligação ao cálcio de baixa afinidade, importantes para a atividade citotóxica da toxina, e locais de ligação ao cálcio de alta afinidade, importantes para a capacidade de ligação à membrana e a atividade hemolítica de CyaA. Embora os locais de baixa afinidade estejam localizados no domínio RTX da toxina, a localização dos locais de alta afinidade é ainda desconhecida. Uma análise da região C-terminal do segmento acilado de CyaA (resíduos 908 a 1008) revelou que existem dois blocos de resíduos de aminoácidos com um padrão semelhante ao dos locais de ligação ao cálcio altamente conservados do domínio RTX, exibindo uma sequência consenso GGxGxD. Deste modo, usando mutagénese dirigida, testou-se a hipótese

de estes dois blocos de resíduos de aminoácidos no segmento acilado de CyaA formarem os locais de ligação ao cálcio de alta afinidade, os quais desempenhariam um papel fundamental na ligação à membrana e atividade hemolítica de CyaA. Portanto, o presente trabalho teve dois objetivos principais: (1) construção, isolamento e purificação de variantes de CyaA com substituições nos locais previstos de ligação ao cálcio, seguido da sua caracterização funcional em ensaios de atividade e por medições eletrofisiológicas em preparações membranares de bicamadas lipídicas, e ainda (2) construção, isolamento e purificação da parte C-terminal do segmento acilado de CyaA ($CyaA_{908-1008}$) e suas variantes, bem como a sua caracterização por cromatografia líquida acoplada a análises de espectrometria de massa e de espectroscopia de dicroísmo circular.

Neste estudo, conseguiu-se expressar e purificar variantes de CyaA que continham mutações não conservativas em ambos os blocos I e II do segmento acilado da toxina, e comparar as suas atividades (ligação à membrana, translocação do domínio AC e atividade hemolítica) com a proteína nativa. Observámos que algumas das substituições introduzidas aboliram as atividades de ligação e as atividades invasivas da enzima AC, bem como a capacidade de formação de poros de CyaA, tanto em membranas de células de mamíferos, como em membranas artificiais. Além disso, conseguimos expressar e purificar com sucesso o polipeptídeo $CyaA_{908-1008}$, bem como as suas variantes mutantes que continham mutações nos locais previstos de ligação ao cálcio. Os resultados de espectroscopia de dicroísmo circular nas variantes de $CyaA_{908-1008}$ indicaram a existência de dois sítios de ligação ao cálcio na toxina CyaA, um localizado no bloco I e outro localizado no bloco II da sua região acilada.

Os resultados obtidos são a base para investigações futuras, especialmente para uma caracterização estrutural mais aprofundada da parte C-terminal da região acilada de CyaA, nomeadamente estudos de cristalografia de raios-X e ressonância magnética nuclear.

Palavras-chave: Tosse convulsa, *Bordetella pertussis*, CyaA, toxina adenilato ciclase, sítios de ligação ao cálcio

ACKOWLEDGMENTS

This master's dissertation was marked by countless challenges and there are many people to whom I owe my most sincere acknowledgment.

First of all, I would like to thank João Barros, Ph.D. for his precious testimony and for introducing me the laboratory in Prague where all the experimental work of this project took place. Furthermore, I would like to thank Professor Peter Sebo, a head of the Laboratory of Molecular Biology of Bacterial Pathogens, for providing me the opportunity to integrate his group, for helping me finding accommodation and for the outstanding lab meetings, which were crucial for the familiarization with the projects and members of the laboratory. I truly admire his knowledge, enthusiasm, readiness to help and endless energy.

I am also very grateful to my supervisor, Ing. Adriana Osickova, Ph.D., for excellent tutelage, for the patience, motivation, invaluable advices and the time she dedicated to answer all my questions. Besides the knowledge transmitted and help in the thesis, since the beginning Adriana always treated me like a daughter. Thank you for all the gifts and treats, for introducing me to your lovely daughters and for the amazing picnics in the Institute with Klára, where we shared amazing moments and stories. To her husband, Ing. Radim Osicka, Ph.D., I also owe my deepest gratitude not only for being always available to help me in stressful moments, but also for his technical expertise and for the extremely useful knowledge he always transmitted. I will never forget what both of you have done for me. This dissertation would not be possible without you! Also, I would like to express my acknowledgment to my co-supervisor Carlos de São José, Ph.D., who also contributed for the realization of this dissertation and whose help was of utmost importance.

To all the members of the Laboratory of Molecular Biology of Bacterial Pathogens I address my gratitude, for the advice, practical help and great working atmosphere. My special thanks go to Jirka Masin, Ph.D., who helped me with the analysis of protein activities, which I really enjoyed doing, and to the technicians Sona, Iva, Hanka and Vladimíra for being so helpful and for the excellent technical support. I would also like to thank my colleagues, in particular those who have also endowed me with some of their skills. In special, I want to thank Carlos, "specialist in SDS-PAGE electrophoresis and CD spectroscopy", for being such a good teacher and helpful person. I could always come to you with lots of questions that you have always adjusted what you were doing to answer me with kindness and a smile on your face. To Waheed and Humaira, a big thank you for all the support provided, especially with what I considered the biggest challenge in my dissertation, working with the BLM machine! Thank you for the enormous sympathy and for letting me running to your home all the time I was in trouble and for receiving me always in the best way possible, offering delicious Pakistani food.

Last but not least, I would like to express my gratitude to my friends and family. Coming from the most diverse nationalities, I am very grateful for the amazing friends I have met in Prague. Thank you for all your support, for the trips we have done and for all the moments we have shared together. This experience would not have been so epic without you. I would also like to thank all my Portuguese friends for the video calls, messages and support they sent me constantly during my stay in Prague. To my mum, dad and brother a huge thank you for always supporting my decisions, for helping me achieve my goals and for all your precious advices. To thank you for everything I would have to write another dissertation. Mum, dad and brother: you were definitely my biggest motivation!

TABLE OF CONTENTS

ABBREVIATIONS

ABC transporter	ATP-binding cassette transporter
AC	Adenylate cyclase
ACIP	Advisory Committee on Immunization Practices
ADP	Adenosine diphosphate
aP	Acellular pertussis
ATP	Adenosine triphosphate
CaM	Eukaryotic calmodulin
cAMP	Cyclic adenosine monophosphate
CD	Circular dichroism
CR3	Complement receptor 3, integrin CD11b/CD18, αMβ2, Mac1
CyaA	Adenylate cyclase toxin, ACT
CyaC	Cyclolysin-activating lysine-acyltransferase
DNT	Dermonecrotic toxin
DTP	Diphtheria-tetanus-pertussis
EDTA	Ethylenediamine tetraacetic acid
EGTA	Triethylene glycol diamine tetraacetic acid
ER	Endoplasmic reticulum
FHA	Filamentous hemagglutinin
FIM	Fimbriae
IPTG	Isopropyl-β-D-thiagalactopyranosid
Hly	Hemolysin
LC-MS	Liquid chromatography-mass spectrometry
LOS	Lipooligosaccharide
LPS	Lipopolysaccharide
MFP	Membrane fusion protein
PCR	Polymerase chain reaction
PEP	Postexposure prophylaxis
PRN	Pertactin

PT, PTX	Pertussis toxin
RT	Room temperature
RTX	Repeats in toxin
SOPMA	Self-optimized prediction from multiple alignment
TCT	Tracheal cytotoxin
TLR4	Toll-like receptor 4
T1SS	Type I secretion system
T3SS	Type III secretion system
U.S. CDC	United States Centers for Disease Control and Prevention
wP	Whole-cell pertussis

1. INTRODUCTION

1.1 Pertussis

1.1.1 Disease

Being recognized since the sixteenth century, pertussis was first described in the seventh century as “the cough of 100 days” and later referred in France as “quinte”, due to the 5 hour periodicity of the paroxysms observed in acute episodes of disease [1,2]. Also known as whooping cough (because of its characteristic cough), pertussis is considered a highly contagious infectious disease of the respiratory tract which is mainly caused by the Gram-negative bacterium *Bordetella pertussis* [3,4]. Despite the availability and world-wide use of pertussis vaccines, whooping cough remains the least controlled vaccine-preventable disease with about 16 million cases and 200-300 thousand deaths occurring per year worldwide [5].

The reservoir of *B. pertussis* is exclusively human [6,7] and the bacterium is transmitted by aerosolized droplets from cough or sneeze. *B. pertussis* infects the ciliated epithelial cells of the airways, where bacteria multiply and resist elimination by inflammatory cells, and may reach the bronchioles and lung alveoli of the host [8,9]. Although the disease affects especially young children and non-vaccinated new-borns and infants, adolescents and adults can also be infected, thus serving as carriers of the pathogen [10]. Many studies have highlighted the role of close household members, like mothers and siblings, as the main source of pertussis transmission to infants, putting them at the greatest risk of severe outcomes of this disease [11-13]. While one might think that symptomatic disease is required for transmission, prolonged close contact with infected individuals with asymptomatic disease appears to be sufficient for transmission [7,14].

The clinical presentation of the disease including severity and duration of symptoms may vary depending on patient age, vaccination status, previous infection, as well as co-infection with other pathogens [15]. Following initial infection, the incubation period of *B. pertussis* usually lasts from 7 to 10 days, but it can range from 5 to 28 days [4]. After infection and incubation, the typical presentation of the disease involves three consecutive stages lasting from about 1 to 3 weeks each: catarrhal, paroxysmal, and convalescent, wherein patients remain infectious for 3 weeks following symptoms onset if left untreated [1,16]. The catarrhal phase is the most infectious one and patients develop mild symptoms like cough, sore throat, runny nose, and conjunctivitis similar to other infectious diseases, making the diagnosis process more difficult at this stage. The gradual increase in cough frequency characterizes the beginning of the paroxysmal phase, where patients experience repetitive series of severe coughing episodes followed by a characteristic inspiratory whoop and/or vomiting. In the third phase, the frequency, duration, and severity of coughing episodes gradually decreases. However, cough paroxysms patterns can recur in case of another viral respiratory infection [1,2,4]. In severe cases, clinical complications such as apnea, pneumonia, convulsions, pulmonary hypertension, extreme lymphocytosis, as well as co-infections with respiratory viruses occur among infants who have not completed vaccine series, leading ultimately to respiratory failure and death. Older patients can develop symptoms like insomnia, apnea, weight loss, urinary

incontinence, syncope and rib fractures. However, unlike infants, these patients rarely develop pneumonia or require hospitalization [1,3].

1.1.2 Diagnosis

Early recognition of pertussis might facilitate an effective clinical management of patients, as well as limit the spread to other susceptible people. The accurate diagnosis of *B. pertussis* infection is dependent on the clinical presentation of the disease and progression of the symptoms previously described. The diagnosis of pertussis in the catarrhal phase can be usually confused with other viral infections that mimic the signs and symptoms of *Bordetella* infection. Furthermore, pertussis can be also manifested by atypical clinical symptoms in neonates and adults, which makes the recognition process difficult, leading to significant delays in treatment [1]. Therefore, it is extremely important to apply rapid and reliable laboratory diagnostic technics, which involve obtaining a nasopharyngeal specimen, as well as keeping the clinical and public health management informed. Polymerase chain reaction (PCR) based assays are the most common methods used in the diagnosis of pertussis, having the advantage of higher sensitivity and continually improving specificity compared to the existing culture and serological assays [17,18].

1.1.3 Treatment

Healthcare providers generally treat pertussis with antibiotics, but other strategies can be used including corticosteroids, bronchodilators, antihistamines, or pertussis-specific immunoglobulins. However, these methods are not usually recommended as there is a lack of evidence about their effectiveness [19,20]. For severe cases of pertussis, exchange transfusions can also be done with some success, especially when applied early in the disease course [21].

For an effective treatment, antibiotics are recommended not only for confirmed cases but also for close contacts as postexposure prophylaxis (PEP). When given early in the course of the disease (optimally during the first 3 weeks), antimicrobials may attenuate severity and duration of the disease, as well as help cleaning the nasopharynx from *B. pertussis* and preventing its spreading to other susceptible individuals [1,4]. Therefore, the antibiotic treatment should be considered on the basis of a clinical diagnosis even before the laboratory confirmation [1,22]. Macrolide antibiotics such as erythromycin, azithromycin, or clarithromycin constitute the principal treatment for children and adults with pertussis as well as for PEP [23]. However, treatment with erythromycin can be associated with adverse events in neonates less than 1 month old, such as hypertrophic pyloric stenosis [24]. In these cases, azithromycin is usually the preferred option not only because it allows for less frequent dosing, resulting in better adherence to therapy, but also because unlike erythromycin and clarithromycin it has limited, if any effect on the cytochrome P450 system [25]. Trimethoprim-sulfamethoxazole can be used as an alternative agent to macrolides in cases of allergy, intolerance, or infection with some macrolide-resistant strain of *B. pertussis* [4].

1.1.4 Prevention

Despite the high vaccination coverage, worldwide pertussis is ranked among the 10 leading causes of childhood mortality, which leads to question the limits of current pertussis vaccination programmes [26,27]. In 1934 (prevaccine era), the greatest number of pertussis cases (26,000 cases per year) was reported to the U.S. Centres for Disease Control and Prevention (CDC) [28]. Pertussis vaccines have been introduced in many countries in the 1940s and 1950s, and since 1974 immunization against pertussis has been recommended by World Health Organization (WHO) [29].

There are two types of pertussis vaccines: whole-cell (wP) vaccines consisting of the entire *B. pertussis* bacteria that have been inactivated either by heat, or treatment with formalin; and acellular pertussis (aP) vaccines consisting usually of 1 to 5 purified components of *B. pertussis*, including detoxified forms of pertussis toxin (PT) either alone or in combination with other *B. pertussis* components such as filamentous hemagglutinin (FHA), pertactin (PRN) and fimbriae (FIM) types 2 and 3. Depending on vaccine type and manufacturer, the composition and amount of pertussis antigens differs. Both wP and aP vaccines are usually combined with diphtheria and tetanus toxoids in combinations called diphtheria-tetanus-pertussis vaccines (DTwP or DTaP). More recently, some pertussis vaccines are also combined with other vaccines such as hepatitis B, *Haemophilus influenzae* type b, or even inactivated poliovirus [27,29]. Routine infant vaccination against pertussis is comprised of three primary doses of DTaP, administered at 2, 4, and 6 months of age, followed by two booster doses at 15 to 18 months and 4 to 6 years [30].

Following introduction of wP vaccines in the late 1940s, the number of reported cases rapidly decreased, reaching an historic low of 1010 cases in 1976 in the United States. However, in 1970s focus gradually shifted towards side effects after immunization [8,30]. Adverse reactions such as local pain, redness, induration at the injection site, fever, drowsiness, irritability and anorexia are frequently associated with wP vaccines. More severe reactions are uncommon and rare [4,27]. As the frequency of adverse reactions tends to increase with age and with the number of injections, wP vaccines are not recommended for children aged ≥7 years, adolescents and adults [29]. Efforts to develop improved pertussis vaccines were made, resulting in the subsequent development of aP vaccines in the late 1990s [31]. Because aP vaccines contain minimal to none amount of the lipopolysaccharide (LPS), they are less reactogenic than wP vaccines, but unfortunately also less effective [4,8,28]. Although the frequency of adverse events following primary aP immunisation is very low or zero, with each successive aP dose the frequency and severity of local reactions tend to increase. Thus, aP vaccines with reduced antigen concentrations have been developed for adolescents and adults [29].

Vaccine-induced immunity to pertussis is not lifelong, and although differences in the immune response triggered by both types of pertussis vaccines (wP and aP) exist, cellular immunity is considered to play a pivotal role in both cases [1]. Some studies highlighted the role of cellular immunity induced by wP vaccines (that is similar to that induced by natural infection) in the clearance of a *B. pertussis* primary infection and protection against rechallenge, consisting in a Th1-like response with elevated production of T-helper-cell type 1 cytokine IFN-γ, and low/no production of type 2 cytokines (IL-4 and

IL-5) [31,32]. More recently, a study conducted using the baboon model showed that previously infected animals and wP-vaccinated animals possess a robust Th1/Th17 memory, while aP vaccination induces higher Th2 but lower Th1/Th17 responses, decreasing symptom severity but not transmission [33]. Nevertheless, due to the demonstrated similar efficacy and improved safety over wP vaccines [34,35], aP vaccines have gradually replaced wP vaccines in many developed countries. However, the significantly higher production costs associated with aP vaccines make the wP the vaccine of choice in many developing countries [27].

1.1.5 Resurgence of pertussis as a public health threat

After introduction and widespread use of pertussis vaccines, dramatic epidemic cycles have been registered in the past 30 years [36,37]. Despite the cyclic nature of pertussis, with peaks occurring every 3 to 5 years, in 2012 the greatest burden of pertussis in 60 years was registered, with about 48,000 cases and 18 deaths reported to the U.S. CDC, even though there were other outbreaks occurring in 2004, 2005, and 2010 [8,30]. Besides that, vaccination against pertussis led to alterations in the epidemiology of the disease. In the prevaccine era, pertussis incidence was mainly linked to children between 6 months and 2 years of age. In contrast, it is now becoming more frequent among adolescents and adults [27]. This alterations in pertussis epidemiology have been reported not only to the U.S. CDC but also to the European Centre for Disease Prevention and Control (EUVAC).

Several factors have been attributed to this shift in the epidemiology of pertussis, including *B. pertussis* strain adaptation, waning immunity after immunization with aP vaccines, the spread of other *Bordetella* species, as well as increased awareness and diagnostic capabilities [1,4,27]. There is evidence that the switch from wP vaccines to aP vaccines is the most important factor that explains the underlying causes that had precipitated the global increase in a disease that had been so well controlled for decades. Studies performed in different states of U.S. after 2012 pertussis outbreak found a significant decrease in DTaP vaccine efficacy in adolescents over time, indicating that waning immunity is likely to play a major role in increasing pertussis incidence in this age group [38,39].

Beyond the increased incidence among adolescents and adults and corresponding risk of transmission to susceptible individuals, older children affected with pertussis are often fully vaccinated in accordance to the recommended vaccination guidelines [40]. A study conducted during the transition to aP vaccines found an increased risk of developing disease in children vaccinated only with aP vaccines comparing to those who have ever received prior wP vaccines as part of their primary series [41]. To avoid the increase of infections in this age group, in 2005, the Advisory Committee on Immunization Practices (ACIP) recommended the inclusion of a single dose of a tetanus toxoid, reduced diphtheria toxoid, and acellular pertussis (Tdap) vaccine in the pre-existing vaccination programs [42]. However, the lack of evidence on whether the resurgence of pertussis is exclusively related to waning immunity with aP vaccines or even related to differences in the immune response triggered by these vaccines makes unclear the benefits of this approach [8].

To protect those at higher risk of this disease, several strategies have been put into place. The "cocooning" strategy consists of immunizing close contacts (parents, siblings, and grandparents) after the birth of a new child to prevent the transmission of the disease. However, the implementation of this strategy is often impeded by logistics and cost-effectiveness issues. Another strategy includes the passive transfer of pertussis antibodies to infants (transplacental transfer) by immunizing pregnant women [27]. Although several studies have shown an efficient transfer of antibodies against pertussis from vaccinated mothers to babies via the placenta [43,44], there are still some concerns associated with this strategy [1,37]. Therefore, in 2012, the ACIP advised TdaP vaccine for pregnant women without respect of the interval between pregnancies [45]. Another approach would be starting immunizing infants at birth, with shorter intervals between doses, which would still leave new-borns vulnerable until protective antibody levels are achieved. Furthermore, the potential risk of interference with the antibody response to other recommended vaccines, such as the hepatitis B, *H. influenzae* type b and diphtheria vaccines highlights the weakness of this approach [27]. Other possibilities include the reinstitution of DTP vaccines and addition of another *B. pertussis* antigens (like CyaA or BrkA antigen) to existing DTaP vaccines [1].

The re-emergence of pertussis as a global public health threat clearly demonstrates the need for the development of more effective vaccines that have an improved safety profile and confer long-term immunity. In the absence of better vaccines, the development of better treatment strategies is crucial, in order to protect young infants from pertussis. The achievement of this goals is dependent on a better understanding of the etiological agent of the disease, as well as the molecular mechanisms of *B. pertussis* pathogenesis, which will be described in the following sections.

1.2 The genus *Bordetella*

Members of the genus *Bordetella* include human and animal pathogens within the family *Alcaligenaceae*, comprising 10 main species: *B. pertussis*, *B. parapertussis*, bovine-associated *B. parapertussis*, *B. bronchiseptica*, *B. avium*, *B. hinzii*, *B. holmesii*, *B. trematum*, *B. petrii*, and "*B. ansorpii*" [1]. However, only *B. pertussis*, *B. parapertussis* and *B. bronchiseptica* are the most relevant species regarding mammalian infection, and due to their very close phylogenetic relationship these strains are collectively referred as *B. bronchiseptica* cluster [2,8,46].

Moreover, the genus also contains a number of additional and more distantly related species. For example, *B. avium* and *B. hinzii* are both bird pathogens, however *B. hinzii* has also occasionally been described to affect humans. *B. holmesii* has been associated with septicaemia and pertussis-like disease in humans [2,47]. *B. trematum* and *B. ansorpii* are not associated with respiratory tract infections but were isolated from human ear infections and skin wounds. *B. petrii* represents the first *Bordetella* species isolated from the environment, being further isolated from immunocompromised patients with ear infection and pulmonary disease. Furthermore, novel environmental *Bordetella* species have been obtained recently from mural paintings in ancient tombs [47].

1.2.1 *B. bronchiseptica* cluster

Despite the genetic proximity among the three species belonging to the *B. bronchiseptica* cluster, they differ in several phenotypic traits such as growth characteristics, several biochemical particularities, as well as differences in their host range and severity of disease they cause [8,46]. *B. pertussis* is a strict aerobe and human pathogen with no known animal or environmental reservoir. *B. parapertussis* can be divided into two distinct lineages: the human-adapted *B. parapertussis*$_{Hu}$, which is less capable of causing severe pertussis in humans compared with *B. pertussis*, but still responsible for a limited number of cases; and the ovine-adapted *B. parapertussis*$_{Ov,}$ which causes choric infection of respiratory tract in sheep. In contrast, *B. bronchiseptica* has a broad host range, causing chronical and often asymptomatic infection in a wide range of animals and even humans [2,8].

Phylogenetic analyses together with comparative genome sequencing support the hypothesis that both *B. pertussis* and *B. parapertussis*$_{Hu}$ have evolved independently from different *B. bronchiseptica*-like ancestors [2,48,49]. Concomitant to the transition by *B. pertussis* and *B. parapertussis*$_{Hu}$ to the human-restricted niche there was a considerable increase in the number of insertion elements, an accumulation of pseudogenes, many chromosomal rearrangements and a big reduction of their genome size, thus narrowing their metabolic potential and keeping most virulence factors in the streamline genomes of these human pathogens [49,50]. Moreover, multilocus sequence typing studies of *Bordetella* isolates have established two distinct *B. bronchiseptica* complexes, complex I and IV, with the majority of *B. bronchiseptica* complex IV strains being isolated from humans, as opposed to the primarily animal origin of *B. bronchiseptica* complex I isolates. Based on whole-genome sequencing analysis it was further demonstrated that *B. pertussis* and *B. parapertussis* evolved from different complexes, with *B. parapertussis* sharing a more recent ancestor with complex I, whilst *B. pertussis* with complex IV [8].

Indeed, adoption of a host-restricted lifestyle by *B. pertussis* and *B. parapertussis* may have been favoured by gene loss, rather than gene acquisition, simultaneously with the proliferation of transposons. These genomic modifications were, in turn, responsible for the alteration of regulatory networks, metabolic pathways, or even the elimination of some antigenic proteins that made these bacterial strains more susceptible to immune surveillance [49,50]. Similar patterns of adaptation to a specific niche are observed in other pathogens, such as in *Salmonella typhi*, a human-restricted pathogen, in contrast to *Salmonella enterica* serovar Thyphimurium, which has a broader host range. Similarly to *B. pertussis*, *S. typhi* possesses many pseudogenes and has experienced a loss of several proteins possibly involved in interactions with multiple hosts [51].

Despite being present in all three species, not all the genes encoding for virulence factors are equally expressed among these strains. For example, while PT is only produced by *B. pertussis* strains, both *B. parapertussis* and *B. bronchiseptica* contain PT genes without expressing them. Apart from toxins, these highly related virulence factors also include different adhesins, both controlled by the regulatory Bvg two-component system, which is also conserved and can be functionally exchanged between *B. pertussis*, *B. parapertussis* and *B. bronchiseptica* [46].

At the other end of the evolutionary spectrum, although numerous shifts on the allelic profile of *B. pertussis* have been documented after vaccine introduction, diversity at the gene-level remains very limited when compared to other pathogenic bacteria. Nonetheless, introduction of pertussis vaccines has prompted some important changes to circulating alleles, thus accelerating *B. pertussis* gene-level evolution. These variations are observed in terms of both gene- and genomic-level and include changes in the allelic profile, proliferation of some strains deficient in one or more of the antigens used in aP vaccines, as well as inter-strain genome rearrangements, deletions and large tandem duplications. However, the contribution of both gene- and genomic-level changes in the resurgence of whooping cough is still not fully understood. It is important to continue these analyses, specially based on whole-genome sequencing, as well as on other long-read sequencing technologies [52].

1.3 *Bordetella pertussis*

Being recognized as the causative agent of pertussis since the 19th century, *B. pertussis* was for the first time isolated by Bordet and Gengou in 1906. *B. pertussis* is a Gram-negative, pleomorphic aerobic coccobacillus with an optimal growth on both Bordet-Gengou and Regan-Lowe blood-supplemented agar mediums between 35 °C and 37 °C. Furthermore, it is a fastidious, nonmotile, catalase- and oxidase-positive species [1].

1.3.1 Regulation of virulence factors

Bacterial virulence is dependent on the expression of different virulence factors, which may be required at different stages of infection. Regulation of these virulence factors occurs in response to changing environmental conditions in many bacterial pathogens [53,54]. *Bordetella* species are known for being able to change the expression of sets of virulence factors alternating between virulent and avirulent forms [55].

The expression of virulence factors in *B. pertussis* is regulated by a central regulatory locus *bvg* (*Bordetella* virulence genes) [53], which consists of three genes: *bvgA*, *bvgS* and *bvgR* [56]. The *bvgAS* genes encode a two-component regulatory system comprising a sensor protein (BvgS) and a transcriptional activator protein (BvgA). A schematic representation of the BvgAS function is depicted in **Figure 1**. These proteins were shown to share homology with the "two-component" family of prokaryotic regulatory proteins that respond to environmental stimuli [57]. Examples include the EnvZ/OmpR system involved in regulation of outer membrane proteins of *Escherichia coli*, as well as the CheA/CheB/CheY system involved in chemotaxis also in *E. coli*, as well as in *Enterobacter aerogenes* and *S. typhimurium* [55]. BvgS in the inner membrane senses external signals and transfers them to the cytosolic BvgA via a complex phosphorelay [58]. The signals to which BvgS responds *in vivo* are unknown, however *in vitro*, the system is activated at 37 ºC and inactivated either in the presence of chemical modulators like $MgSO_4$ and nicotinic acid or at low temperatures (~25 ºC) [8,59].

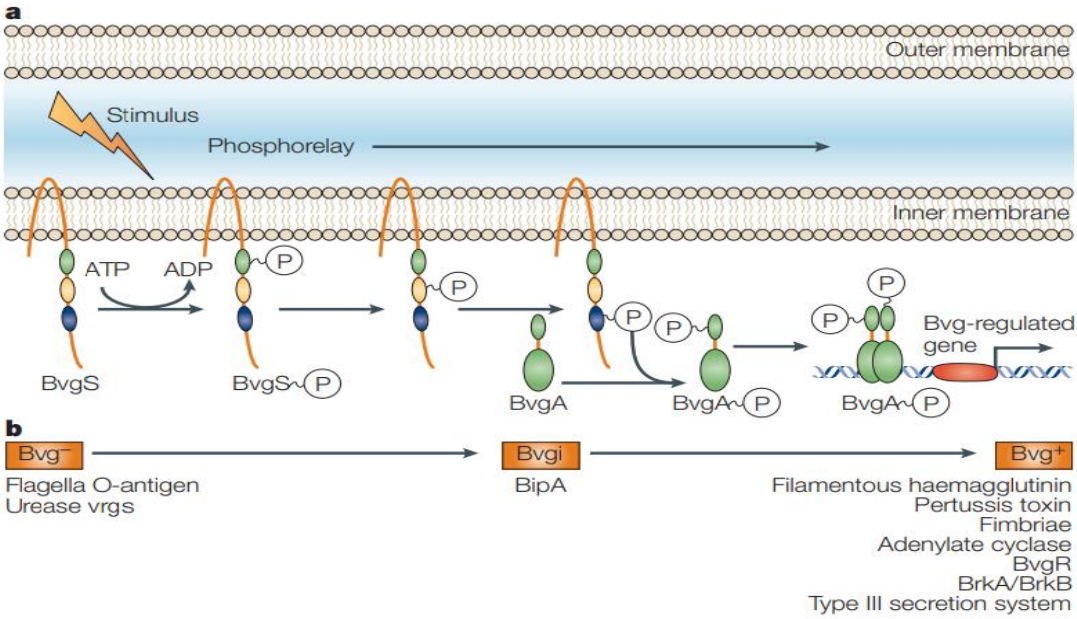

Figure 1. A schematic picture that represents the mode of action of the Bvg two-component system. **a**. Periplasmic stimulus activates BvgS, which experiences autophosphorylation. The phosphate group is relayed along BvgS and finally to BvgA. Phosphorylated BvgA then activates transcription of several genes. This Bvg-active state is called Bvg^+ phase. **b.** In the absence of activating stimuli, BvgS is inactive, thus BvgA remains unphosphorylated. The bacteria are in the so-called Bvg^- phase, being characterized by the expression of a subset of Bvg^- phase-specific genes. With low BvgA activation an intermediate phase (Bvg^i) is observed, but with increasing BvgA activity it is common to observe a switch from Bvg^- phase conditions to Bvg^+ phase conditions. The figure lists factors that are expressed at each Bvg phase. Vrg, *vir*-repressed genes. Adapted from [60].

BvgAS is used by the bacteria to modulate the gene expression in different environmental conditions and according to the host organism and stage of infection. The expression levels of four classes of genes are dependent on the phenotypic phase adopted by the system, favouring a temporal regulation of the virulence factors to promote the infection and avoid the host defence. When BvgAS is fully active (the so-called Bvg^+ phase), the expression of virulence-activated genes (*vags*) including many genes implicated in pathogenesis (such as *ptx* and *cyaA*) are positively regulated, suggesting that this phase is required for virulence. On the contrary, the Bvg^- phase is characterized by the expression of virulence-repressed genes (*vrgs*), such as those needed for flagella synthesis and motility in *B. bronchiseptica*. The role of this phase is not fully understood, however it has been hypothesized to contribute either in bacterial intracellular uptake and persistence or transmission between different hosts. It was also demonstrated to be important for survival under nutrient-limiting conditions in *B. bronchiseptica*. In the Bvg-intermediate (Bvg^i) phase, the BvgAS system is not fully induced, being characterized for the expression of *bipA* (which encodes an outer membrane protein of unknown function) or other early response genes such as *fhaB* (which encodes FHA) and *fim* (which encodes fimbriae). The Bvg^i phase may play a role in transmission by the aerosol route or the initial stages of infection [8,59].

Additional regulatory systems are known to participate in the expression of some virulence factors of *B. pertussis*, including regulation by iron availability [61] and regulation by physiological changes in CO_2 concentrations [62]. Although these systems are of extreme importance during the *Bordetella* spp. infectious cycle, they have not been fully described yet. More regulatory circuits are likely to be discovered.

1.3.2 Virulence factors

Upon infection of the human host and subsequent activation of the phosphorelay system, the pathogen enters the Bvg^+ phase, which is characterized by the expression of different adhesins, toxins and metabolic proteins. A schematic representation of the virulence factors of *B. pertussis* is shown in **Figure 2**. A recent study predicted more than 140 proteins specifically secreted by *B. pertussis* during the Bvg^+ phase [63]. Pertussis results from the coordination of several virulence factors, which include toxins such as pertussis toxin (PT), adenylate cyclase toxin (CyaA or ACT), dermonecrotic toxin (DNT), and tracheal cytotoxin (TCT). Other factors include surfaces structures, such as filamentous hemagglutinin (FHA), pertactin (PRN), fimbriae (FIM), the type III secretion system (T3SS), lipooligosaccharide (LOS), and metabolic proteins. These virulence factors of *B. pertussis* will be described in more detail below.

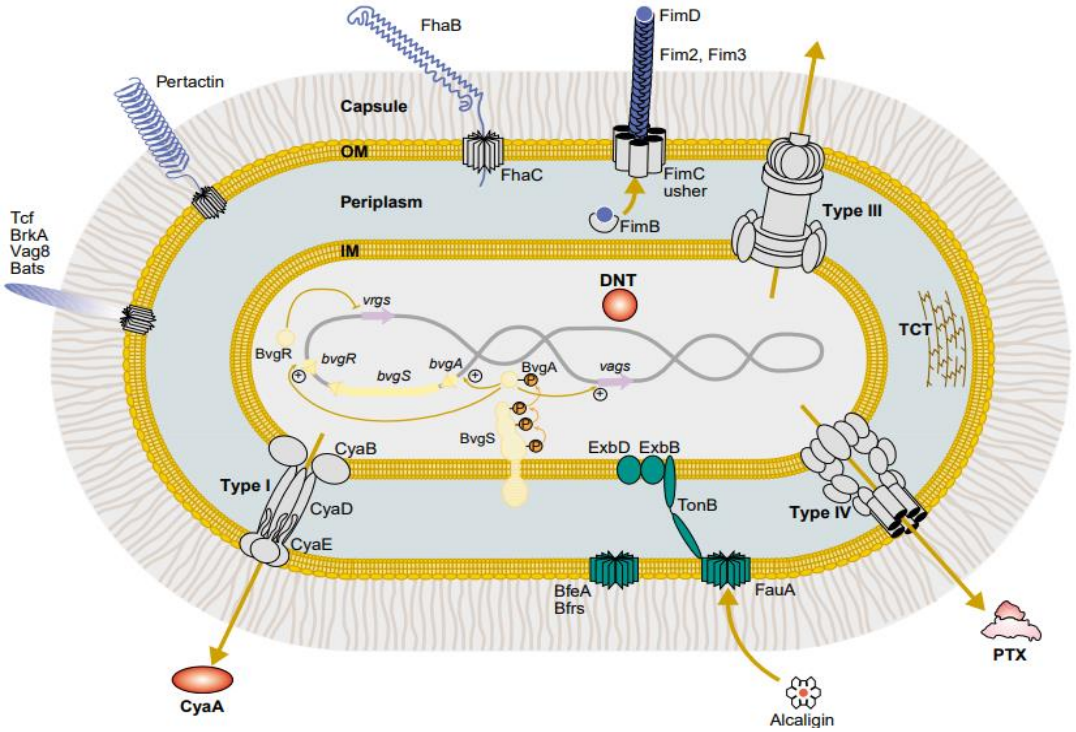

Figure 2. Virulence factors of *B. pertussis*. *B. pertussis* is depicted as a Gram-negative organism with inner and outer membranes (IM and OM), a periplasm and a capsule. The adhesins Fim, FhaB, pertactin, Tcf, BrkA, Vag8 and Bats are shown in blue; pertussis toxin (PTX), adenylate cyclase toxin (CyaA) and dermonecrotic toxin (DNT) are in red; the accessory proteins FhaC, FimB, FimC, Type III, Type IV and Type I are in grey; the iron uptake systems ExbB/ExbD, TonB, FauA, BfeA and Bfrs are in green; and the regulatory systems BvgA, BvgS and BvgR are in beige. The large brown arrows represent the orientation of export and import of virulence

factors and siderophores, respectively. The inner brown arrows show the phosphorelay and the regulation circuit. Adapted from [64].

1.3.2.1 Surface Structures

Adhesins are surface structures of bacteria important for its adherence to the host, mediating the attachment and colonisation. Some of the most important adhesins of *B. pertussis* are FHA, FIM, PRN and LOS. Many additional surface proteins may play a role in *B. pertussis* pathogenesis. These are BvgAS-activated autotransporter proteins, such as BrkA, TcfA, BapC, BatB, Vag8, SphB1 and Phg, and their function in pathogenesis include mediating adherence, complement resistance, evasion of antibody-mediated clearance, as well as proteolytic processing of other surface proteins [1,8].

1.3.2.1.1 Filamentous hemagglutinin

FHA is a highly immunogenic, hairpin-shaped protein having an important role in the attachment to the host cell surface. It is synthesized as a 367 kDa precursor polypeptide (called FhaB), which is then exported to the periplasm via the Sec machinery and secreted to the extracellular milieu by FhaC with the help of the SphB1 protease, while it is processed into a mature ~230 kDa protein [65]. FHA mediates the adhesion of *B. pertussis* to several eukaryotic cell types *in vitro* [66,67]. Three different binding motifs of FHA refer to its important role in the adhesion [68] and represent how this molecule can mimic eukaryotic cell adhesion mechanisms for mediating adherence of bacteria to mammalian cells. It was proposed to bind different integrins due to the interaction with its RGD (Arg-Gly-Asp) motif [69-72]. Whether it interacts with these or other mammalian receptors *in vivo* has yet to be determined [8]. Among its multiple functions, FHA mediates the initial adhesion of *B. pertussis* to ciliated epithelium of upper respiratory tract, driving the infection from upper to lower respiratory tract [73,74]; promotes phagocytosis of *B. pertussis* by macrophages and polymorphonuclear neutrophils [75,76]; induces release of IL-6 and suppresses IL-12 production by macrophages and dendritic cells [77,78]. Furthermore, it has been shown that FHA may play a role in the delivery of CyaA toxin from the bacterium to the target cell [79], but the importance of this phenomenon *in vivo* is still poorly understood. Nevertheless, Irie *et. al* [80] have demonstrated that the CyaA-FHA interaction may inhibit biofilm formation.

1.3.2.1.2 Fimbriae

FIM are type 1 pili *i.e.*, surface projections necessary for the colonization of the host cells. *B. pertussis* produces two major protein subunits depending on the strain, Fim2 and Fim3, encoded by *fimB* and *fimC*, respectively. Both subunits have identical molecular weight (~20 kDa) but are serologically distinct [81] and beyond that, their expression can undergo phase variation [82]. Even though it is usual for many bacteria to have a single gene cluster encoding for the major fimbriae subunits and accessory proteins required for export and assembly of its structure [83], *Bordetella* fimbriae subunits are not located

within a single gene cluster. The Fim operon (*fimBCD*) is located between the *fhaB* and *fhaC* genes [84]. This may represent a selective advantage, allowing the co-regulation of virulence genes that function together in infection. Alternative major fimbrial subunits known as FimA, FimN and FimX have also been identified [85-87]. Furthermore, a tip adhesin (FimD) has also been described [84]. This adhesin constitutes a minor subunit common to all fimbriae, which mediates binding to monocytes [88]. Fim 2 and 3 are important components for the colonization of the lower respiratory mucosa [89,90]. Similarly to FHA, they seem to be involved in adherence and suppression of the initial inflammatory response to infection [91], which might facilitate bacterial persistence.

1.3.2.1.3 Pertactin

PRN is an autotransporter protein which mediates eukaryotic cell binding via RGD motif. It is highly immunogenic and highly polymorphic [92]. Like other autotransporter proteins, it consists of a central passenger domain flanked by an N-terminal signal sequence and a C-terminal porin domain [93]. PRN has been proposed to play a role in adherence to the host due to the presence of several motifs commonly involved in eukaryotic cell binding [94,95]. However, similarly to fimbriae, studies addressing this issue have yielded equivocal results [74,92]. While PRN was shown to participate in adhesion on ciliated rabbit tracheal explant cultures [96], the role of PRN *in vivo* was not confirmed in the mouse model [97]. Nevertheless, in the murine model of *B. bronchiseptica* infection PRN may be involved in resistance to neutrophil-mediated clearance and promoting persistence in the lower respiratory tract [74,92]. Pertactin is included in most current aP vaccines, due to the protective antigenic properties demonstrated in mice [98]. However, polymorphisms in PRN toxin may have been implicated in escape from immunity to *B. pertussis* in vaccinated populations [99], which is now a major concern with several implications for the development of improved vaccines.

1.3.2.1.4 Lipooligosaccharide

LPS is a component of the outer membrane cell wall of Gram-negative bacteria, consisting of three different parts: the lipid A, the core oligosaccharide and the O-antigen. Unlike *B. bronchiseptica* and *B. parapertussis*, the LPS of *B. pertussis* lacks the O-antigen, being for this reason often referred to as lipooligosaccharide (LOS) [100]. LPS can be recognized by CD14, toll-like receptor 4 (TLR4) and by its co-receptor MD-2 in several cell types, including monocytes, macrophages, dendritic cells and B cells, which leads to the formation of TLR4-MD-2-CD14 complexes with the subsequent activation of signalling pathways and release of pro-inflammatory cytokines [101]. Studies have shown distinct recognition abilities of different forms of lipid A between human and murine TLR4-MD-2-CD14 complexes. While the murine TLR4-MD-2-CD14 has a similar response to both penta- and hexa-acylated lipid A, human TLR4-MD-2-CD14 responds strongly to hexa-acylated lipid A, but only weakly to penta-acylated lipid A [102]. In addition, the phosphate groups of the lipid A can be modified by glucosamine (GlcN) moieties in many *B. pertussis* strains. This modification is positively regulated by

the BvgAS regulatory system and has the ability to further alter the magnitude of the TLR4 stimulation [103-105]. While murine TLR4-MD-2-CD14 has a similar response whether the phosphate groups of the lipid A are modified or not, human TLR4-MD-2-CD14 responds strongly to *B. pertussis* lipid A containing GlcN-modified phosphate groups than to lipid A with unmodified phosphates [103]. *B. pertussis* produces a penta-acylated lipid A, suggesting that its ability to stimulate TLR4 in humans is even weaker than in mice, even though *B.* pertussis LOS is mainly composed of GlcN-modified phosphate groups [105]. Furthermore, it was shown that $TLR4^{-/-}$ mice are only modestly impaired in their ability to control infection by *B. pertussis* [106-108] and *B. pertussis* LOS interaction with murine dendritic cells was shown to result in the development of anti-inflammatory regulatory T cells [106]. Altogether these results suggest that *B. pertussis* have evolved in such a way it became relatively non-inflammatory in humans. However, some precautions must be taken in extrapolating results obtained from mice studies to humans, since the TLR4-MD-2-CD14 immune responses are dependent on the host.

1.3.2.2 Toxins

In addition to adhesins, *B. pertussis* also produces a number of toxins and most of them are proteins, except for LOS and TCT. Some of the most important *B. pertussis* toxins are PT, CyaA, DNT and TCT. CyaA, DNT and TCT are all expressed by *B. pertussis*, *B. parapertussis* and *B. bronchiseptica*. However, as previously stated, production of functional PT is exclusive to *B. pertussis*. Furthermore, *B. pertussis* uses the T3SS to deliver different effector proteins from bacterial cytosol directly into host cells.

1.3.2.2.1 Pertussis toxin

PT is one of the first identified and most extensively studied virulence factors of *B. pertussis* [8]. It is an ADP-ribosylating exotoxin of the AB_5 family [109], composed of 6 polypeptides (S1 to S5) [2]. The catalytic subunit A is a monomer comprising the polypeptide S1, while the pentameric B subunit consists of polypeptides S2, S3, S4, and S5 assembled in a 1:1:2:1 ratio [2]. PT is secreted by the type IV secretion system encoded by the *ptl* locus [110]. Once it is secreted, the B subunit (polypeptides S2 to S5) binds to sialic acid-containing glycoprotein [111,112]; the toxin is endocytosed by the host cell and follows a retrograde transport pathway to the endoplasmic reticulum (ER) [113]. Then, the A subunit translocates from the ER to the cytoplasm [114], where it catalyses the transfer of ADP-ribose from NAD^+ to the alpha subunit of heterotrimeric G-proteins, blocking their ability to inhibit adenylate cyclase activity (resulting in uncontrolled production of cyclic AMP (cAMP) in the cells) and leading consequently to the dysregulation of the immune response [112]. The outcome of such activity has a remarkably broad range of pharmacological effects in different models of infection. Experiments using the mouse model suggested that the primary targets for PT are alveolar macrophages [115]. The toxin inhibits the migration of neutrophils, monocytes and lymphocytes *in vitro* [116]. In mouse models, PT production by *B. pertussis* is directly correlated with reduced inflammatory responses and chemotaxis of neutrophils to the site

of infection, as well as to increased bacterial burdens early in infection [117,118]. Furthermore, its production at the peak of the infection is consistent with aggravated inflammation and pathology in the airways [119]. At the clinical level, PT production is directly related with the extreme lymphocytosis observed in patients and appears to be also involved in pulmonary hypertension, which accounts for the morbidity and mortality of the disease [120,121]. Besides that, antibodies against PT protect against severe disease, being this a crucial fact for its inclusion in all aP vaccines [112,122]. Nowadays, it is clear that although PT is an important virulence factor for infection, *B. pertussis* interaction with its host is more complex than currently recognized and involves not only different adhesins and toxins but also a series of other virulence determinants [64]. As opposed to what was believed, PT does not cause the typical paroxysmal cough in pertussis, since *B. parapertussis* also causes paroxysmal cough and this organism does not produce PT [123].

1.3.2.2.2 Dermonecrotic toxin

DNT is a protein with transglutaminase activity that can activate Rho GTPases by deamidation of Rho proteins [124,125]. It can alter the function of osteoblast cells *in vitro* [126] and yields necrotic lesions by subcutaneous injection in mice [127]. DNT appears to remain within the bacterial cytoplasm during infection and to be only released upon bacterial cell lysis [127,128], which may suggest that it acts indirectly in pathogenesis. A recent study showed that DNT affects neural cells through specific binding to the T-type voltage-gated Ca^{2+} channel that is highly expressed in the central nervous system and leads to neurological disorders in mice after intracerebral injection. These results may suggest a role for DNT as an etiological agent for pertussis encephalopathy, a severe complication of *B. pertussis* infection [129].

1.3.2.2.3 Tracheal cytotoxin

TCT is a natural breakdown product of the *Bordetella* cell wall peptidoglycan that is produced during cell wall remodelling [130]. TCT is the only known virulence factor of *Bordetella* whose expression is not dependent on the BvgAS regulatory system. It can be released in large amounts to the extracellular milieu, most likely due to the lack of a functional protein required for its transport back into the cytoplasm, which results in its ineffective recycling by *B. pertussis* [2]. TCT acts synergistically with LOS to induce the production of pro-inflammatory cytokines (like TNF-α, IL-1, IL-1β, and IL-6) and induces nitric oxide synthase for nitric oxide production, which causes destruction of ciliated cells from the epithelial surface and inhibits DNA synthesis [131-133]. This activity is dependent on the nucleotide-binding oligomerization domain-containing protein 1 (NOD1), a cytosolic pattern recognition receptor (PRR) sensitive to peptidoglycan. However, this is mainly restricted to the mouse NOD1, as human NOD1 poorly recognize TCT [134]. Nevertheless, it is hypothesized that this toxin might have a role in the characteristic cough observed in pertussis, however its contribution to the pathogenesis of pertussis in humans is still poorly understood.

1.3.2.2.4 Type III secretion system

The *Bordetella spp*. T3SS is used by *B. pertussis* to deliver effector proteins from the bacterial cytosol directly into the target cell, thus hijacking the intracellular machinery of the infected cells [135-137]. These effectors reach the cytosol of the host cell with the help of a translocon, which consists of two conserved hydrophobic proteins that form a pore in the eukaryotic cell membrane [138]. The T3SS is highly conserved between all members of the *Bordetella* genus and the corresponding loci are tightly regulated by the BvgAS system [2,139,140]. T3SS is a complex apparatus consisting of about 30 proteins showing homology with the Ysc T3SS apparatus genes of *Yersinia spp.* (**Figure 3**), namely with the T3SS ATPase (BscN-YscN), the needle (BscF-YscF), and the translocon components (BopB-YopB, BopD-YopD) [140,141].

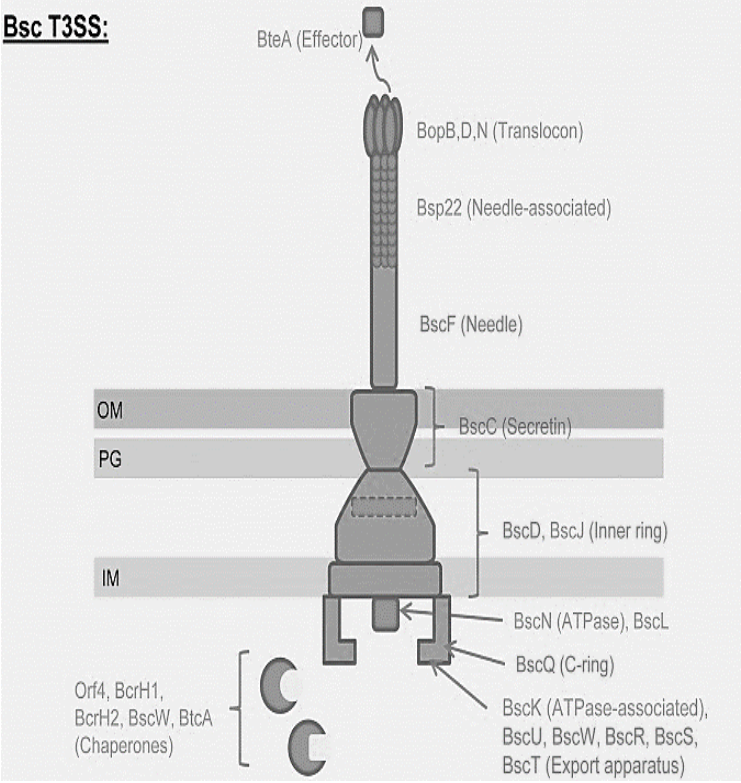

Figure 3. Schematic representation of *Bordetella* secretion complex (Bsc) T3SS structure. IM, inner membrane; OM, outer membrane; PG, peptidoglycan. Adapted from [142].

So far, only BteA has been definitively identified as a translocated substrate of the Bsc T3SS [143,144]. In *B. bronchiseptica*, T3SS was demonstrated to induce cell necrosis *in vitro* [145]. Moreover, it was suggested to have an immunomodulatory role by promoting persistence in the lower respiratory tract of mice [140,146,147]. However, the mechanisms behind this phenomenon are not fully understood. Regarding the human host, no requisite of T3SS activity for *B. pertussis* cytotoxicity was reported, which is quite surprisingly given that the genes are intact, highly conserved, transcribed and regulated, and that the BteA effector is interchangeable between *B. pertussis* and *B. bronchiseptica* [148,149]. The underlying causes of such paradox are now becoming better understood. It seems that laboratory-adapted strains do not secrete these proteins,

as opposed to the majority of low passage clinical isolates of *B. pertussis* [150-152]. This interesting event suggests that adapted *B. pertussis* strains are able to restore the type III secretion following contact with the host, such as during experimental infections of mice [152]. Recently, *B. pertussis* T3SS expression was shown to be stimulated under glutamate or iron depletion [61,153], which is in accordance with the previous findings, since under laboratory conditions *B. pertussis* is usually cultivated in Stainer-Scholte medium containing high glutamate concentration.

1.4 Adenylate cyclase toxin

Discovery of the adenylate cyclase toxin (CyaA, ACT, or AC-Hly) in *B. pertussis* dates back to 1976 [154]. Since then, it has been shown to be a crucial virulence factor of *B. pertussis* and considered as one of the few virulence factors that is conserved and produced by all pathogenic *Bordetella* species [155]. CyaA is secreted by *cyaBDE*-encoded type I secretion system and acylated by the product of *cyaC* [156,157]. The toxin is a member of the RTX (repeats in toxin) family and consists of two functional parts: the N-terminal domain, which is a calmodulin-dependent adenylate cyclase that converts ATP to cAMP [158,159], and the C-terminal hemolysin moiety, where a pore-forming domain, an acylated segment and calcium-binding RTX repeats are located [160,161]. CyaA binds with high affinity to complement receptor 3 (CR3, CD11b/CD18, $\alpha_M\beta_2$, Mac-1) of neutrophils, monocytes/macrophages and dendritic cells [162], where it exerts multiple effects, such as inhibition of bactericidal oxidative burst and opsonophagocytic killing mechanisms of neutrophils and macrophages [163,164]. In addition, CyaA was also shown to block the activation and chemotaxis of T-cells [165]. Studies using a mouse model have demonstrated that CyaA-deficient bacteria are cleared faster than wild-type bacteria, and studies using immunodeficient and neutropenic mice have suggested a role for CyaA in facilitating bacteria to resist neutrophil-mediated clearance [166,167].

The importance of CyaA was recently confirmed by Eby and co-workers, who detected significant levels of CyaA in nasopharyngeal fluids and washes using the baboon model of pertussis. They found that CyaA concentration could reach 100 ng/ml near target cell surface in the host nasopharynx [168]. CyaA was also shown to suppress TLR-induced secretion of pro-inflammatory IL-12 and TNF-α cytokines and to promote secretion of immunosuppressive IL-10 cytokine from mouse and human dendritic cells [169-174]. These facts together suggest that CyaA is able, either directly or indirectly, to influence a broad spectrum of processes of both innate and adaptive immunity of the host, which makes the CyaA toxoid a leading antigen candidate for inclusion into the next generation of pertussis vaccines [175].

1.4.1 CyaA biogenesis

CyaA is expressed from the *cya* locus, which is composed of 5 genes (*cyaA*, *cyaB*, *cyaC*, *cyaD* and *cyaE*) (**Figure 4**). The *cyaA* gene, encoding the inactive protoxin (proCyaA), is transcribed as the first gene of the *cyaABDE* operon, where the *cyaB*, *cyaD* and *cyaE* genes encode the components of the type 1 secretion system (T1SS) required for CyaA secretion. The *cyaC* gene encodes an acyltransferase enzyme that is required for the post-

translational activation of proCyaA and is located upstream to *cyaA*, being transcribed from a different promoter than *cyaA* gene, in the opposite orientation to this gene [176,177]. Unexpectedly, in the *cyaABDE* operon two distinct promoters were identified: one located 115 bp upstream the *cyaA* gene and other located in the intergenic *cyaA-cyaB* region [178]. The importance of the second promoter is evidenced by the fact that most of the transcripts from the *cyaA* promoter are terminated in the intergenic region between *cyaA* and *cyaB* genes, thus leading to a majority of monocistronic transcripts. As opposed to the *cyaA* promoter, which is under the control of the BvgAS regulatory system, the *cyaBDE* promoter seems to display a low-level constitutive expression, which is independent of virulence control [178].

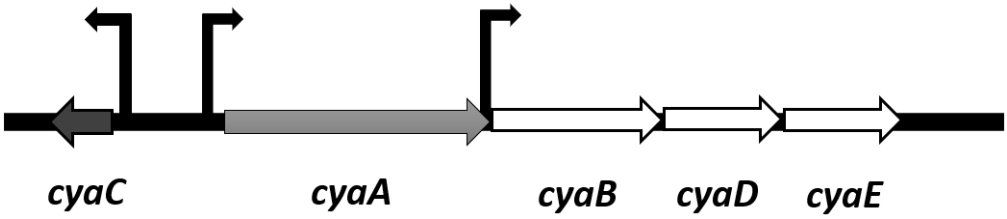

Figure 4. Schematic representation of the *cya* locus. The genes *cyaA, cyaB, cyaD* and *cyaE* are transcribed in the same direction from the same promoter located upstream of *cyaA*. Another promoter located upstream of *cyaB* allows separate transcription of *cyaB, cyaD* and *cyaE*. The activator gene, *cyaC*, is transcribed from another promoter in the opposite direction to the other genes of the locus.

However, CyaA expression was also found to be regulated to some extent by the CO_2 responding element [62]. As a consequence of the low affinity the response-regulator protein BvgA-P has for the *cyaA* promoter, *cyaA* gene is among the so-called "late-response" genes.

In addition to the regulation at the transcriptional level, sRNA-mediated regulation of CyaA expression in the presence of the Hfq RNA chaperon has also been described [179]. Although the amount of *cyaA* mRNA transcribed in an *hfq* deletion mutant (Δ*hfq*) is the same as in the wild-type bacteria, the amount of CyaA protein is lower in the case of the mutant. This might suggest a regulation mechanism for CyaA expression at the level of mRNA stabilization [179].

Like other RTX toxins, CyaA is secreted by T1SS after translation and post-translational acylation by CyaC. The T1SS consists of three different components (**Figure 5**): (i) an ABC (ATP-binding cassette) transporter incorporated in the inner bacterial membrane (called CyaB in *Bordetella*); (ii) a membrane fusion protein (MFP) that extends from the inner membrane into the periplasm (called CyaD in *Bordetella*); and (iii) an outer membrane protein (OMP) from the TolC family that spans into periplasm from the outer membrane (called CyaE in *Bordetella*) [180,181]. The mechanism of CyaA secretion resembles that used for the secretion of the RTX α-hemolysin (HlyA) of *E. coli* through the HlyAB/TolC apparatus [182]. After recognition of the secretion signal of CyaA by CyaB, a sealed channel-tunnel assembly across the entire Gram-negative cell envelope is formed and CyaA protein is then exported in a single step directly from bacterial cytoplasm into the external medium, without passage through the periplasmic

space [175]. The recognition signal of the toxin occurs within the last 74 residues of the C-terminal part of the toxin and remains unprocessed after secretion [183]. Once the C-terminus of CyaA emerges from the outer opening of the T1SS conduit on the bacterial surface, a folding nucleus (spanning 1636 to 1642 amino acid residues) is formed, initiated by the Ca^{2+} driven folding of the RTX repeat blocks into β-rolls [184]. At conditions of Ca^{2+} deprivation, most of the secreted CyaA molecules remain associated with FHA on the bacterial surface, exhibiting no activity and capacity to penetrate the target cells. In contrast, at 2 mM Ca^{2+} concentration typical for body fluids, CyaA is efficiently folded and is quantitatively released into culture supernatant [184].

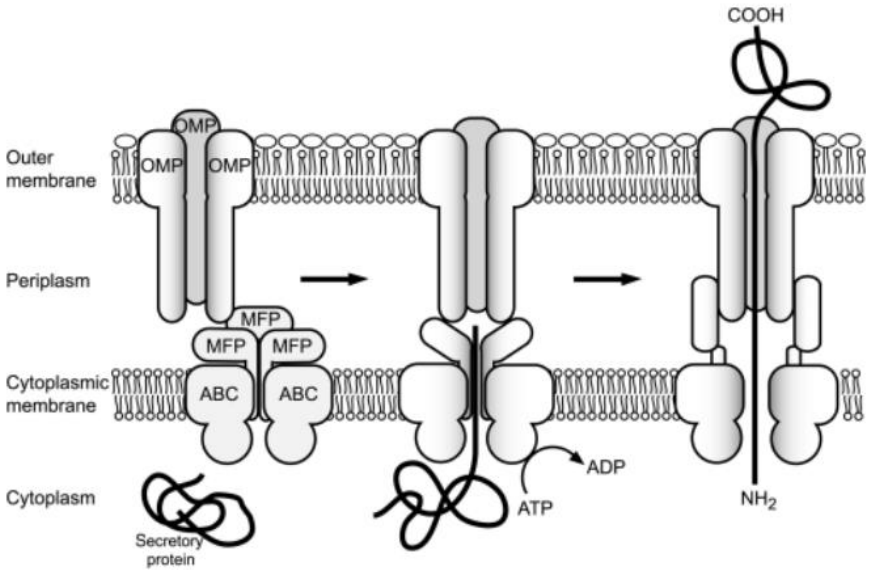

Figure 5. Schematic representation of the T1SS assembly operation. Upon recognition of the C-terminal secretion signal of the RTX protein, the inner membrane complex formed by an energy-providing ABC transporter and an MFP contacts the trimeric OMP, forming then a sealed channel–tunnel assembly spanning across the entire Gram-negative bacterial cell envelope for the passage of the RTX protein. Exportation of the protein through the conduit occurs in a single step from the bacterial cytoplasm directly to the external bacterial surface, without transiting through the periplasmic space. Millimolar calcium concentrations are typically encountered in host extracellular space colonized by pathogenic bacteria, allowing for the proper folding and acquisition of biological activity by the toxin, while the typical <100 nM of Ca^{2+} encountered in the bacterial cytoplasm retains the toxin unfolded. Adapted from [185].

1.4.2 CyaA structure

The completely secreted and folded CyaA molecule is a 1706 residue-long polypeptide (**Figure 6**) consisting of two functional parts: an N-terminal ~400 residue-long adenylate cyclase (AC) enzyme linked to a ~1300 residue-long RTX hemolysin (Hly) moiety [176]. The Hly moiety is further divided into the following subdomains: (i) the hydrophobic pore-forming domain [186]; (ii) the acylated segment, where the posttranslational modification of two specific lysine residues takes place [157,187]; (iii) the receptor-binding RTX domain harbouring the characteristic calcium-binding aspartate and glycine-rich nonapeptide repeats of a consensus sequence GGxGxDxxx (where x

represents any amino acid residue) [188,189]; and (iv) the C-terminal secretion signal for T1SS [183,184].

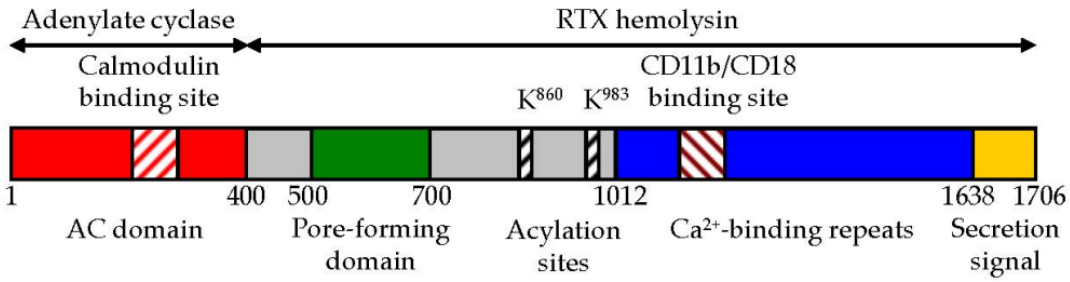

Figure 6. Schematic representation of the CyaA molecule with its relevant functional domains. The N-terminal AC enzyme domain (~400 residues) and the C-terminal Hly moiety (~1300 residues) of CyaA are linked together by a ~100 residue-long segment (residues 400 to 500). The Hly moiety itself harbours distinct functional subdomains: (i) a hydrophobic pore-forming domain (residues 500 to 700); (ii) an acylated segment (residues 800 to 1000), where the posttranslational acylation at two lysine residues (K860 and K983) occurs; (iii) a typical calcium-binding RTX domain with the CD11b/CD18-binding segment (residues 1166 to 1287); and (iv) a C-terminal secretion signal. Adapted from [190].

1.4.2.1 Adenylate cyclase domain

The adenylate cyclase (AC) domain of CyaA consists of 385 amino acid residues (~40 kDa) and catalyses the conversion of ATP into cAMP that is able to hijack the cellular signalling when present at pathologic levels in the cytosol of the host cell [191,192]. The AC enzyme is only activated upon binding of eukaryotic calmodulin (CaM) in a 1:1 stoichiometry inside the host cell cytosol [193,194]. Upon activation by CaM, the catalytic activity of the enzyme can be increased up to ~1000 fold, reaching an extremely rapid (k_{cat}~2000 s^{-1}) conversion of ATP into cAMP [191]. CaM binds to four distinct regions of the AC enzyme, as it was shown by the crystal structure of the AC enzyme with the C-terminal domain of CaM (C-CaM) [195]. The interactions between the four regions of the AC enzyme and CaM induce major conformational changes that are required for AC catalytic activity [158,159,196]. Two functional subdomains within the AC domain of CyaA were identified by limited proteolysis: T25 and T18 [194]. While the T18 subdomain is responsible for calmodulin binding, the N-terminal T25 subdomain harbours the catalytic site of the AC enzyme [158,159].

Mechanistic insight into AC catalytic activity revealed that aspartates D188 and D190 and histidine H298 of the AC domain are crucial for the binding of Mg^{2+} ions, while asparagine N304 plays a role in the positioning of ribose, and arginine R37 and lysine residues K58, K65, and K84 are required for the binding of the triphosphate of ATP [195]. Deprotonation of 3'-OH of ATP is then accomplished by the key catalytic residue H63 of the AC enzyme, which is further involved in the reaction mechanism of adenylyl cyclization [197].

Besides catalysing the formation of cAMP, the AC domain of CyaA was also shown to catalyse the formation of cCMP and cUMP, and all these multiple cNMP-forming

enzyme activities come from a single catalytic site [198]. Thus, cCMP and cUMP formation may cooperate with cAMP formation in the modulation of the immune responses [199].

1.4.2.2 AC to Hly-linking segment

A ~100 residue-long segment linking the AC enzyme to the Hly moiety is located between residues 400 and 500 of CyaA and has no homologs in other RTX proteins. Although little is known about the structure and function of this segment in the CyaA activity, it was demonstrated that deletion of the residues 375 to 485 within CyaA abrogated the translocation of the catalytic domain into target cells [200]. Another study further identified a peptidic segment within this region (residues 454 to 484) exhibiting membrane interaction properties [201]. These observations suggest a role for the AC to Hly-linking segment of CyaA in translocation of the AC domain across the cell membrane. Moreover, this segment was further proposed to be involved in restricting the propensity of CyaA to form pores in target cell membranes. Masin *et al.* showed that combined substitutions of negatively charged residues clustered within the N-terminal half of the linker segment by neutral residues (D445N + D446N + E448Q) strongly enhanced the specific pore-forming capacity of the toxin without altering its specific capacity to translocate the AC domain across target cell membrane [202]. The AC to Hly-linking segment thus appears to account for the relatively modest cell-permeabilizing capacity of CyaA, as compared to typical hemolysins of the RTX family [202].

1.4.2.3 Pore-forming domain

Formation of cation-selective oligomeric pores within target cell membranes can be attributed to the pore-forming domain of CyaA. This hydrophobic domain comprises residues 500 to 700 and consists of several amphipathic alpha-helical structures [203-205] that form an oligomeric pore of approximately 0.6 to 0.8 nm in diameter [206]. Permeabilization of the target cell membrane for small cations by CyaA [207] can result in colloid-osmotic lysis of erythrocytes, which in turn accounts for the hemolytic halo surrounding *Bordetella* colonies grown on blood agar plates [208]. However, the specific hemolytic activity of CyaA is quite low when compared with other typical RTX pore-forming toxins, like the α-hemolysin of *E. coli* [186,206,209]. This suggests that the main role of the pore-forming domain of CyaA is the support of the AC domain delivery, rather than cell permeabilization *per se*.

The pore-forming activity of CyaA is directly related with the cooperative calcium-dependent folding of the RTX domain [189]. As the concentration of free calcium ions crosses the narrow threshold of 0.7 to 0.8 mM Ca^{2+}, the propensity of CyaA to form pores increases to ~50-fold, while the half-maximal pore-forming activity can be at 2 to 4 mM Ca^{2+} [210]. Moreover, CyaA pores are voltage-dependent and its characteristics may vary regarding the level and orientation of the electrical potential across the membranes [211]. Deletion of ~500 N-terminal amino acid residues was shown to result in a substantial increase of the hemolytic potency of CyaA, suggesting that prevention of translocation of the AC domain or its deletion favours the toxin to acquire a hemolytic conformation

[212]. CyaA cation-selective pores elicits potassium ion efflux from nucleated cells [213,214], contributing to the overall cytotoxicity of the toxin [214,215].

1.4.2.4 Acylated segment

In order to acquire its biological activity, proCyaA requires posttranslational activation by the co-expressed acyltransferase CyaC in the so-called acylated segment [177,216]. In this segment, the ε-amino group of the lysine residue 983 (K983) is acylated by CyaC [157]. Acylation of the K983 was found to be necessary and sufficient for toxin activities on erythrocytes [217]. In addition, a second lysine residue (K860) was found to be acylated when proCyaA is expressed in the presence of CyaC in *E. coli* cells [187]. CyaA toxin variants having either K860 or K983 acylation sites individually ablated by arginine substitutions exhibited significantly reduced toxin activities on erythrocytes that lack the CD11b/CD18 integrin receptor [218,219]. However, use of acylated CyaA variants on either K860 or K983 alone allowed to conclude that independently of its acylation status, K860 plays a structural role in membrane insertion and translocation of the toxin into sheep erythrocytes [217]. Acylation of K860 alone is also sufficient for tight CD11b/CD18 receptor binding on murine macrophage-like cells but the toxin activity was largely impaired. In addition to its requirement for toxin activity, K983 plays a structural role in determining the cation selectivity of CyaA pores and its acylation controls the pore-forming propensity of the toxin [219].

Curiously, the non-acylated proCyaA is still able to form pores in planar lipid bilayers, even though with a lower propensity than the fully acylated toxin. Besides that, the formed pores have the same properties as the pores created by the fully active CyaA. The non-acylated toxin is also able to penetrate membranes of liposomes [220].

1.4.2.5 RTX domain and C-terminal secretion signal

The RTX domain of CyaA consists of the last C-terminal ~700 amino acid residues of the toxin and comprises five distinct RTX blocks (I to V) that harbour the typical glycine and aspartate-rich RTX nonapeptide repeats [188]. These blocks are connected by segments of variable lengths. Models of the RTX domain structure were predicted based on the homology of the solved structures of other T1SS-secreted RTX proteins, such as lipases and proteases of *Pseudomonas aeruginosa* and *Serratia marcescens* [221-223]. According to these models, the first six residues (GGxGxD) of the nonapeptide RTX motif constitute a turn with a bound calcium ion, while the last three residues form a short β-strand. Calcium ions are then periodically coordinated by carboxyl groups of the side chains of conserved aspartic acid residues and protein-backbone carbonyl groups [190]. The X-ray structure of $CyaA_{1529-1681}$ fragment comprising the RTX block V was recently solved (**Figure 7**) [184].

Calcium-driven folding of the RTX domain is required for efficient toxin binding to target cells and different regions of this domain were shown to be important for the activity of the toxin [189]. Deletions in block III or insertion of peptides into a specific

position within the RTX moiety strongly impaired toxin binding and penetration into target cells [188].

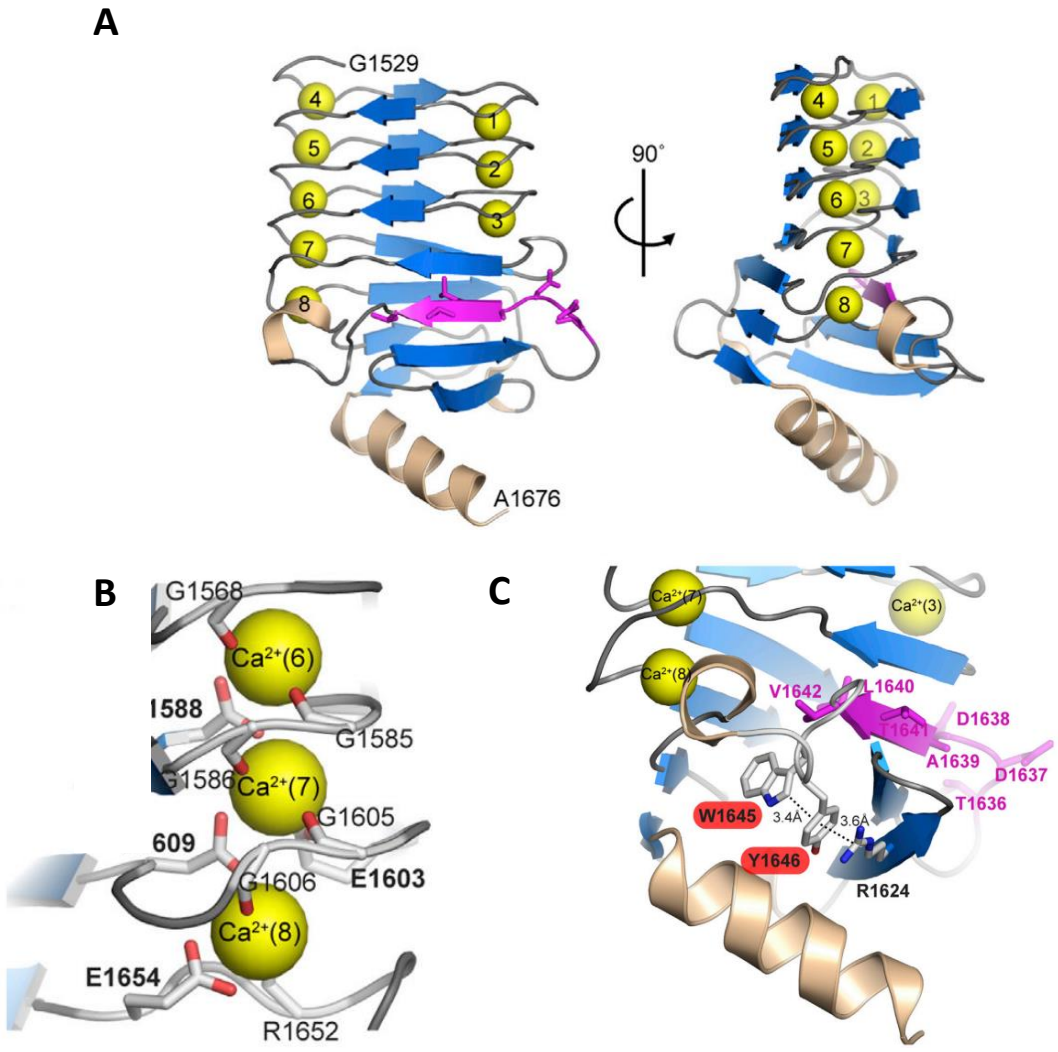

Figure 7. X-ray structure of CyaA$_{1529-1681}$. (A) The N-terminal consecutive nonapeptide tandem repeats (GGxGxDxxx) are arranged in a regular right-handed helix of parallel β-strands (β-roll). The first six residues (GGxGxD) of the RTX motif constitute a turn with bound calcium ion (yellow ball), while the last three non-conserved residues (xxx) form a short β-strand. Calcium ions are numbered for clarity, and the residues 1636–1642 constituting the "Ca^{2+}-induced folding nucleus" are coloured in magenta. **(B)** Close-up view of calcium-binding sites within the C-terminal segment of CyaA$_{1529-1681}$. Ca^{2+}(6) and Ca^{2+}(7) are completely buried within the turns and are regularly coordinated by the side chains of aspartate residues in position 6 (D1588 and D1609) and backbone carbonyl groups of glycine residues of the GGxGx**D**xxx motif, respectively. Ca^{2+}(8) is more exposed to the solvent and is coordinated by side chains of aspartate D1609 and glutamate E1654 along with backbone carbonyls of glycine G1606 and arginine R1652 and two water molecules (data not shown). The carbon and oxygen atoms are represented in grey and red colour, respectively. **(C)** Detailed view of the C-terminal capping structure of the CyaA$_{1529-1681}$ segment. The TDDALTV heptapeptide is highlighted in magenta. The indole ring of tryptophan W1645 is positioned perpendicularly to the benzene ring of tyrosine Y1646, which itself interacts with the positively charged guanidinium group of arginine R1624 in a cation-π-π interaction. Adapted from [184].

The main CD11b/CD18-interaction domain of CyaA was demonstrated to be located within a glycine and aspartate rich region located in blocks II and III of the RTX domain. Indeed, insertion of a FLAG epitope in this region completely abolished the capacity of the toxin to interact with the $CD11b^+$ cells [188]. Furthermore, CyaA interaction with the CD11b/CD18 receptor could be efficiently blocked by antibodies elicited by the immunization of mice with the RTX domain [224]. A stretch of 15 amino acid residues located at the C-terminal part of CyaA appears to be essential for toxin activity and also for CyaA insertion into host cell membrane [184,225,226].

The last 74 amino acid residues of the Hly moiety form the unprocessed secretion signal of CyaA [183]. Driven by the C-terminal segment, CyaA is extruded in an unfolded form from the Ca^{2+}-depleted cytosol of bacteria directly into the Ca^{2+}-rich external milieu, passing through the T1SS duct [176,184]. At the low concentrations of calcium ions within bacterial cytosol, the RTX domain of the toxin remains structurally disordered and highly hydrated, while the millimolar concentrations of free calcium ions in body fluids trigger the folding of this domain [227-232]. Successive calcium binding then promotes formation of a capping structure and scaffolds the Ca^{2+}-driven folding of the consecutively extruded RTX domain, which progresses vectorially from the C-terminus towards the N-terminal end, thus accelerating the translocation of the polypeptide through the T1SS conduit [184].

1.4.3 Interaction of CyaA with target cells

Identification of CyaA receptor on myeloid cells was one of the major breakthroughs for a better understanding of *Bordetella* pathophysiology [233]. The study carried out by Guermonprez and co-workers allowed to demonstrate that CyaA binds to the β_2 integrin CD11b/CD18 on myeloid phagocytic cells [233]. Due to the extremely high specific enzymatic activity of the AC domain of the toxin, CyaA was also found to bind and penetrate a broad range of other eukaryotic cell types from various origins, most likely due to a low affinity binding to glycan moieties of gangliosides and N-linked glycans of surface glycoproteins [234-236]. CyaA interaction with the CD11b subunit of the CD11b/CD18 receptor increases the efficacy of the binding by about two orders of magnitude [162]. The selectivity of the binding to CD11b/CD18 is dictated by a highly specific protein–protein interaction, involving negatively charged glutamate and aspartate residues of the 1166–1287 segment of CyaA and positively charged and hydrophilic residues within the 614–682 segment of the CD11b subunit of CD11b/CD18 [237]. This binding site is unique for CD11b and is not present in the two closest relatives of CD11b, the highly homologous CD11a and CD11c subunits of the β_2 integrins CD11a/CD18 and CD11c/CD18, respectively [162,237]. Moreover, the contacts of the toxin were established not only with the segment between residues 614 to 682 but also with other CD11b segments, as well as with the adjacent glycan chains located in the C-terminal portion of CD11b [237,238]. Thus this type of multivalent interaction may be responsible for specific and high affinity binding of CyaA to its receptor and subsequent penetration of the toxin across cellular membrane and its biological activities [238].

After binding to CD11b/CD18, the toxin either forms oligomeric cation-selective transmembrane pores or translocates its AC domain across the membrane into cell

cytosol, as schematically depicted in **Figure 8** [239]. There the AC enzyme is activated by binding of cytosolic CaM and catalyses an uncontrolled conversion of intracellular ATP into cAMP [191]. Accumulation of this key signalling molecule inside the cells then contributes for deregulation of numerous signalling pathways downstream to protein kinase A (PKA) and Epac (exchange protein directly activated by cAMP) [240]. This subverts cellular physiology and rapidly suppresses bactericidal functions of phagocytes, such as the oxidative burst and opsonophagocytic killing of bacteria by neutrophils and macrophages [163,165,240,241]. In parallel, the hemolysin moiety oligomerizes into cation-selective pores and permeabilizes cells for the efflux of cytosolic potassium ions and possibly also sodium and water influx [207,213,242,243], which can lead consequently to the lysis of cells [206]. Altogether, both cAMP signalling and ATP depletion, as well as the pore-forming activity of the toxin, can synergize in causing apoptosis or necrosis of phagocytes [215,244-246].

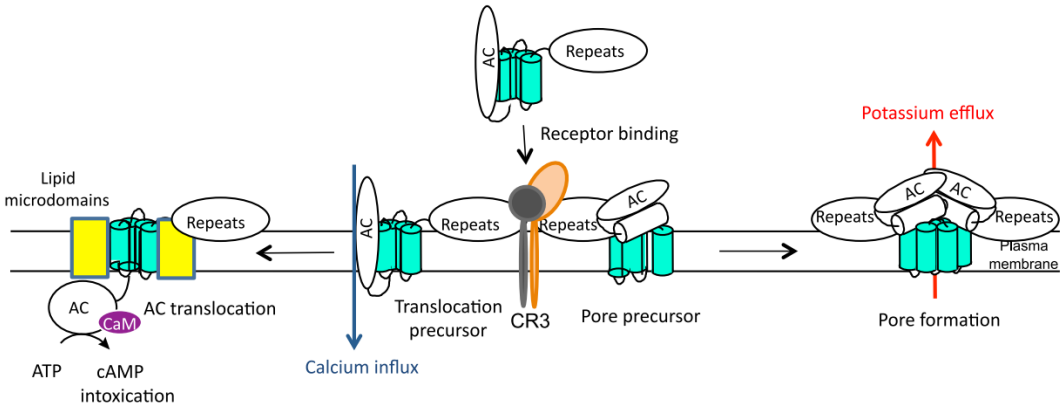

Figure 8. Schematic model of CyaA action on target membrane. This model predicts the insertion of two distinct CyaA conformers into target cell membrane. One would be the translocation precursor that would account for delivery of the AC domain across the lipid bilayer and provokes also a concomitant influx of calcium ions into cells; the other conformer would form a pore precursor that would oligomerize into CyaA pores, provoking potassium efflux from target cells. These two activities would then be to large extent independent and mutually exclusive. Both conformers would operate in parallel and existing in an equilibrium that can be shifted in either direction by alterations of temperature, free calcium concentration, antibody binding, acylation status of CyaA, or by specific residue substitutions within the CyaA molecule Adapted from [239].

The AC domain penetrates the host cell in two sequential steps (**Figure 9**). Insertion of this domain into the cell membrane with the rest of the CyaA molecule permeabilizes cells for the influx of Ca^{2+} ions, which then triggers the mobilization of the CyaA-integrin complex into lipid rafts via activation of calpain and cleavage of talin that tethers CD11b/CD18 to the actin cytoskeleton [247]. AC translocation across the lipid bilayer appears to be controlled by the membrane potential [248] and by the transmembrane α-helices localized in the hydrophobic pore-forming domain of CyaA [203,205]. In addition, this process is independent on membrane permeabilization by CyaA pores [214], exhibiting a very short half-time of several dozens of seconds [249].

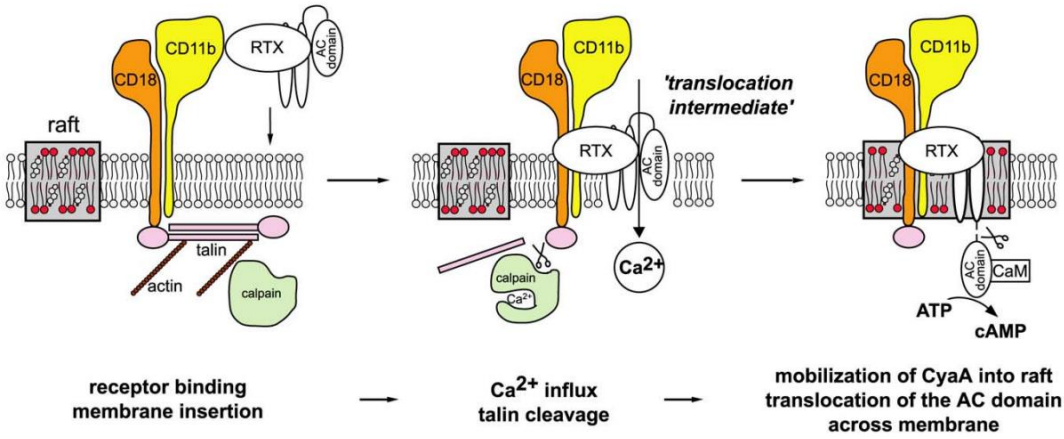

Figure 9. Model of CyaA translocation across target cell membrane. Firstly, CyaA binds the CD11b/CD18 integrin receptor dispersed in the bulk of the membrane phase outside of lipid rafts, having the cytoplasmic tail of the CD18 subunit tethered to actin cytoskeleton via the linker protein talin. Upon receptor engagement, the AC domain partially inserts into cell membrane and participates in formation of a Ca^{2+}-conducting path across cell membrane. Influx of external Ca^{2+} into cells induces activation of the Ca^{2+}- dependent protease calpain, yielding talin cleavage and liberation of the CyaA-CD11b/CD18 complex from binding to actin cytoskeleton. Consequently, the complex is recruited into cholesterol-enriched lipid rafts, where the specific lipid organization and composition allows completion of AC domain penetration across the target cell membrane. Adapted from [247].

Binding and penetration of CD11b/CD18-expressing cells by CyaA strongly depends on the toxin loading by calcium ions and on the acylation of the K860 and K983 residues, with the acylation of K983 being necessary and sufficient in supporting toxin action [157,219]. Non-acylated proCyaA exhibits a decreased capacity to bind the integrin and the interaction of proCyaA with CD11b/CD18 poorly supports the penetration of the AC domain into target cells [160]. It has recently been shown that swapping of the acylated segment and the RTX domain of HlyA into the CyaA toxin molecule retargets the AC toxin from the CD11b/CD18 β_2 integrin for binding to one of the HlyA receptors, the CD11a/CD18 β_2 integrin. These results helped to delimit residues 400–710 of CyaA as an "AC translocon" sufficient for translocation of the AC polypeptide across the plasma membrane of target cells [250].

1.4.4 Calcium-binding sites of CyaA

In a previous work, Rose *et al*. have analysed the calcium interacting properties of CyaA, suggesting that the toxin harbours two classes of calcium-binding sites [189]. The first class consists of a small number of high affinity calcium-binding sites (K_D <1 nM), whereas the second class consists of about 45 calcium-binding sites of low affinity (K_D >0.3 mM). Calcium binding to the low affinity sites may be involved in the delivery of the AC domain into target cells, while calcium binding to the high affinity sites appears to be critical for the membrane binding and the pore-forming activity of the toxin [189]. However, the localization of these high affinity sites in the CyaA molecule is not known, but they appear to be not located in the last 700 residues of the RTX portion of the toxin

[189], where the ~45 low-affinity calcium-binding sites are formed. A primary sequence analysis of the C-terminal part of the acylated segment of CyaA revealed that it contains two blocks of amino acid residues ^{912}I**GG**D**G**D**D**V^{919} and ^{930}D**GG**A**G**T**N**T^{937} with a similar pattern as can be observed in the highly conserved calcium-binding sites of the C-terminal RTX domain, exhibiting a consensus sequence GGxGxD (**Figure 10**). Similar blocks of amino acid residues were also predicted in the acylation segment of other RTX toxins (**Figure 10**).

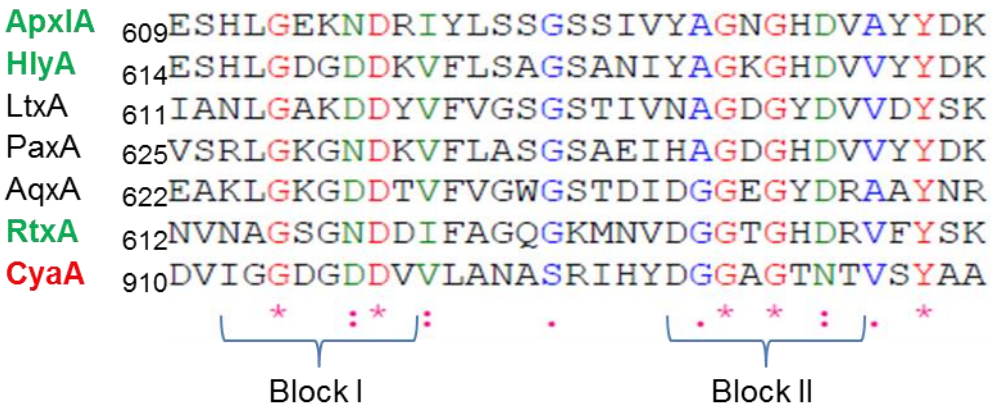

Figure 10. ClustalW sequence alignment of a partial sequence of the acylated domain of CyaA and corresponding sequences of related RTX toxins. ApxIA, *Actinobacillus pleuropneumoniae*; HlyA, *Escherichia coli*; LtxA, *Aggregatibacter actinomycetemcomitans*; PaxA, *Pasteurella aerogenes*; AqxA, *Actinobacillus equuli*; RtxA, *Kingella kingae*; and CyaA, *Bordetella pertussis*. * identity, : strongly similar, . weakly similar amino acid residues.

Furthermore, a secondary structure prediction analysis of the segment by the SOPMA algorithm [251] indicated mainly presence of β-structures in the C-terminal part of the acylated region of CyaA (**Figure 11**).

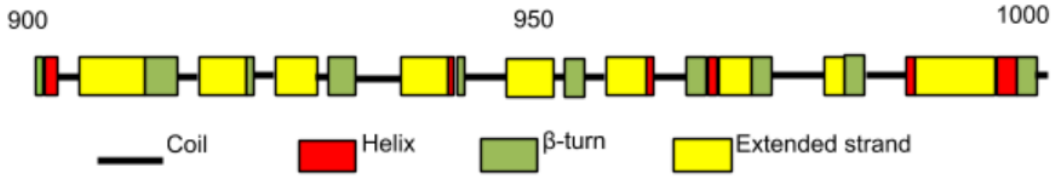

Figure 11. Schematic representation of secondary structures in the C-terminal part of the acylated segment of CyaA. Prediction was performed between residues 900 and 1000 of CyaA using the SOPMA software.

Altogether, the data obtained by Rose *et al*. suggests that (i) CyaA binds few calcium ions that cannot be removed by the chelating agents EDTA or EGTA without denaturation and (ii) these bound ions are necessary and sufficient for the membrane-binding and hemolytic activities of the toxin, but insufficient for its cytotoxic activity [189]. Thus, it opens doors to further investigate the exact location of these few high affinity sites within the CyaA molecule that would play a key role in CyaA membrane binding and hemolytic activities, as well as to provide some insights into the structural layout of this region of the toxin. The following section will describe a proposed approach for the experimental-based procedures that might help to solve this structural/functional puzzle.

2. OBJECTIVES

The main goal of this project is the investigation of two predicted calcium-binding sites located in the acylated segment of CyaA of *B. pertussis*. Using site-directed mutagenesis, we will test the hypothesis that the two blocks of amino acid residues located in the C-terminal part of the acylated segment of CyaA might form the high-affinity calcium-binding sites that could play a key role in CyaA membrane binding (membrane insertion) and pore-forming (hemolytic) activities. Circular dichroism (CD) spectroscopy will be used to test whether binding of calcium ions to the acylated segment of CyaA (residues 908-1008) results in formation of secondary structures in the polypeptide. Furthermore, the acylation status of the acylated segment of CyaA will be analysed by liquid chromatography-mass spectrometry (LC-MS).

In order to achieve this goal, the following specific aims were established:

1- Construction, isolation and purification of CyaA variants carrying substitutions in the predicted calcium-binding sites and their characterization by functional biochemical and biophysical assays;
2- Construction, isolation and purification of $CyaA_{908-1008}$ variants and their analyses by CD spectroscopy and LC-MS.

This study might represent a step forward for understanding *B. pertussis* fundamental biological mechanism of action, which can be useful for the development of more effective pertussis vaccines, namely that could help interrupt the vicious cycle of colonization and transmission of the bacterium, something that the current aP vaccines fail to achieve**.**

3. MATERIAL AND METHODS

3.1 Bacterial strains, growth conditions and plasmids

The *Escherichia coli* K12 strain XL1-Blue (Stratagene, La Jolla, CA; *recA1 endA1 gyrA96 thi-1 hsdR17 supE44 relA1 lac* [F´*proAB lac1*^{q}ZΔ*M15* Tn*10*(Tet^{r})]) was used throughout this work for DNA cloning. The *E. coli* BL21/pMM100 strain (*E. coli* B F^{-} *dcm ompT hsdS* (r_B^- m_B^-) *gal* [*malB*$^{+}$]$_{K\text{-}12}$(λ^S)) transformed by the plasmid pMM100 [252], which carries the gene for tetracycline resistance and a gene encoding LacI^{q}. It was used for expression of recombinant proteins.

Bacteria were grown at 37 °C in Luria-Bertani (LB) medium (DNA manipulation) or in MDO medium (protein expression; yeast extract, 20 g/l; glycerol, 20 g/l; KH_2PO_4, 1 g/l; K_2HPO_4, 3 g/l; NH_4Cl, 2 g/l; Na_2SO_4, 0.5 g/l; thiamine hydrochloride, 0.01 g/l) supplemented with appropriate antibiotic(s).

pT7CACT1 (**Figure 12,** Osicka *et al*., 2000) is a construct for co-expression of *cyaC* and *cyaA*, and it allows production of recombinant CyaC-activated CyaA in *E. coli* under control of the isopropyl-β-D-thiogalactopyranoside inducible lacZ promoter. This plasmid carries gene for ampicillin resistance. It was used for production of CyaA and construction of pT7CACT1-derived plasmids for production of CyaA mutant variants.

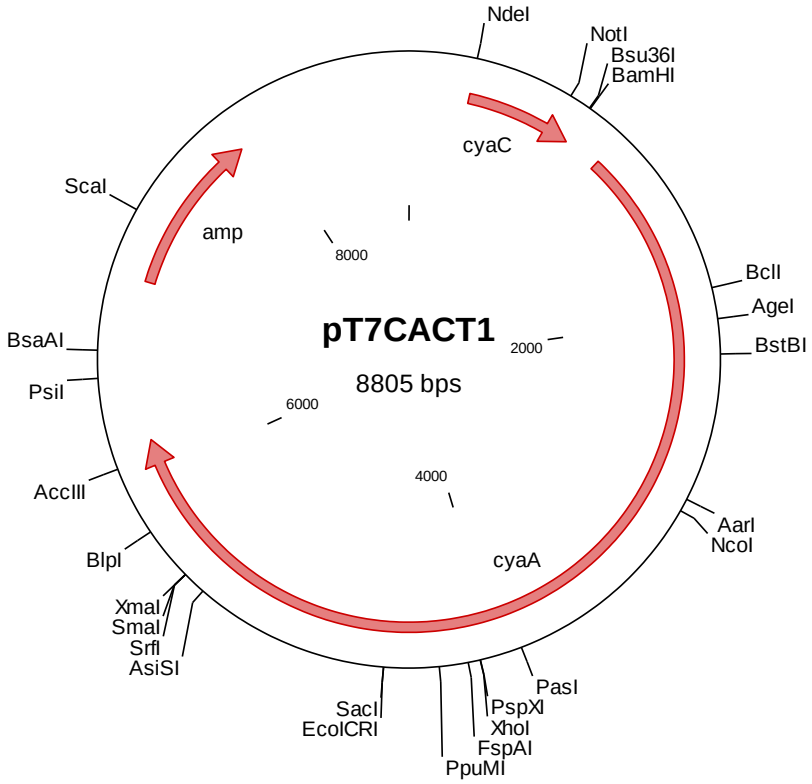

Figure 12. A map of pT7CACT1 plasmid.

3.2 Human cell line

Monocytic THP-1 cells (ATCC TIB-202) were obtained from the American Type Culture Collection (ATCC, Manassas, VA) and cultured in RPMI 1640 (Sigma-Aldrich, St. Louis, MO) supplemented with 10% fetal calf serum (FCS) (GIBCO Invitrogen, Grand Island, NY) and antibiotic antimycotic solution (0.1 mg/ml streptomycin, 1000 U/ml penicillin and 0.25 mg/ml amphotericin; Sigma-Aldrich, St. Louis, MO).

Prior to the activity experiments, the phosphate-buffered RPMI medium was replaced with HEPES-buffered D-MEM (Sigma-Aldrich, St. Louis, MO) supplemented with 10% FCS, since phosphate chelates the calcium ions required for the activity of the toxin. The D-MEM medium contains 1.9 mM Ca^{2+}, which corresponds approximately to the concentration of calcium ions in the body fluids and is the optimal concentration for the action of the toxin. The human monocytes were then allowed to rest and adapt to the D-MEM for 2 hours at 37 °C in a humidified 5% CO_2 atmosphere prior to use.

3.3 Preparation of E. coli supercompetent cells

Bacterial strains XL-1 Blue or BL21/pMM100 (section 3.1) were grown overnight at 37 ºC on LB-agar plates supplemented with appropriate antibiotics. A 5-10 ml amount of the overnight culture was inoculated into 500 ml of super optimal broth medium (2% Bacto Tryptone, 0.5% Yeast Extract, 10 mM NaCl and 2.5 mM KCl) with added $MgSO_4$ and $MgCl_2$ (10 mM both) and cultivated at 30 °C until $OD_{600} \approx 0.6$ was reached. Fully grown culture was consequently cooled on ice and centrifuged (3,000 g, 4 ºC, 10 minutes). The pellet was resuspended in 20 ml of ice-cold transformation buffer (10 mM HEPES, 15 mM $CaCl_2$, 250 mM KCl and 50 mM $MnCl_2$ (pH 6.7)). The cell suspension was incubated on ice for 10 minutes, repeatedly centrifuged (3,000 g, 4 ºC, 10 minutes), and re-suspended in 4 ml of ice-cold transformation buffer. Dimethyl sulfoxide in final concentration 7% (v/v) was added to the cell suspension and after incubation on ice for additional 10 minutes aliquots of 200 µl were quickly frozen in liquid nitrogen and stored at -70 ºC.

3.4 Heat-shock transformation of competent cells by plasmid DNA

For transformation of cells by plasmid DNA, 1 µl of plasmid DNA solution (DNA concentration 100 – 500 ng/µl) was added to 30 µl of competent cells suspension. For transformation of cells by plasmid DNA obtained by ligation, 15 µl of ligation mixture was added to 150 µl of competent cells suspension. The cell suspensions were incubated on ice for 10 minutes, followed by heat-shock at 37 ºC for 5 minutes and quickly chilled on ice for additional 5 minutes. Preheated liquid LB medium without antibiotics (1 ml) was then added to mixture, which was subsequently incubated for 1 hour at 37 ºC, so the gene for resistance to ampicillin carried by transformed plasmid DNA could be expressed. Cells were then incubated overnight on LB agar plates supplemented with appropriate antibiotic(s) at 37 ºC.

3.5 Minipreparation of plasmid DNA

LB medium (2 ml) with ampicillin (150 µg/ml) was inoculated with a single bacterial colony and cultivated at 37 ºC for 14 hours under vigorous shaking. The bacterial culture was centrifuged (13,000 g, 20 ºC, 1 minute). The resulting pellet was resuspended in 100 µl of Solution I (50 mM glucose, 10 mM EDTA, 25 mM Tris-HCl (pH 8.0)) and incubated for 5 minutes at room temperature (RT). Cells were then lysed by adding 200 µl of Solution II (0.2 M NaOH, 1% SDS), the mixture was gently mixed by inversion and stored for 5 minutes on ice. After that, 150 µl of Solution III (pH 4.8, prepared as mixture of 60 ml of 5 M potassium acetate with 11.5 ml of glacial acetic acid and 28.5 ml H_2O) was added, the mixture was mixed by finger flicking and stored for another 5 minutes on ice. Precipitated proteins, chromosomal DNA and other cellular components were removed by centrifugation (13,000 g, 4 ºC, 15 minutes) and the supernatant (400 µl) with the plasmid DNA was carefully transferred into a fresh tube. An equal volume of isopropanol was added and the mixture was vortexed and stored for 5 to 10 minutes on ice to allow precipitation of plasmid DNA, which was further separated by centrifugation (13,000 g, 4 ºC, 15 minutes). The pellet of precipitated plasmid DNA was washed with 1 ml of 70% ethanol and dried in vacuum desiccator. After drying, the DNA pellet was resuspended in 40 µl of TE buffer with pancreatic RNAase (20 µg/ml) and incubated for 30 minutes at 70 ºC in water bath. The isolated DNA was stored at -20 ºC.

3.6 Manipulation with plasmid DNA

3.6.1 Construction of cyaA mutants

The pT7CACT1 plasmid was used for site-directed mutagenesis of the *cyaA* gene and subsequent production of recombinant CyaA proteins by *E. coli* bacteria. The gene *cyaA* of the pT7CACT1 plasmid was modified by single and multiple substitutions within the sequence encoding both block I and II of amino acid residues, located in the acylated segment of CyaA. To design these substitutions the software Clone Manager Professional Suite version 8 (Sci Ed Software, Westminster, CO) was used.

3.6.2 Site-directed PCR mutagenesis of cyaA

All substitutions were introduced into the *cyaA* gene by site-directed PCR mutagenesis using the proof-reading Q5 polymerase and pairs of suitable PCR primers (**Table 1**, Generi Biotech, Hradec Kralove, Czech Republic). In a first step, two complementary mutagenic primers were used to introduce the mutation into two partially overlapping PCR products (**Table 2**), which were then purified and used as a template in a second PCR amplification (**Table 3**) with another pair of primers to assemble the whole mutagenized fragment. Systematically, silent single base substitutions creating new restriction sites were introduced into the PCR primers to allow straightforward screening of the mutants. The final PCR products, fragments carrying the desired mutations, were recloned into the parental *cyaA* gene in the pT7CACT1 plasmid.

Table 1. Primers used for site-directed PCR mutagenesis of *cyaA*

Name	***Sequence***	***Number of bases***	***Tm (°C)****
Mutated primers			
G914Lfor	GATGTGATAGGCCTAGATGGCGATGACGTCGTG	33	60
G914Lrev	GCCATCTAGGCCTATCACATCCAGTTTGATGCTG	34	62
D915Lfor	GTGATCGGCGGCCTAGGCGATGACGTCGTGCTTG	34	62
D915Lrev	GCCTAGGCCGCCGATCACATCCAGTTTG	28	62
D917Lfor	GGCCTTGACGTCGTGCTAGCCAATGCTTCGCGCATCC	37	62
D917Lrev	CTAGCACGACGTCAAGGCCATCTCCGCCGATCAC	34	60
D918Lfor	AGCTTGATGTGATCGGCGGAGATGGCGATCTCGTCGTGCTTGCCAATGC	49	58
D918Lrev	CGAGATCGCCATCTCCGCCGATCACATCAAGCTTGATGCTGTGCTTGAGCAC	52	60
D915L+D917L++D918Lfor	GGCCTAGGCCTTCTCGTCGTGCTTGCCAATGC	32	58
D915L+D917L++D918Lrev	GACGAGAAGGCCTAGGCCGCCGATCACATCCAGT	34	58
D930Lfor	CATTATCTCGGCGGCGCGGGTACCAACACGGTCAGCTATG	40	58
D930Lrev	GTACCCGCGCCGCCGAGATAATGGATGCGCGAAGCATTG	39	64
G931Lfor	GACCTCGGCGCGGGTACCAACACGGTCAGCTATGC	35	60
G931Lrev	GGTACCCGCGCCGAGGTCATAATGGATGCGCGAA	34	58
G932Lfor	GACGGGCTAGCGGGCACCAACACGGTC	27	62
G932Lrev	GTGCCCGCTAGCCCGTCATAATGGATGCGCG	31	60
G934Lfor	GGCGGAGCGCTCACCAACACGGTCAGCTATG	31	62
G934Lrev	GTTGGTGAGCGCTCCGCCGTCATAATGGATGC	32	60
N936Lfor	CGCGGGTACCCTCACGGTCAGCTATGCCGC	30	60
N936Lrev	CCGTGAGGGTACCCGCGCCGCCGTCATAATG	31	68
D930L+N936Lfor	TCTCGGCGGCGCGGGCACGTTAACGGTCAGCTATGCCGCC	40	60
D930L+N936Lrev	TTAACGTGCCCGCGCCGCCGAGATAATGGATGCGCGAAGCATTG	44	64
G931L+G932L++G934Lfor	TATGACCTCCTAGCGCTCACCAACACGGTCAGCTATG	37	62
G931L+G932L++G934Lrev	GGTGAGCGCTAGGAGGTCATAATGGATGCGCGAAG	35	60

Flanking primers			
1791-SeqFor-CyaA	CAGCGGCTTGCAGGTGGC	18	62
XhoIRev2	CACATGCTCGAGCGTGTC	18	58

**Theoretical melting temperature*

Table 2. Components of PCR 1

Fragment	**1A**	**1B**
0.5 µl template	**pT7CACT1**	
10 µl 5xQ5 Buffer HF		
10 µl GC Enhancer		
21 µl water		
5 µl 2mM dNTP		
1.5 µl 10 µM FOR primer	1791-SeqFor-CyaA	Forward primer with the mutation
1.5 µl 10 µM REV primer	Reverse primer with the mutation	XhoIRev2
0.5 µl Q5 DNA Polymer. HF		

Cycles of PCR 1:

1. 98 °C 30″
2. 98 °C 10″
3. 54 °C 30″
4. 72 °C 45″
5. 30× repetition of cycles 2-4
6. 72 °C 10′
7. 4 °C keeping

Table 3. Components of PCR 2

5 µl template	**1A**
5 µl template	**1B**
10 µl 5xQ5 Buffer HF	
10 µl GC Enhancer	
11 µl water	
5 µl 2mM dNTP	
1.5 µl 10 µM FOR primer	1791-SeqFor-CyaA
1.5 µl 10 µM REV primer	XhoIRev2
1 µl Q5 DNA Polymerase HF	

Cycles of PCR 2:

1. 98 °C 30″
2. 98 °C 10″
3. 52 °C 30″
4. 72 °C 45″
5. 30× repetition of cycles 2-4
6. 72 °C 10′
7. 4 °C keeping

3.6.3 DNA digestion and plasmid dephosphorylation

The isolated and purified DNA fragments obtained after the second PCR reaction and the pT7CACT1 plasmid were digested in different tubes by the same pair of restriction enzymes (NcoI and XhoI). Each tube consisted of a mixture of 1 µl of each enzyme, 4 µl of CutSmart buffer and 10 or 20 µl of the plasmid DNA or PCR fragment, respectively. Water was added to each tube in order to achieve a final volume of 40 µl. The digestion process was allowed to occur between 1-2 hours at 37 ºC. Dephosphorylation was then accomplished by adding 1 µl of a heat-labile recombinant version of calf intestinal alkaline phosphatase (Quick CIP), only to the plasmid DNA for 5 minutes at 37 ºC, in order to avoid re-circularization of the vector during ligation. To confirm the correct

digestion of the samples, electrophoresis on agarose gel was performed and the digested samples were isolated from the gel (described below).

3.6.4 DNA Ligation

Insertion of the purified PCR fragments into the pT7CACT1 plasmid was accomplished using NEB's Quick ligation kit (for cohesive ends). The ligation mixture (a final volume of 30 µl) consisted of the following components:

- 15 µl of Quick ligation Buffer;
- 2 µl of digested and dephosphorylated plasmid DNA;
- 8 µl digested PCR fragment DNA;
- 3.5 µl of H_2O;
- 1.5 µl Quick Ligase.

The mixture was kept at RT for 5 minutes, then shifted to ice for another 5 minutes. To confirm the efficacy of the process a negative control was used, where the fragment DNA was replaced by 8 µl of water.

3.6.5 Electrophoresis in agarose gel

The agarose gel for electrophoresis was prepared by mixing agarose in TBE buffer (90 mM Tris-borate, 2 mM EDTA, pH 8.3) to a final concentration of 0.6 - 2% (w/v) with the addition of ethidium bromide to a final concentration of 0.5 µg/ml. The DNA sample (maximum used volume was 20 µl) was mixed with 5 µl of 5x concentrated DNA loading dye (0.25% (w/v) bromophenol blue, 40% (v/v) glycerol) and applied to the wells on the gel. λ DNA digested by the restriction endonuclease PstI was used as a standard size ladder. Electrophoresis was run at a constant voltage of 100V for 40 minutes in TBE buffer and the DNA bands with intercalated ethidium bromide were visualized afterwards using UV transilluminator.

3.6.6 Isolation of PCR fragments from agarose gel

Desired DNA fragments were excised from agarose gel and isolated using New England BioLabs' (NEB) Monarch DNA Gel Extraction Kit according to manufacturer´s instructions.

3.6.7 Restriction analysis

For verification of restoration of the cloning sites and introduction of the desired mutations, minipreps of pT7CACT1-derived plasmids carrying mutations within the *cyaA* gene were digested by two pairs of suitable restriction enzymes (**Table 4**). NcoI and XhoI were used in all cases to verify the restoration of the cloning sites. To confirm the substitution in the different mutants, an enzyme carrying both the desired mutation and an additional silent mutation (resorting to the online tool WatCut, University of Waterloo)

was first selected. The second enzyme (AgeI) was chosen so that the size of the DNA fragments obtained after cutting the plasmid with these pair of enzymes would allow good separation and visualization on the agarose gel. The digestion occurred for 1 hour in the water bath at 37 ºC and the reaction mixture consisted of the following components:

- 5 µl of plasmid miniprep;
- 2 µl of CutSmart buffer,
- 12 µl of water;
- 0.5 µl of restriction enzyme I;
- 0.5 µl of restriction enzyme II.

Finally, all *in vitro* mutagenized DNA fragments subcloned into the pT7CACT1 plasmid and verified by the restriction analysis were entirely sequenced (Eurofins Genomics, Ebersberg, Germany) to confirm the presence of the desired substitutions and the absence of inappropriate additional mutations.

Table 4. Enzymes used for verification of pT7CACT1 variants by restriction analyses

Substitutions	Plasmid	Digestion (to verify restoration of cloning sites)*	Digestion (to verify the substitution)*
None	pT7CACT1 (original plasmid)	NcoI, XhoI (1160,7645)	_____
G914L	pT7CACT1-G914L	NcoI, XhoI (1160,7645)	AgeI, StuI (1783,7022)
D915L	pT7CACT1-D915L	NcoI, XhoI (1160,7645)	AgeI, BlnI (1787,7018)
D917L	pT7CACT1-D917L	NcoI, XhoI (1160,7645)	AgeI, NheI (1805,7000)
D918L	pT7CACT1-D918L	NcoI, XhoI (1160,7645)	AgeI, HindIII (1767,7038)
D915L+D917L+D918L	pTCACT1-D915L+D917L+D918L	NcoI, XhoI (1160,7645)	AgeI, BlnI (1787, 7018)
D930L	pT7CACT1-D930L	NcoI, XhoI (1160,7645)	AgeI, KpnI (1849,6956)
G931L	pT7CACT1-G931L	NcoI, XhoI (1160,7645)	AgeI, KpnI (1849,6956)
G932L	pT7CACT1-G932L	NcoI, XhoI (1160,7645)	AgeI, NheI (1838,6967)
G934L	pT7CACT1-G934L	NcoI, XhoI (1160,7645)	AgeI, Eco47III (1843,6962)
N936L	pT7CACT1-N936L	NcoI, XhoI (1160,7645)	AgeI, KpnI (1849,6956)
D930L+N936L	pT7CACT1-D930L+N936L	NcoI, XhoI (1160,7645)	AgeI,HpaI (1852,6953)
G931L+G932L+G934L	pT7CACT1-G931L+G932L+G934L	NcoI, XhoI (1160,7645)	AgeI, Eco47III (1843,6962)

*The expected sizes of digested fragments in base pairs are indicated in parentheses.

3.6.8 Production and purification of CyaA and its mutant variants

50 ml of MDO medium supplemented with ampicillin and tetracycline (final concentration of 150 µg/ml and 12.5 µg/ml, respectively) were inoculated with 3 to 5 *E. coli* BL21/pMM100 colonies carrying an appropriate plasmid. Bacteria were cultivated overnight (~15 hours) at 37 ºC. In the next day, 500 ml of pre-warmed (37 ºC) MDO medium supplemented with ampicillin (150 µg/ml) were inoculated with 10 ml of grown bacterial culture and the cultivation of bacteria followed until exponential phase was reached (OD_{600} = ~0.8). The 500 ml cultures were then supplemented with 1 mM isopropyl-1-thio-β-D-galactopyranoside (IPTG) and cultivated under constant shaking at 37 ºC, so that the gene for the toxin could be expressed. After 4 hours, the cultivation was stopped by a sudden cooling at 4 ºC and 1 ml of bacterial culture was collected from each flask to assess the amount of produced toxin by SDS-PAGE analysis. These 1 ml samples were centrifuged (13,000 g, RT, 1 minute) and the pellet resuspended in 50 mM Tris-HCl (pH 8.0), 8 M urea, 2 mM EDTA. The big bacterial cultures were then centrifuged (3,800 g, 4 ºC, 20 minutes), the pellet was resuspended in 50 mM Tris-HCl (pH 8.0), centrifuged again (5,000 g, 4 ºC, 10 minutes) and stored at -20 ºC.

On the following day, 32 ml of 50 mM Tris-HCl (pH 8.0) buffer was added to the frozen pellets. Bacterial walls were disrupted on ice by ultrasound with a large probe for 4 minutes (30 seconds pulse-ON, 1 minute pulse-OFF, 55W), then the cells were centrifuged (18,000 g, 4 ºC, 30 minutes) and supernatants were discarded. Cell membranes were mechanically removed by washing with 50 mM Tris-HCl, 4 M urea (pH 8.0) buffer. The toxin, which was present in inclusion bodies of bacteria, was dissolved in 4.8 g of solid urea with 6 ml of 50 mM Tris-HCl (pH 8.0) and centrifuged (18,000 g, 4 ºC, 30 minutes). Finally, 20 µl samples were collected for further SDS-PAGE analysis and resulting supernatants were stored at -20 ºC.

To the prepared urea extract of CyaA (or its mutant variant), NaCl was added to a final concentration of 50 mM. The sample was then loaded onto a diethyl-aminoethyl-Sepharose (DEAE-Sepharose) ion-exchange chromatography column previously washed with deionized water and equilibrated with solution A (50 mM Tris-HCl (pH 8.0), 8 M urea, 120 mM NaCl). The toxin was captured and most of the other proteins were removed with solution A. After removal of unbound proteins, the toxin was eluted with solution B (50 mM Tris-HCl (pH 8.0), 8 M urea, 200 mM NaCl) in 1-ml fractions. The presence of the toxin in eluted fractions was tested using Bradford method and the fractions with the toxin were collected into a sterile Falcon tube.

The collected toxin fractions were 4 times diluted with 50 mM Tris-HCl (pH 8.0), 1 M NaCl and further purified on a Phenyl-Sepharose column, which was similarly washed with deionized water and equilibrated with 50 mM Tris-HCl (pH 8.0), 1 M NaCl. The toxin was captured and most of the other proteins were removed by the equilibration solution. The toxin was then eluted with 50 mM Tris-HCl (pH 8.0), 8 M urea, 2 mM EDTA in 1-ml fractions and Bradford test was used for determination of presence of the toxin in the eluted fractions and those fractions which contained enough of the toxin were mixed together and stored at -20 ºC until use. The toxin concentration was determined by the Bradford assay (Bio-Rad, Hercules, CA) using bovine serum albumin as a standard and the purity of the toxin was analysed on SDS-PAGE gel.

3.6.9 SDS-electrophoresis in polyacrylamide gel (SDS-PAGE)

For proper separation and visualization of CyaA and CyaA-derived proteins, 5% stacking and 7.5% resolving polyacrylamide gels were prepared. Briefly, 20 µl of the collected samples were mixed with 5 µl of SDS sample buffer (5x concentrated; 0.25 M Tris-HCl (pH 6.8), 0.5 M DTT, 10% (w/v) SDS, 50% (v/v) glycerol, 0.5% (w/v) bromophenol blue) and subsequently heated up to 100 ºC for 2 minutes before loading into wells in the polyacrylamide gels, which were submersed in Tris-glycin buffer (25 mM Tris, 250 mM glycine (pH 8.3), 0.1 (w/v) SDS). The analysed proteins were separated according to their size in an electric field (30 mA per gel). After ~1 hour, the buffer was discarded and the gels were put out and stained with staining solution (45% (v/v) methanol, 10% (v/v) acetic acid, 0.25% (w/v) Coomassie Brilliant Blue R-250) for 1 hour (RT, gentle shaking). Then the gels were destained with destaining solution (25% (v/v) methanol, 10% (v/v) acetic acid) for 1 hour (RT, gentle shaking), washed and dried in cellophane foil. Unstained protein ladder (PageRuler^{TM}, Fermentas, Waltham, MA) was used for assessment of relative molecular weights of proteins.

3.7 Functional characterization of purified CyaA variants

3.7.1 Hemolytic activity of CyaA variants on sheep erythrocytes

To prepare sheep erythrocytes, 30 ml of TN buffer (20 mM Tris-HCl, 150 mM NaCl, pH 8.0) cooled to 4 °C were added to 3 ml of sheep blood (LabMediaServis, Jaromer, Czech Republic) and the sample was centrifuged (2,000 g, 4 °C, 15 minutes). The pelleted cells were resuspended in 30 ml of TN buffer and centrifuged (2,000 g, 4 °C, 15 minutes). This step was repeated twice. The cells were then resuspended in 30 ml of TN buffer and adjusted to 5×10^8 cells per ml of suspension. Finally, $CaCl_2$ solution was added to erythrocyte suspension to a final concentration of 2 mM.

CyaA proteins were then incubated with erythrocytes at 37 ºC (final concentration of the toxins was 10 µg/ml). The negative control, which represents the basal lysis, consisted only of erythrocytes and TUC buffer (50 mM Tris-HCl (pH 8.0), 8 M urea and 2 mM $CaCl_2$). Hemolytic activity was measured by photometric (A_{541}) determination of the amount of hemoglobin released every hour (during 4 hours) to determine the percent of erythrocyte lysis in the presence of the individual toxins.

3.7.2 Binding and cell-invasive activities of CyaA variants on sheep erythrocytes

Sheep erythrocytes, prepared as described above were incubated with CyaA and CyaA-derived proteins at 37 ºC (final concentration of the toxins was 1 µg/ml). After 30 minutes, cell suspensions were washed with TNC buffer (50 mM Tris-HCl (pH 7.4), 150 mM NaCl, 2 mM $CaCl_2$) to remove unbound CyaA and divided into two aliquots. One aliquot was directly used for the measurement of cell-bound AC enzyme activity (membrane binding capacity). The other aliquot was treated with trypsin (final concentration of 20 µg/ml) for 15 minutes at 37 ºC in order to inactivate the extracellular AC domain that did not translocate across the cell membrane. Soybean trypsin inhibitor (final concentration of 40 µg/ml) was then added to the mixture to stop the reaction before the samples were

washed with TNE buffer (20 mM Tris-HCl (pH 7.4), 150 mM NaCl and 5 mM EDTA). Both the tubes for analysing the AC binding and invasive capacity were then incubated with radioactive mixture (60 mM Tris-HCl (pH 8.0), 7 mM $MgCl_2$, 0.1 mM $CaCl_2$, 0.1% (v/v) Triton X-100, 1 mg/ml BSA, 1 µM calmodulin, 0.1 mM cAMP, ~200 CPM/µl of (2,8-^{3}H)cAMP, 2 mM ATP, ~10,000-20,000 CPM/µl of (α-^{32}P)ATP) at 30 ºC. After 10 minutes, the reaction was stopped by addition of 0.5 M HCl. The samples were then denatured at 100 ºC and neutralized after 5 minutes with 1.5 M unbuffered imidazole. Thereafter, the samples were loaded onto aluminium oxide columns and the cAMP that had previously formed was eluted by 10 mM imidazole (pH 7.6). After elution, the columns were removed and, to each tube, a scintillation cocktail was added for further radioactivity measurement on the liquid scintillation counter Hidex 600 SL (Hidex, Turku, Finland).

3.7.3 Binding of CyaA variants and cAMP elevation in THP-1 monocytes

Cells (1×10^6) were incubated in D-MEM with CyaA or CyaA-derived proteins (1 µg/ml) for 30 min at 4 °C, prior to removal of unbound toxin by three washes in D-MEM. After the transfer to a fresh tube, the cells were lyzed with 0.1% Triton X-100 for determination of cell bound AC enzyme activity. Activity of CyaA was taken as 100%.

For determination of the elevation of intracellular cAMP, 1.5×10^5 THP-1 monocytes were incubated with different toxin dilutions for 30 minutes at 37 ºC in D-MEM medium and the reaction was stopped by addition of 0.2% (v/v) Tween 20 in 50 mM HCl, followed by boiling of the samples for 15 minutes at 100 ºC to denature cellular proteins (cAMP is acid- and heat-resistant) and subsequent neutralization with 150 mM unbuffered imidazole. cAMP measurements were done by an ELISA assay. Briefly, ELISA plates were coated with a cAMP-BSA conjugate, washed 3 times with TBS-Tween (50 mM Tris-HCl (pH 8.0), 0.15 mM NaCl, 0.1% (v/v) Tween 20) and incubated for 2 hours with 2% (w/v) BSA in TBS-Tween (TBS-BSA) for prevention of nonspecific protein-binding sites. After repeated washing with TBS-Tween, boiled samples were then added to the plate wells coated with cAMP-BSA conjugates, followed by diluted rabbit anti-cAMP antibodies (1:3,000 dilution in 2% TBS-BSA). Upon overnight incubation at 4 ºC, the plates were extensively washed with TBS-Tween, and anti-rabbit antibodies conjugated with horseradish peroxidase (HRP) were added (1:1000 dilution in 2% TBS-BSA) and incubated for 2 hours at 30 °C. After washing, peroxidase activity was revealed by *o*-phenylenediamine (Sigma-Aldrich, St. Louis, MO), a water-soluble substrate for HRP that produces a product detectable at 492 nm by an ELISA plate reader (Tecan Spark, Männedorf, Switzerland). cAMP concentrations were calculated from a standard curve established with known concentrations of cAMP diluted in TBS-Tween.

3.7.4 Measurements of CyaA variants on planar lipid bilayers

Measurements on planar lipid bilayers (black lipid membranes) were performed in a Teflon cell separated by a diaphragm with a circular hole (diameter 0.5 mm) bearing the membrane and separating two chambers. The membrane was formed by the painting method using soybean lecithin in n-decane–butanol (9:1, v/v). Both chambers contained

150 mM KCl, 10 mM Tris-HCl (pH 7.4) and 2 mM $CaCl_2$ and the experiments were performed at 25 ºC. CyaA proteins were prediluted in TUC buffer (50 mM Tris-HCl (pH 8.0), 8 M urea and 2 mM $CaCl_2$) and added into the grounded cis compartment with a positive potential, where they can interact with the phospholipid bilayer, oligomerize and form pores. The membrane current was registered by Ag/AgCl electrodes (Theta) with salt bridges (applied voltage was 50 mV), amplified by an LCA-200-100G amplifier (Femto, Berlin, Germany), and digitized by use of a LabQuest Mini A/D convertor (Vernier, Beaverton, OR). For lifetime determination, approximately ~200 of individual pore openings were recorded and the dwell times were determined using QuB software with 10 Hz low-pass filter. The kernel density estimation was fitted with a double-exponential function using Gnuplot software. The relevant model was selected by the $\chi 2$ value.

3.8 Construction of CyaA$_{908\text{-}1008}$ variants

The nucleotide sequences encoding the C-terminal part of the acylated segment of CyaA (residues 908-1008) with different substitutions were amplified by PCR from the pT7CACT1-derived plasmids with specific primers containing restriction sites, allowing to place the PCR products into the plasmid pT7CT7cyaC-cyaA$_{908\text{-}1008}$ (A. Osickova, Institute of Microbiology, Prague) instead of a sequence encoding an intact CyaA$_{908\text{-}1008}$ polypeptide (**Figure 13**). Moreover, the DNA sequences encoding CyaA$_{908\text{-}1008}$ and its mutant variants were fused in frame to a specific sequence encoding an N-terminal double-hexahistidine tag (d6His). The resulting plasmids allowed the expression of the d6His-CyaA$_{908–1008}$ variants (abbreviated as CyaA$_{908\text{-}1008}$). The steps taken in this mutagenesis process were identical to the full-length toxin mutagenesis previously described (see sections 3.6.2 to 3.6.6). However, either the border primers (**Table 5**) or the enzymes used for verifying by restriction analysis (**Table 6**) differed this time.

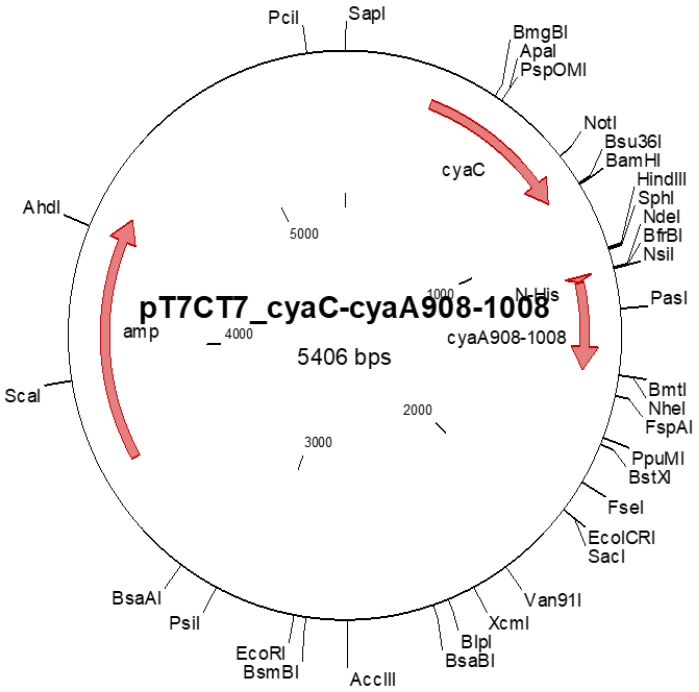

Figure 13. A map of pT7CT7cyaC-cyaA$_{908\text{-}1008}$ plasmid.

Table 5. Border primers used for PCR amplification of *cyaA*$_{908\text{-}1008}$ fragments

Name	*Sequence*	*Number of bases*	*Tm (°C)**
zkrBsu36IFor	GGCACCGCCTAAGGATCC	18	60
zkrNheIRev	CGAATAGCTAGCTATTCGAGC	21	62

** Theoretical melting temperature*

Table 6. Enzymes used for verification of pT7CT7cyaC-cyaA$_{908\text{-}1008}$ variants by restriction analyses

Substitutions	Plasmid	Digestion (to verify restoration of cloning sites)*	Digestion (to verify the substitution)*
D915L+D917L+D918L	pT7CT7cyaC-cyaA$_{908\text{-}1008}$ -D915L+D917L+D918L	Bsu36I, NheI (606,4800)	BlnI(=AvrII), SacI (735,4671)
G931L+G932L+G934L	pT7CT7cyaC-cyaA$_{908\text{-}1008}$ -G931L+G932L+G934L	Bsu36I, NheI (606,4800)	Eco47III, SacI (679,4727)
N936L	pT7CT7cyaC-cyaA$_{908\text{-}1008}$ -N936L	Bsu36I, NheI (606,4800)	KpnI-HF, SacI (673,4733)

*The expected sizes of digested fragments in base pairs are indicated in parentheses.

3.9 Production and purification of CyaA$_{908\text{-}1008}$ variants for CD spectroscopy

The CyaA$_{908\text{-}1008}$ variants were produced in the presence of the activating acyltransferase CyaC in *E. coli* BL21/pMM100 cells. The expression and subsequent isolation of the CyaA$_{908\text{-}1008}$ variants in the form of soluble urea extracts was done as described above (section 3.6.8). Purification of the small CyaA$_{908\text{-}1008}$ fragments was then accomplished on Ni-NTA agarose columns. Firstly, the columns were equilibrated with 50 mM Tris-HCl (pH 8.0), 200 mM NaCl, 8 M urea, then the urea extracts containing the CyaA$_{908\text{-}1008}$ fragments were loaded onto the Ni-NTA agarose columns and contaminating *E. coli* proteins were washed out with 50 mM Tris-HCl (pH 8.0), 200 mM NaCl, 20 mM imidazole, 8 M urea. The CyaA$_{908\text{-}1008}$ fragments were eluted with 50 mM Tris-HCl (pH 8.0), 200 mM NaCl, 600 mM imidazole, 8 M urea and concentrated on Phenyl-Sepharose columns. For this purpose, the collected CyaA$_{908\text{-}1008}$ samples were diluted in a ratio of 1:4 with 50 mM Tris-HCl (pH 8.0,) 1 M NaCl and loaded onto the Phenyl-Sepharose mini-columns (Bio-Rad, Hercules, CA) equilibrated with 50 mM Tris-HCl (pH 8.0), 1 M NaCl. Thereafter, the columns were washed with 50 mM Tris-HCl (pH 8.0) and the CyaA$_{908\text{-}1008}$ fragments were eluted with 50 mM Tris-HCl (pH 8.0), 8 M urea, 2 mM EDTA. The presence of the proteins was verified by Bradford test, the most concentrated fractions were collected in the same tube and the purity of the samples was analysed on 18% SDS-PAGE gels.

3.10 CD spectroscopy

The secondary structure content of the purified CyaA$_{908\text{-}1008}$ polypeptides was analysed by CD spectroscopy. To eliminate the EDTA present in the samples, the buffer (50 mM

Tris-HCl (pH 8.0), 150 mM NaCl, 2 mM EDTA) was exchanged to 8 M urea. For doing so, the polypeptide preparations were centrifuged several times (12,000 g, 25 ºC, 15 minutes) using Amicon Ultra-0.5 ml centrifugal filters (MWCO 3kDa). Freshly prepared 8 M urea solution was added after each centrifugation step to reduce the EDTA content to traces amounts. Afterwards, the samples were centrifuged to obtain a highly concentrated preparation. Right before the measurement, the polypeptides were diluted in 20 mM Tris-HCl (pH 8.0), 50 mM NaCl buffer to a final concentration of 0.2 mg/ml, which was selected based on previous screening of the optimal concentration to get a good signal/noise ratio in the used wavelength range. The exact protein concentration was further checked by absorbance at 280 nm using a NanoDrop device (Denovix, Delaware, United States). The circular dichroism spectrum was collected in the range 200-260 nm at 1 nm/sec, 3 accumulations per measurement. Increasing concentrations of calcium ions were added and the spectra were collected per each cation concentration. The Software Pro-Data Viewer was used throughout the experiment. The obtained secondary structure content estimation was compared to that predicted by SOMPA.

3.11 Statistical analysis

Results are expressed as the arithmetic mean ± standard deviation (SD) of the mean. Statistical analysis was performed by one-way ANOVA followed by Dunnett's post-test using GraphPad Prism 8.0 (GraphPad Software, La Jolla, CA).

4. RESULTS

4.1 Construction, isolation and purification of CyaA variants

A primary sequence analysis of the acylated segment of CyaA revealed that it contains two blocks of amino acid residues (**Figure 14**) with a pattern similar to that of the highly conserved calcium-binding sites of the RTX domain of the toxin. To test the hypothesis that these two blocks might form calcium-binding sites playing an important role in cell binding, cell invasive and pore-forming (hemolytic) activities of CyaA, we substituted one or more residues within these blocks (**Figure 14**) that could be involved in coordination of calcium ions.

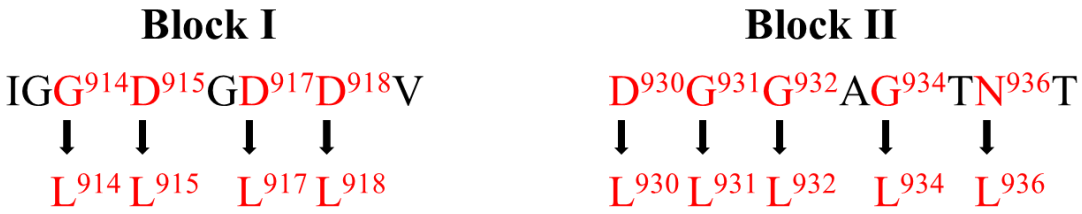

Figure 14. Two blocks of amino acid residues of the acylated segment of CyaA with indicated substitutions (in red colour).

The single or multiple substitutions were introduced into the *cyaA* gene by site-directed PCR mutagenesis and PCR products were subcloned into the parental *cyaA* gene in the pT7CACT1 plasmid (**Figure 12,** Osicka *et al*., 2000). The pT7CACT1-derived plasmids were analysed for the presence of the PCR fragments with inserted mutations by restriction analysis, using newly created restriction sites, which were introduced into the PCR primers as silent mutations (**Appendix**). The presence of the desired substitutions and the absence of any inappropriate additional mutations was confirmed by sequencing. The wild-type (WT) CyaA, included in all experiments as a positive control, and the different CyaA mutant variants were produced in the presence of the activating protein CyaC, using the *E. coli* strain BL21/pMM100 transformed with the appropriate plasmid construct, derived from pT7CACT1. The WT and mutant CyaA proteins were isolated from inclusion bodies of disrupted bacteria, purified by a combination of ion-exchange and hydrophobic chromatography, and analysed by SDS-PAGE (**Figure 15**).

The CyaA-derived proteins carried the following substitutions in the first block: G914L, D915L, D917L, D918L and D915L+D917L+D918L; and in the second block: D930L, G931L, G932L, G934L, N936L, D930L+N936L and G931L+G932L+G934L.

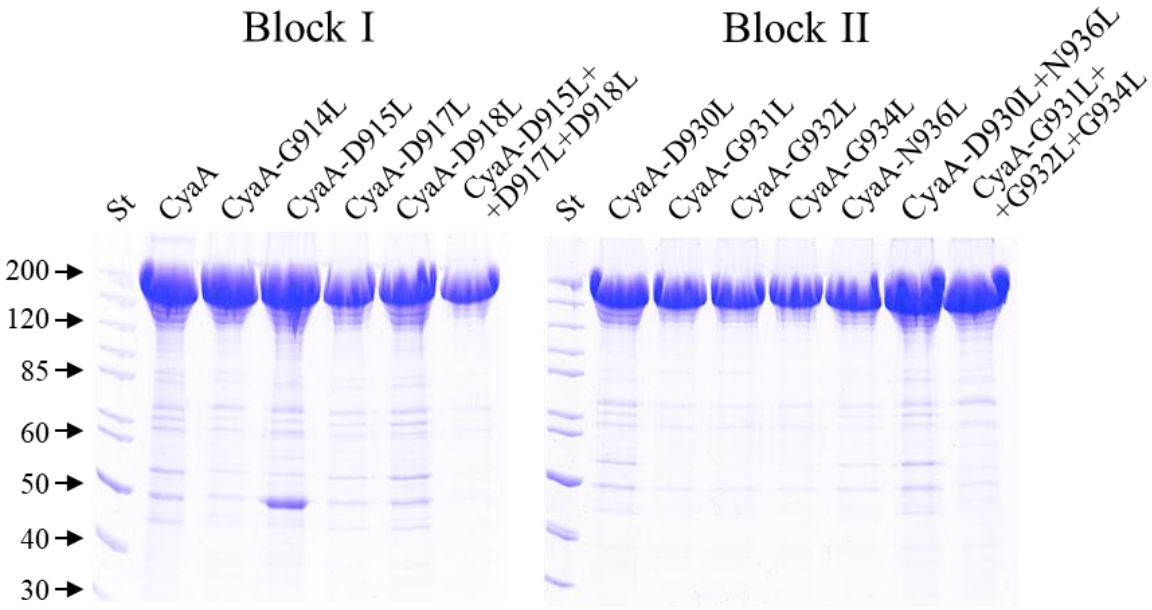

Figure 15. Analysis of the purified CyaA variants by SDS-PAGE. The plasmid pT7CACT1 and twelve pT7CACT1-derived constructs were used for the production of CyaA and its mutant variants in *E. coli* BL21/pMM100 cells. The proteins were purified close to homogeneity from urea-solubilized inclusion bodies by ion-exchange and hydrophobic chromatography on DEAE-Sepharose and Phenyl-Sepharose, respectively. The samples were analysed on 7.5% polyacrylamide gels and stained with Coomassie Blue. St, molecular mass standards.

4.2 Cell binding and cell invasive activities of CyaA variants

Sheep erythrocytes were used as model cells lacking the toxin receptor CD11b/CD18. The ability of CyaA and its mutant variants to bind erythrocyte membrane and to deliver the invasive AC domain across the lipid bilayer was determined by the measurement of membrane associated AC activity, or of internalized and membrane associated AC activity protected against digestion by externally added trypsin.

As shown in **Figure 16**, binding and invasive AC capacities of the CyaA-G914L, CyaA-D915L, CyaA-D917L and CyaA-D918L toxins on erythrocytes were comparable to those of the WT CyaA. In contrast, simultaneous substitution of the D915, D917 and D918 residues by leucine residues strongly reduced (by ~80%) the capacity of the CyaA-D915L+D917L+D918L construct to bind erythrocytes and completely abolished its ability to deliver the AC domain into the cell cytosol (**Figure 16**).

As further shown in **Figure 16**, replacement of D930, G931 and G932 by leucine residues had no effect on the binding and invasive activities of the toxins carrying these single mutations. However, the CyaA-G934L, CyaA-N936L, CyaA-D930L+N936L and CyaA-G931L+G932L+G934L constructs exhibited a substantial decrease (by ~75-90%) or complete loss of their binding and invasive capacities when compared with the WT CyaA toxin.

All these results demonstrate that the blocks I and II of the acylated segment of CyaA contain amino acid residues that are important for cell binding and cell invasive activities of the toxin.

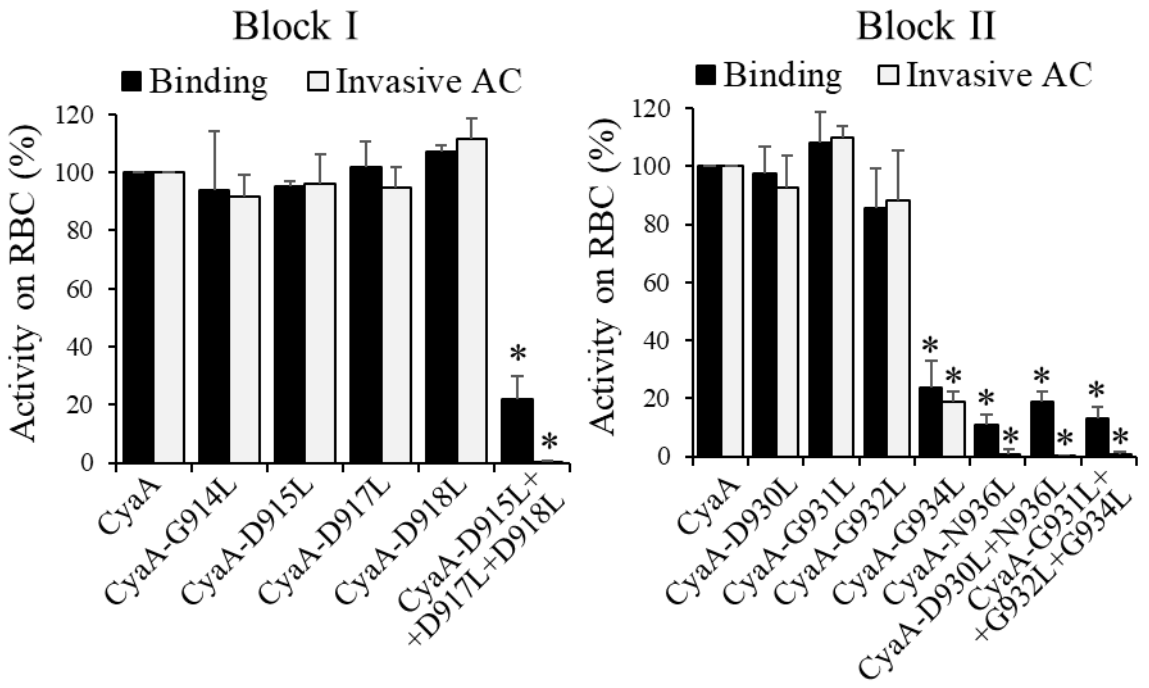

Figure 16. Binding and invasive AC activities of CyaA and its mutant variants on erythrocytes. Sheep erythrocytes (5×10^8/ml) were incubated at 37 °C with 1 μg/ml of CyaA or its mutant variants and after 30 minutes aliquots were taken for determinations of the cell-associated AC activity and of the AC activity internalized into erythrocytes and protected against digestion by externally added trypsin. Activities are expressed as percentages of CyaA activity and represent average values ± standard deviations from at least three independent determinations performed in duplicate with two different toxin preparations. Significantly reduced binding and invasive AC activities of the CyaA mutant variants to erythrocytes in comparison with intact CyaA are indicated (*, $p<0.0001$; ANOVA).

4.3 Pore-forming (hemolytic) activities of CyaA variants

The ability of CyaA and its mutant variants to form membrane pores was tested as specific hemolytic activity, determined as hemoglobin release from erythrocytes.

As shown in **Figure 17**, all the CyaA mutant constructs containing substitutions in block I of the acylated segment were able to form pores in erythrocyte membrane, except of the CyaA-D915L+D917L+D918L variant.

Regarding the toxins that were mutated in block II, the CyaA-G934L, CyaA-N936L, CyaA-D930L+N936L and CyaA-G931L+G932L+G934L constructs were unable to provoke any lysis of erythrocytes over time, while CyaA-D930L, CyaA-G931L and CyaA-G932L behaved similarly to the WT CyaA (**Figure 17**).

These data demonstrate that the same amino acid substitutions, which substantially reduced cell binding and cell invasive activities of CyaA also abolished the capacity of the toxin to form hemolytic pores in the cell membrane of erythrocytes.

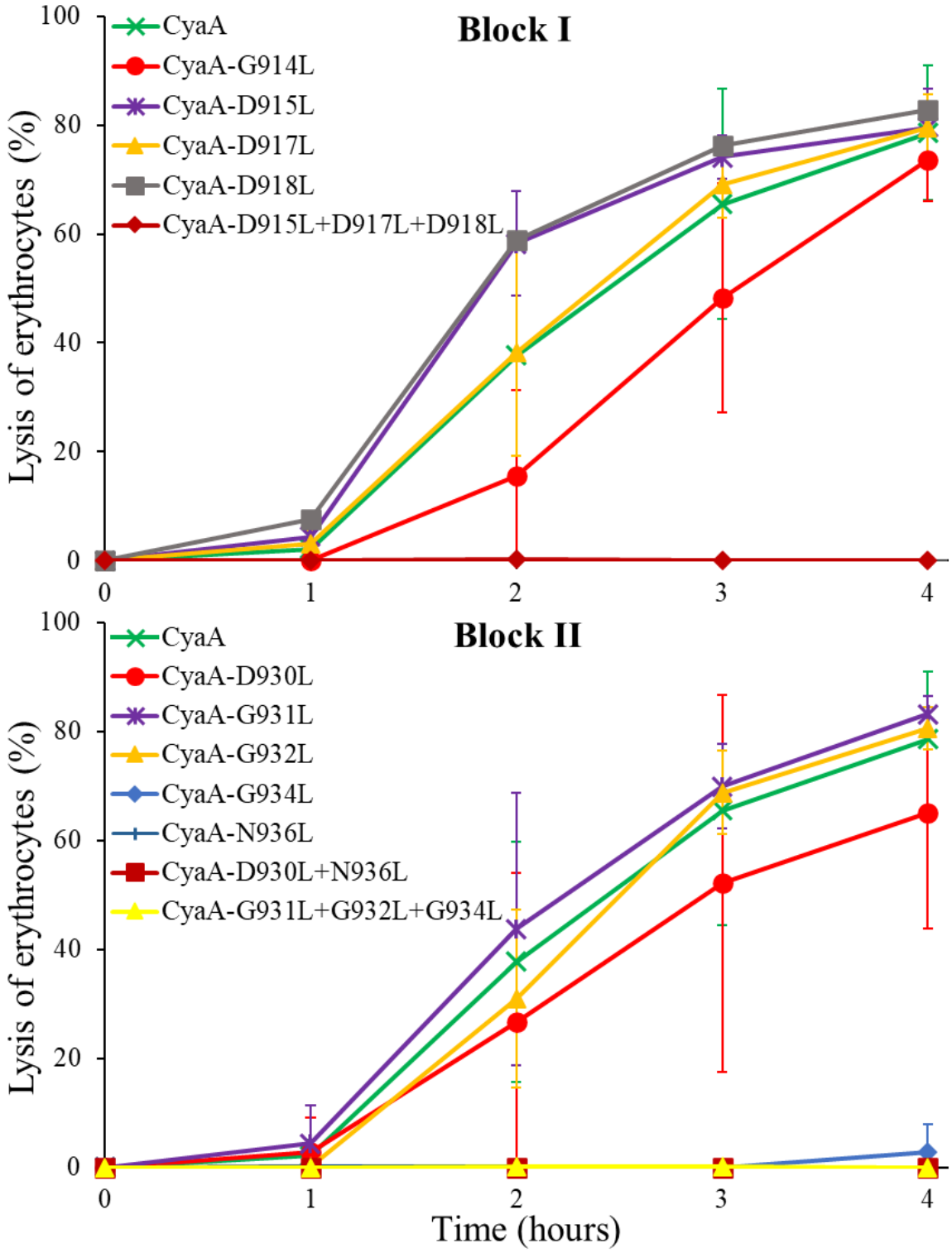

Figure 17. Hemolytic activity of CyaA and its mutant variants on sheep erythrocytes. For determination of hemolytic activity, sheep erythrocytes (5×10^8/ml) were incubated at 37 °C in the presence of 10 µg/ml of CyaA or its mutant variants. Hemolytic activity was measured in time for 4 hours as the amount of released hemoglobin by photometric determination (A_{541} nm). Activities are expressed as percentages of hemolytic activity and represent average values ± standard deviations from at least two independent determinations performed in duplicate.

4.4 Binding of CyaA variants to and cAMP intoxication of THP-1 monocytes

CyaA specifically binds phagocytic cells through their integrin receptor CD11b/CD18 [162,237]. This interaction enables the toxin to exert a complex range of cytotoxic and immunosubversive activities on myeloid phagocytic cells [190]. Therefore, we also examined the binding capacity of the CyaA variants on THP-1 monocytes, which were used as model cells expressing the CD11b/CD18 receptor. Binding of the CyaA mutant variants to THP-1 cells was determined as the amount of total cell-associated AC enzyme activity upon incubation of cells with the CyaA proteins for 30 min at 4 °C. As summarized in **Figure 18**, all the CyaA mutants that bound to CD11b/CD18-negative erythrocytes as WT CyaA (section 4.2) also bound with similar capacities to CD11b/CD18-positive THP-1 cells. But interestingly, the CyaA variants with substantially reduced capacity to bind erythrocytes (CyaA-G934L, CyaA-N936L, CyaA-D930L+N936L and CyaA-G931L+G932L+G934L) were able to bind THP-1 cells with rather high efficacy, ranging from ~70% to 100% of WT CyaA (**Figure 18)**. The exception was the CyaA-D915L+D917L+D918L mutant, which bound THP-1 cells with a reduced capacity (~26%, **Figure 18**), similarly as it bound erythrocytes (section 4.2). These results demonstrate that the substitutions G934L, N936L, D930L+N936L and G931L+G932L+G934L inserted into block II of the acylated segment of CyaA substantially reduced toxin binding to erythrocytes, whereas they have only weak effect on CyaA binding to CD11b/CD18-positive THP-1 cells.

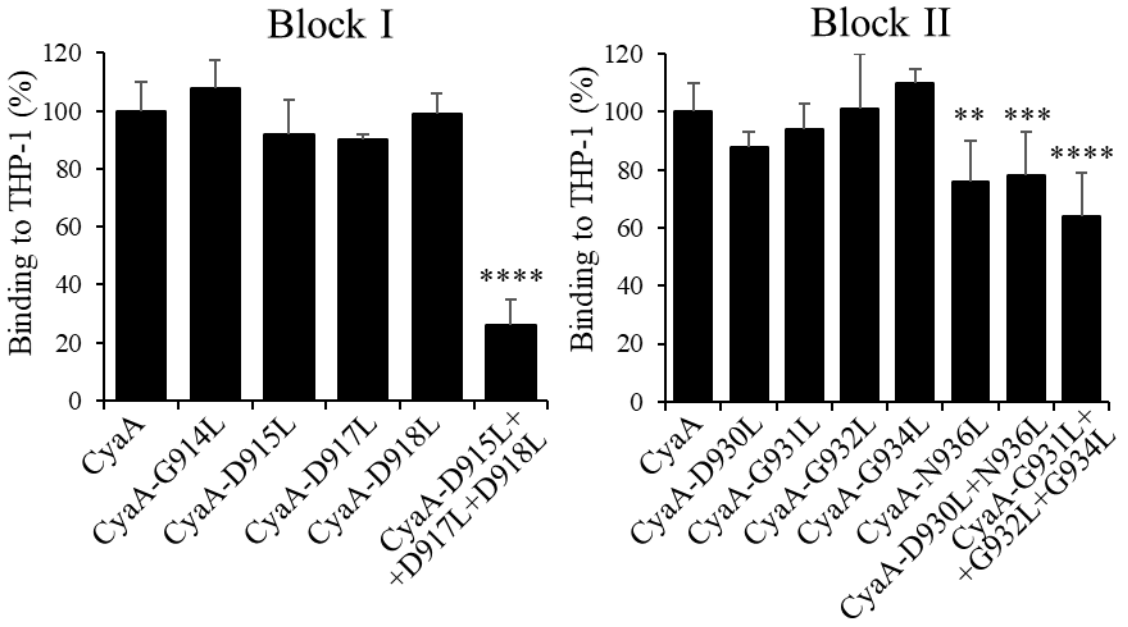

Figure 18. Binding activities of the CyaA variants on THP-1 cells. Binding of the CyaA variants to THP-1 cells (1×10^6) was determined as the amount of total cell-associated AC enzyme activity upon incubation of cells with 1 μg/ml of the protein for 30 minutes at 4 °C. Activities are expressed as percentages of CyaA activity and represent average values ± standard deviations from at least three independent determinations performed in duplicate with two different toxin preparations. Significant differences between binding of the CyaA mutant variants and intact CyaA to THP-1 cells are indicated (**, $p<0.01$; ***, $p<0.001$; ****, $p<0.0001$; ANOVA).

The ability of CyaA and its variants to translocate the AC domain across the cytoplasmic membrane into the cell cytosol was determined as cAMP elevation in THP-1 cells by

cAMP ELISA assay. As summarized in **Figure 19**, all CyaA mutant variants with single substitutions located in block I increased intracellular levels of cAMP to the same extent as the WT CyaA toxin. In contrast, the triple mutant CyaA-D915L+D917L+D918L was unable to elevate cAMP levels in the cytosol of THP-1 monocytes (**Figure 19**).

As further summarized in **Figure 19**, the CyaA-D930L, CyaA-G931L, CyaA-G932L and CyaA-G934L variants with single substitutions located in block II had minor differences in their ability to elevate cAMP levels in the cytosol of THP-1 cells when compared to the WT CyaA. In contrast, the capacity of the CyaA-N936L, CyaA-D930L+N936L and CyaA-G931L+G932L+G934L mutants to elevate cAMP levels in the cytosol of THP-1 cells was almost abolished.

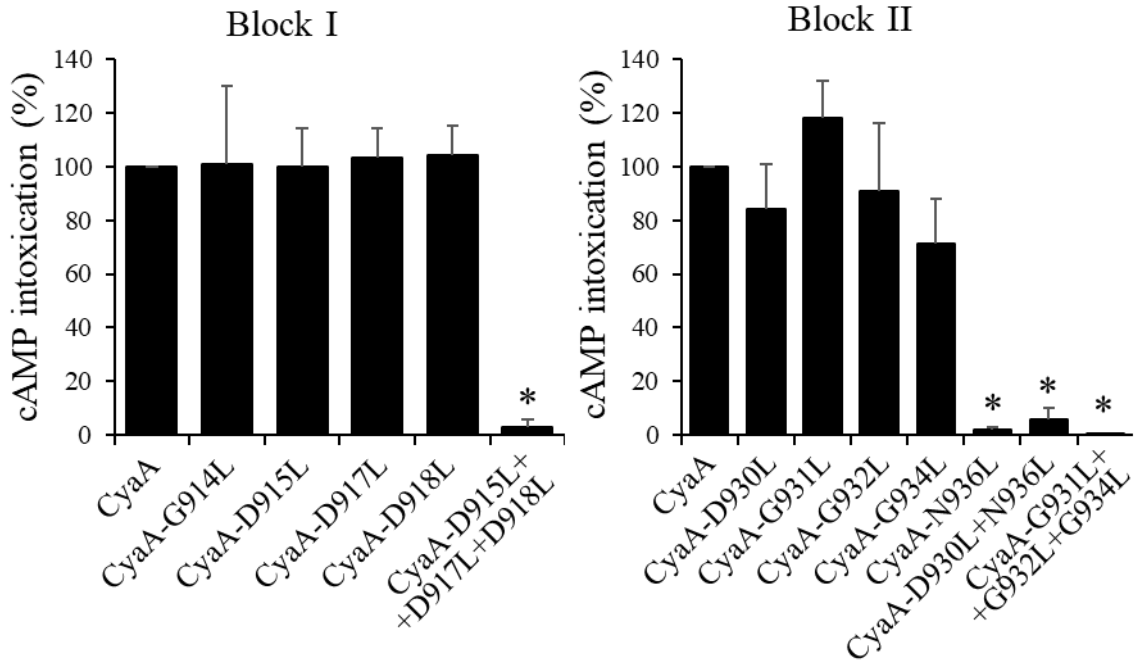

Figure 19. Effect of the CyaA variants on intracellular levels of cAMP in THP-1 cells. cAMP intoxication was assessed by determining the intracellular concentration of cAMP generated in cells after 30 minutes of incubation of THP-1 cells (1.5×10^5) with four different toxin concentrations (15.6, 31, 62.5 and 125 ng/ml) from within the linear range of the dose response curve. Activities are expressed as percentages of intact CyaA activity and represent average values ± standard deviations from three independent determinations performed in duplicate with two different toxin preparations. The CyaA mutant variants, which intoxicated THP-1 cells with significantly lower efficacy than intact CyaA are indicated (*, $p<0.0001$; ANOVA).

Taken together, the blocks I and II located in the acylated domain of CyaA contain several amino acid residues whose substitution can affect binding, invasive AC and hemolytic activities of CyaA on CD11b/CD18-negative erythrocytes, as well as the ability of the toxin to bind CD11b/CD18-positive THP-1 monocytes and elevate cAMP levels in their cytosol.

4.5 Measurements of CyaA variants in planar lipid bilayers

Since the CyaA-G934L and CyaA-N936L constructs were not hemolytic on erythrocytes, we decided to examine whether these mutated toxins exhibit a capacity to

permeabilize lipid bilayer membranes made of 3% asolectin. We analysed their overall membrane activity (i.e., the combined contributions of the number of pore-forming toxin molecules in the membrane, lifetime and conductance of single pores, and the frequency of pore formation), their single-pore conductance and lifetime of opened pores.

As shown in **Figure 20A**, 250 pM CyaA elicited a steep increase of conductance across the lipid bilayer over time, whereas the same amounts of the CyaA-G934L and CyaA-N936L mutants produced negligible conductance across the black lipid membrane. This is in agreement with their residual cytolytic capacity on erythrocytes (**Figure 17**).

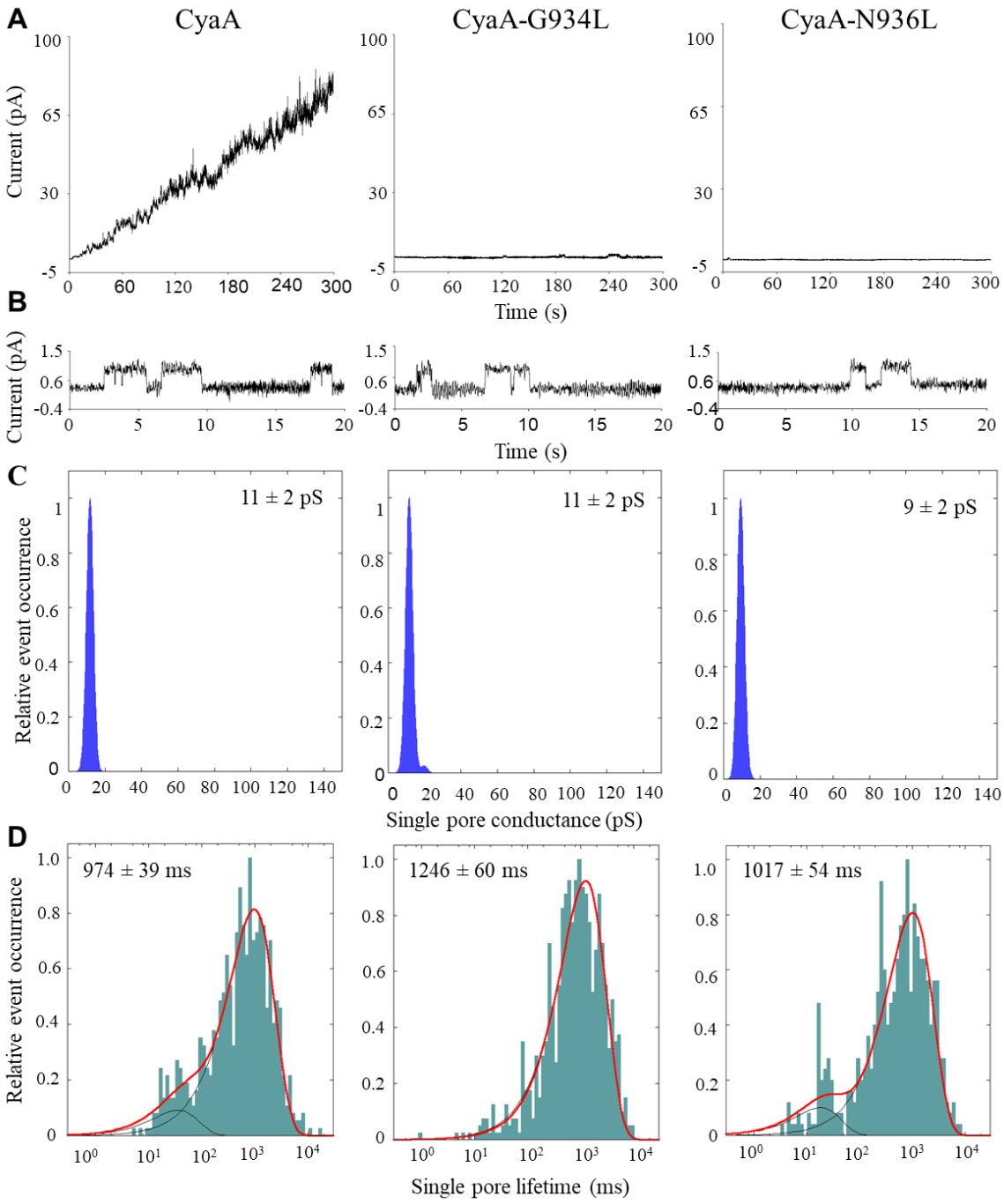

Figure 20. Overall membrane activities, conductances and lifetimes of CyaA and its mutant variants on planar lipid membranes. A, Overall membrane activities of 250 pM purified CyaA

and its mutant CyaA-G934L and CyaA-N936L variants on asolectin/decane:butanol (9:1) membranes. The aqueous phase contained 150 mM KCl, 10 mM Tris-HCl (pH 7.4), 2 mM $CaCl_2$; the applied voltage was 50 mV; the temperature was 25 °C; and the recording was filtered at 10 Hz. **B**, Single-pore recordings of asolectin membranes in the presence of 30 pM purified CyaA and its mutant variants under otherwise identical conditions as in A. **C**, Kernel density estimation of single-pore conductances calculated from single-pore recordings (>300 events) acquired on several different asolectin membranes with 5-500 pM CyaA or its variants under the same conditions as in A. The numbers represent the most frequent conductances ± S.D. of pores formed by the CyaA variants. **D**, For lifetime determination, ~200 individual pore openings were recorded on several different asolectin membranes with 5-500 pM CyaA or its variants under the same conditions as in A. The logarithmic histogram of dwell times was fitted with a double-exponential function. The error estimates of lifetimes were obtained by bootstrap analysis. The numbers in each panel represent the most frequent values ± S.D.

However, both CyaA variants occasionally still formed single pore conductance units that exhibited similar characteristics as the pores formed at much higher frequency by the WT CyaA (**Figure 20B**). The most frequent conductances of pores formed by CyaA-G934L (11 ± 2 pS) and CyaA-N936L (9 ± 2 pS) were quite comparable with that of the WT protein (11 ± 2 pS) (**Figure 20C**). Finally, the CyaA-G934L and the CyaA-N936L mutants formed pores in asolectin membranes with similar lifetimes (1246 ± 60 ms and 1017 ± 54 ms, respectively) as the WT CyaA toxin (974 ± 39 ms) (**Figure 20D**).

It can thus be concluded that the single mutations G934L and N936L inserted into the block II of the acylated segment of CyaA strongly affected the ability of the CyaA-G934L and CyaA-N936L toxins to correctly bind/insert into the asolectin bilayer and/or the propensity of the mutant toxins to form oligomeric pores with the same frequency as the WT toxin. However, once inserted to the membrane, the CyaA-G934L and CyaA-N936L variants formed pores with similar single pore conductance states and lifetimes as the WT CyaA.

4.6 Construction, isolation and purification of $CyaA_{908-1008}$ variants

The pT7CACT1-derived plasmids (section 4.1) were used to PCR amplify nucleotide sequences encoding the C-terminal part of the acylated segment of CyaA (residues 908-1008) with the single (N936L) or multiple substitutions (D915L+D917L+D918L and G931L+G932L+G934L). The PCR products were placed into the plasmid pT7CT7cyaC-$cyaA_{908-1008}$ instead of a sequence encoding an intact $CyaA_{908-1008}$ polypeptide (**Figure 13**). In parallel, the DNA sequences encoding $CyaA_{908-1008}$ variants were fused in frame to a specific sequence encoding an N-terminal double-hexahistidine tag. The presence of the desired substitutions and the absence of any unrelated additional mutations were confirmed by sequencing. The resulting plasmids allowed the expression of the WT $CyaA_{908-1008}$ polypeptide and its mutant variants in the presence of the activating acyltransferase CyaC in *E. coli* BL21/pMM100 cells. The $CyaA_{908-1008}$ polypeptides were then isolated from inclusion bodies of disrupted bacteria, purified on Ni-NTA agarose columns and concentrated on Phenyl-Sepharose columns. Finally, the collected polypeptide fractions were analysed by SDS-PAGE (**Figure 21**).

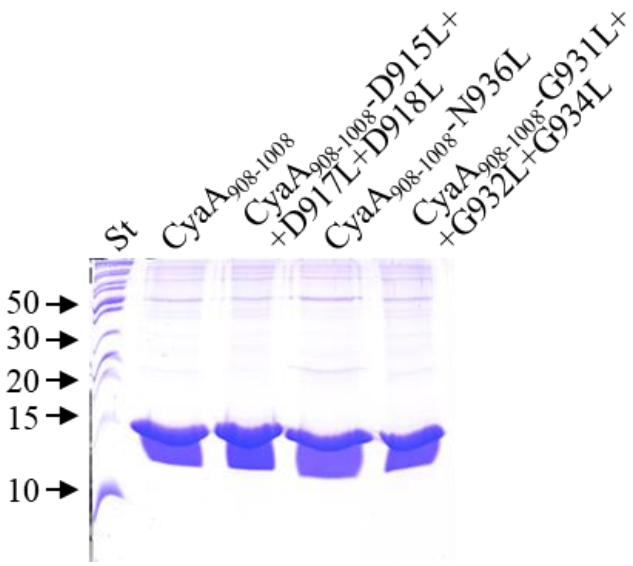

Figure 21. Analysis of the purified CyaA$_{908-1008}$ polypeptides by SDS-PAGE. The plasmid pT7CT7cyaC-cyaA$_{908-1008}$ and three pT7CT7cyaC-cyaA$_{908-1008}$-derived constructs were used for the production of CyaA$_{908-1008}$ and its mutant variants in *E. coli* BL21/pMM100 cells. The proteins were purified close to homogeneity from urea-solubilized inclusion bodies by affinity and hydrophobic chromatography on Ni-NTA agarose and Phenyl-Sepharose, respectively. The samples were analysed on 18% polyacrylamide gel and stained with Coomassie Blue. St, molecular mass standards.

Previously, it was demonstrated that the posttranslational modification of internal lysine residues (K860 and K983) within conserved acylated sites by covalent attachment of fatty acyl residues is crucial for CyaA cytotoxic activities [177,219,253]. Since the second acylation site with the residue K983 is present in the CyaA$_{908-1008}$ variants, the acylation pattern of the purified CyaA$_{908-1008}$ variants was analysed by liquid chromatography-mass spectrometry (LC-MS) (performed at the Centre of Molecular Structure Core Facility, Biocev, Vestec, Czech Republic). As summarized in **Table 7**, WT CyaA$_{908-1008}$ activated by its cognate acyltransferase CyaC exhibited a predominant acylation with palmitoyl (C16:0) and palmitoleyl (C16:1) chains at the K983 residue (~89%).

Table 7. Acylation status of the CyaA$_{908-1008}$ variants modified by the CyaC acyltransferase

Acyl chain*	CyaA$_{908-1008}$	CyaA$_{908-1008}$-D915L+D917L+D918L	CyaA$_{908-1008}$-N936L	CyaA$_{908-1008}$-G931L+G932L+G934L
	K983	K983	K983	K983
None	0	43	0	8
C14:0	2	1	0	1
C16:0	28	4	22	20
C16:1	61	49	59	62
C18:1	10	2	19	9

*****The CyaA$_{908-1008}$ variants were produced in the presence of the CyaC acyltransferase in *E. coli* BL21/pMM100 cells, purified close to homogeneity and analysed by LC-MS. Percentage distributions of fatty acyl chains linked to the ε -amino groups of the lysine residue K983 were estimated semi-quantitatively, from the relative intensities of selected ions in reconstructed ion current chromatograms.

A small proportion of the molecules was also modified by myristoyl (C14:0) and octadecenoyl (C18:1) chains linked to the K983 residue (~12%). As further summarized in **Table 7**, the acylation status of the K983 residue on both $CyaA_{908-1008}$-N936L and $CyaA_{908-1008}$-G931L+G932L+G934L strongly resembled the acylation status of the WT polypeptide. In contrast, the K983 residue of $CyaA_{908-1008}$-D915L+D917L+D918L was primarily modified with the C16:1 chain (~49%) and residually with the C14:0, C16:0 and C18:1 chains (~7%). The rest of the molecules remained unacylated (~43%) (**Table 7**).

4.7 CD spectroscopy of $CyaA_{908-1008}$ variants

CD spectroscopy is a powerful technique based on the differential absorption of left and right circularly polarized light by an optically active molecule. It has been extensively used for determining the secondary structure of proteins and to monitor conformational changes due to inserted mutations, among other factors [254]. In this work, CD spectroscopy was employed to detect the interaction of the polypeptide $CyaA_{908-1008}$ with the divalent cation Ca^{2+} and to analyse the effect of the $CyaA_{908-1008}$ - Ca^{2+} interaction on the secondary structure of the molecule.

The $CyaA_{908-1008}$ polypeptide was diluted at least 15 times with 50 mM NaCl, 20 mM Tris-HCl (pH 8.0) to reduce the urea concentration under 0.5 M and calcium chloride was stepwise added to the quartz cell in the concentration range 0 to 1500 µM. As demonstrated in **Figure 22**, binding of calcium ions to $CyaA_{908-1008}$ occurred in a cooperative way.

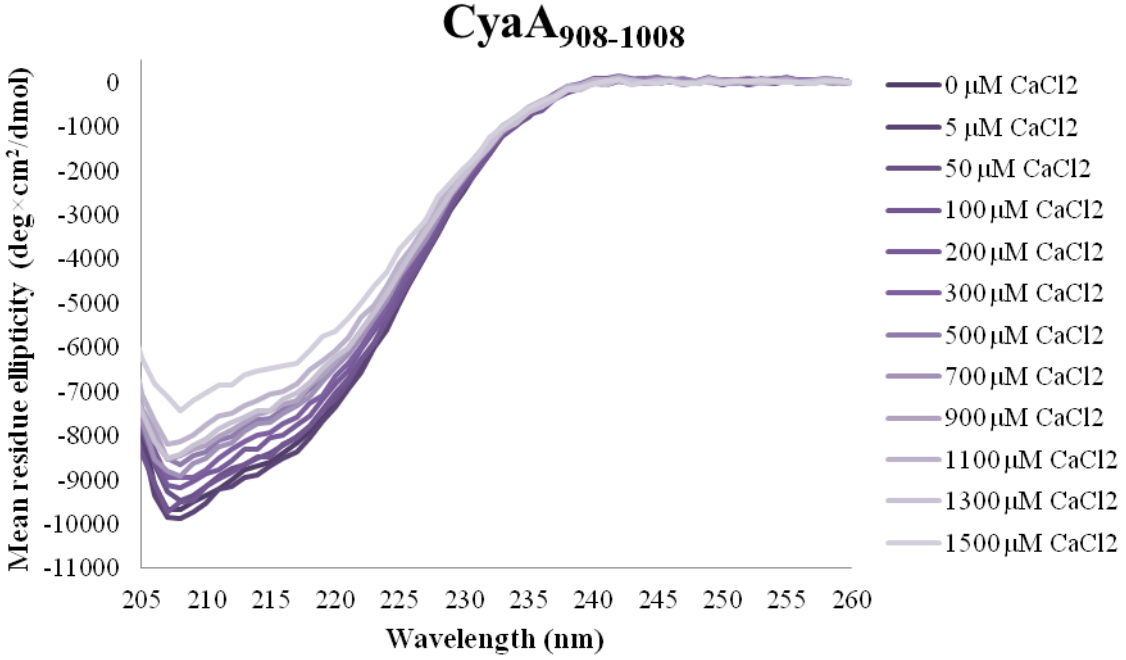

Figure 22. Far-UV CD spectra of $CyaA_{908-1008}$ in the presence of increasing concentrations of calcium ions. $CyaA_{908-1008}$ was incubated with stepwise increasing concentrations (0 to 1500 µM) of $CaCl_2$. Each spectrum represents the average of 3 accumulations, carried out at 25 °C between 200 and 260 nm at 1 nm/sec.

In the absence of calcium ions, the polypeptide shows a partially unfolded configuration, indicated by the negative peak at 205 nm (as result of the π-π* band of the amide bound). However, significant secondary structures are observed in both the π-π* and n-π* bands, especially in the later as indicated by the negative peak (hump) at approximately 217 nm, which is characteristic of beta structures. Binding of calcium ions induced folding of the molecule, evidenced by a reduction in the intensity of the negative peak at 205 nm hence of the random coils content (**Figure 22**). At the same time, the overall secondary structure of the molecule evidenced conformational changes upon addition of calcium ions.

To assess the contribution of the predicted calcium-binding sites, we used for CD measurements the $CyaA_{908\text{-}1008}$ polypeptides with introduced mutations in both block I (D915L+D917L+D918L) and block II (G931L+G932L+G934L or N936L) of the acylated segment. $CyaA_{908\text{-}1008}$-D915L+D917L+D918L showed a well folded conformation even in the absence of calcium ions, and the obtained spectrum suggests the presence of beta structures predominantly due to the significant negative peak at 218 nm and the absence of evident peak at 205 nm (**Figure 23A**). Despite the obvious difference with the WT $CyaA_{908\text{-}1008}$ polypeptide, the calcium binding character was kept. Increasing concentrations of calcium ions induced changes in the secondary structure of the protein. However, instead of an increase in the intensity of the signal, the tendency is toward a reduction of secondary structure content. This phenomenon could suggest that the molecule in solution has a collapsed conformation, and after binding of calcium, some flexible but still collapsed structures are formed.

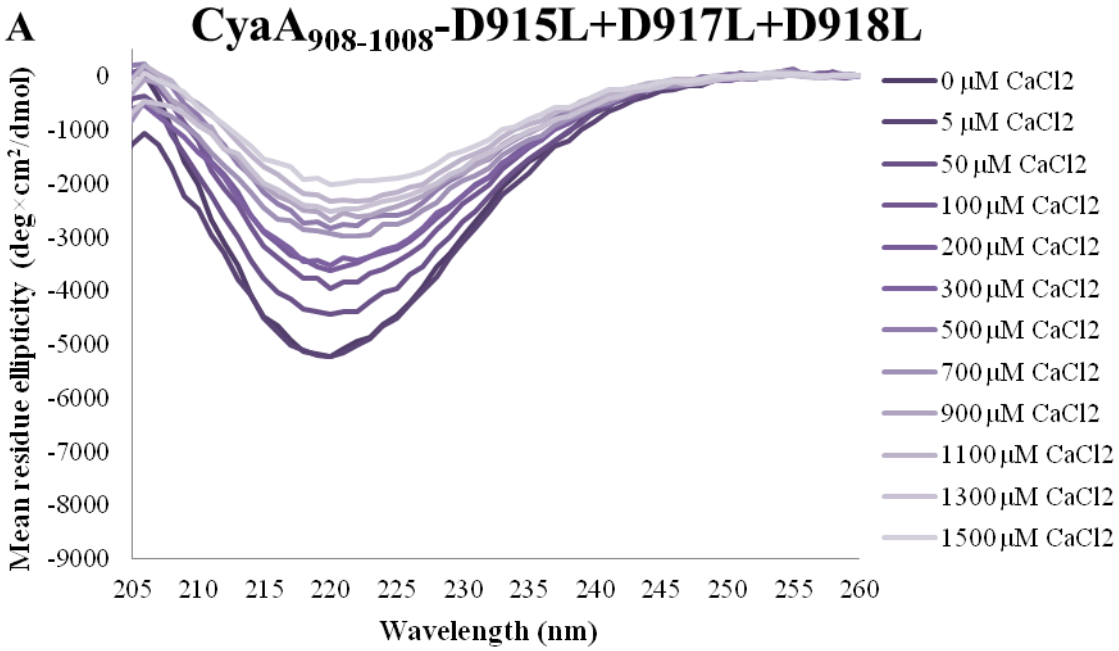

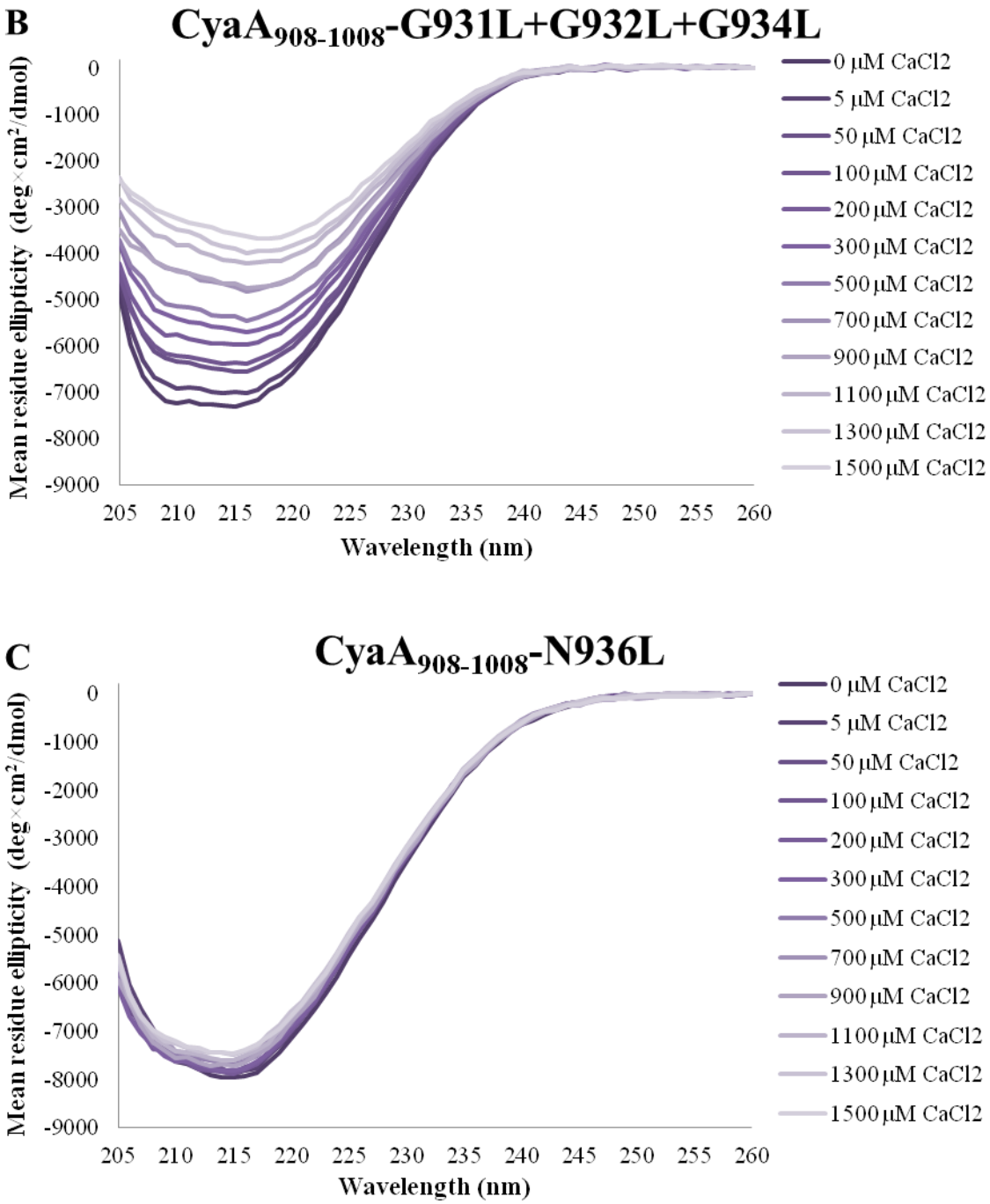

Figure 23. Far-UV CD spectra of the CyaA$_{908-1008}$ variants in the presence of increasing concentrations of calcium ions. The CyaA$_{908-1008}$-D915L+D917L+D918L **(A)**, CyaA$_{908-1008}$-G931L+G932L+G934L **(B)** and CyaA$_{908-1008}$-N936L **(C)** polypeptides were incubated with stepwise increasing concentrations of $CaCl_2$ (0 to 1500 µM). Each spectrum represents the average of 3 scans from determinations performed with two different toxin preparations, carried out at 25 °C between 200 and 260 nm at 1 nm/sec.

In the case of CyaA$_{908-1008}$-G931L+G932L+G934L, a similar tendency was observed (**Figure 23B**). The overall structure seemed to be a mixture of alpha and beta structures

with random coils, but with significant better compaction compared to the precursor polypeptide. $CyaA_{908\text{-}1008}$-N936L, in the other hand, did not show extraordinary changes upon addition of calcium ions (**Figure 23C**). Subtle variations in the spectra corresponded to the different studied concentrations of calcium ions, but in general the polypeptide showed almost no changes in the content of secondary structures, compared to the WT $CyaA_{908\text{-}1008}$ polypeptide.

These results indicate that the C-terminal part of the acylated segment of CyaA binds calcium ions. Interestingly, this binding can be completely abolished by the single substitution N936L introduced into the acylated segment.

5. DISCUSSION

In this work, we have investigated whether two blocks of amino acid residues located in the acylated region of CyaA could form the predicted calcium-binding sites. Using site directed-mutagenesis of these two blocks, we studied the impact of the introduced mutations on CyaA membrane binding, AC invasive and hemolytic (pore-forming) activities. We reported that single and multiple substitutions within block I (D915L+D917L+D918L) and block II (G934L, N936L, D930L+N936L and G931L+G932L+G934L) of the acylated region of CyaA impaired the capacity of the toxin to bind and translocate its AC domain across the membrane of target cells, as well as the hemolytic activity of the toxin. While the individual substitutions of the residues D915, D917 or D918 by a leucine residue did not affect the binding, invasive and hemolytic activities of CyaA, these substitutions, when inserted together (D915L+D917L+D918L) to one toxin molecule, abolished almost completely the activities of the toxin. This suggests that the residues D915, D917 and D918 have a synergistic role in the activities of CyaA. In fact, when introduced in the same CyaA molecule, the leucine substitutions on the aspartate residues might disrupt the characteristic calcium-binding aspartate and glycine-rich nonapeptide repeat of a consensus sequence GGxGxDxxx. This can impair somehow the folding of the CyaA molecule, thus compromising its activity. Indeed, purified CyaA proteins that were stored in 8 M urea (being for this reason denatured), were renatured before the activity experiments in the presence of 2 mM $CaCl_2$. Binding of calcium ions leads to the folding of the CyaA molecule (from the C- to the N-terminus) and is one of the requirements for the activity of the toxin, beyond the post-translational modification of the lysine residues K860 and K983, with the acylation on K983 residue being more important for the activity of the toxin than on the K860 residue [217].

The CyaA-N936L, CyaA-D930L+N936L and CyaA-G931L+G932L+G934L variants exhibited strongly reduced activities on both sheep erythrocytes and THP-1 cells. However, these constructs bound preferentially the THP-1 cells expressing the receptor CD11b/CD18, suggesting that the interaction with the receptor facilitated their binding to the cell surface, although it did not promote their capacity to deliver the AC enzyme across the cell membrane. This indicates that the introduced mutations did not affect the integrity of the CD11b/CD18-binding site of CyaA located between residues 1166 to 1287 of the RTX domain [160], but most likely compromised the structure of the AC to Hly-linking segment (residues ~400-500) and/or of the pore-forming domain (residues ~500-700) that have been shown to be crucial and sufficient for translocation of the AC domain across the cell membrane [250]. In addition, the single substitutions of D930, G931 or G932 by a leucine residue did not affect the binding, AC invasive and hemolytic activities of the CyaA mutant variants on both cell types used. Hence, it indicates that the substitution N936L in the CyaA-D930L+N936L construct and the substitution G934L in the CyaA-G931L+G932L+G934L construct are the mutations with the major impact on the biological activities of the toxin.

Previous experiments with black lipid membranes made of asolectin have shown that CyaA interacts with target membranes and forms pores within seconds [186,255,256]. Moreover, the type of the pores formed by CyaA as well as their voltage dependence are determined by the orientation of the electrical potential across the membranes with

respect to the addition of the toxin [211]. CyaA pores on artificial membranes behave as frequently opening and closing membrane channels, which likely arises by an association equilibrium between non-conducting CyaA monomers and subsequent aggregation of the CyaA monomers into conducting oligomers [257]. Opening of these pores permeabilizes cells for potassium efflux and can eventually lead to colloid-osmotic cell lysis due to the influx of ions and water [186,207,257].

We report here that the overall pore-forming activity of the CyaA variants with the substitutions G934L and N936L on asolectin membranes was very low, which was in agreement with their non-hemolytic activity on erythrocytes. However, once the toxins have inserted into the planar lipid bilayer at a low frequency, the substitutions in the CyaA molecule did not affect anymore the conductance and lifetime of single pores formed by the CyaA-G934L and CyaA-N936L variants, since these exhibited quite similar properties as single pores formed by the WT CyaA. This shows that the leucine substitutions of the G934 and N936 residues of CyaA affected the ability of the mutant toxins to bind/insert into the membrane and to form oligomeric pores, but not the structure of the pores itself.

The acylation status of the $CyaA_{908\text{-}1008}$ polypeptide and its mutant derivatives was assessed by LC-MS. We found that palmitoylation (C16:0) and palmitoleylation (C16:1) are the two major posttranslational modifications not only of the K983 residue of WT $CyaA_{908\text{-}1008}$, but also of the $CyaA_{908\text{-}1008}$-G931L+G932L+G934L and $CyaA_{908\text{-}1008}$-N936L variants. This is in line with previous observations, where the K983 residue of the recombinant CyaA isolated from *E. coli* K12 was both palmitoylated and palmitoleylated at a ratio of ~1:2 [218]. In contrast, the $CyaA_{908\text{-}1008}$-D915L+D917L+D918L was predominantly palmitoleylated on the K983 residue (~49%) and a significant part of the molecules (~43%) remained unacylated. Modification by C16:0 acyl chains was negligible in $CyaA_{908\text{-}1008}$-D915L+D917L+D918L (~4%).

As deduced from the CD spectroscopy experiments, binding of calcium ions to the $CyaA_{908\text{-}1008}$, $CyaA_{908\text{-}1008}$-D915L+D917L+D918L and $CyaA_{908\text{-}1008}$-G931L+G932L+ +G934L constructs induced the folding of the molecules. WT $CyaA_{908\text{-}1008}$ showed a flexible conformation, mainly formed by random coil with some content of alpha and beta structures. In the case of the derived mutants, the overall conformation was more collapsed, indicating a remarkable effect of the mutations in the secondary structure content and the polypeptide conformation. While in the WT $CyaA_{908\text{-}1008}$ polypeptide increasing concentrations of calcium ions reduced the random coils content, in the two variants mentioned above, binding of calcium ions reduced the secondary structure content of the polypeptides as an overall effect, evidenced by the reduction in the intensity of the negative peak at 218 nm (characteristic of beta structures) without appearance of a negative peak at 205 nm (proper random coil). Thus, the reduction in the content of secondary structures, mainly beta structures, in the polypeptides with mutations in block I (D915L+D917L+D918L) or block II (G931L+G932L+G934L) of the acylated segment of CyaA strongly suggests that the introduced mutations compromise two putative calcium-binding sites located in these blocks. Indeed, from the recently solved X-ray structure of the $CyaA_{1529\text{-}1681}$ fragment comprising the RTX block V, we know that the first six residues of the RTX motif (GGxGxD) constitute a turn with bound calcium ion, while the last three non-conserved residues (xxx) form a short beta strand, and that the

consecutive tandem repeats that bind calcium (GGxGxDxxx) form together a regular right-handed helix of parallel beta strands [184]. Assuming that this is also the case of the two putative calcium-binding sites of the acylated region of CyaA, the reduction in the content of beta structures makes more sense now.

In contrast, $CyaA_{908\text{-}1008}$-N936L did not fold in the presence of calcium, which suggests that binding of calcium is completely abolished by the single mutation. The substitution of the asparagine residue (neutral and polar) by a leucine residue (neutral and nonpolar) cannot explain the strikingly lack of reactivity of the polypeptide in the presence of calcium ions, as these amino acid residues have quite similar structures. Furthermore, as evidenced by the LC-MS experiments, $CyaA_{908\text{-}1008}$-N936L is acylated on the K983 residue as the WT polypeptide. A plausible hypothesis would be that the N936 residue, which is located in block II of the acylated region of CyaA, represents an evolutionary advantage of CyaA towards other related RTX toxins. In fact, if we have a look at **Figure 10**, we can notice that in the block I of CyaA the nonapeptide repeat is conserved and it is of the prototype GGxGxDxxx, while in the second block the aspartic acid residue is replaced by an asparagine residue (GGxGxNxxx). This happens only in CyaA and not in the other related toxins (**Figure 10**). Recalling previous results, we observed that the full-length CyaA-N936L construct was unable to bind, translocate its AC domain and release hemoglobin from target cells. Moreover, it was pretty much inactive also on planar lipid bilayers made of asolectin, even at concentrations higher than 250 pM. Taken together, these results suggest that the N936 residue stabilizes in such a way the structure of both predicted calcium-binding sites of block I and II of the acylated segment of CyaA that if we replace it by a leucine residue, the two binding sites lose their capacity to bind calcium ions. Solving the tertiary structure of $CyaA_{908\text{-}1008}$ and its mutant variants by nuclear magnetic resonance (NMR) spectroscopy and/or X-ray crystallography would help deciphering this enigma.

6. CONCLUSIONS AND FUTURE PERSPECTIVES

Strong evidences indicating the existence of two calcium-binding sites located in the acylated segment of CyaA were described in this study for the first time. CyaA-derived proteins carrying substitutions in both block I and II of the acylated segment of CyaA were prepared. Some substitutions abolished the activity of the mutant toxins on cells expressing or lacking the CD11b/CD18 receptor and compromised the overall membrane activities of the mutant toxins on black lipid membranes. The $CyaA_{908\text{-}1008}$ variants carrying critical mutations in the predicted calcium-binding sites were constructed for further evaluation of the acylation status and formation of secondary structures by LC-MS and CD spectroscopy, respectively. The $CyaA_{908\text{-}1008}$-N936L and $CyaA_{908\text{-}1008}$-G931L+G932L+G934L variants were shown to be acylated like the WT $CyaA_{908\text{-}1008}$ polypeptide, exhibiting a predominant acylation with palmitoyl and palmitoleyl chains at the K983 residue. However, the $CyaA_{908\text{-}1008}$-D915L+D917L+D918L variant was only partially acylated by palmitoleyl chains and ~43% of molecules remained unacylated on the K983 residue. From CD experiments, it can be concluded that increasing concentrations of calcium ions induced changes in the secondary structure of the $CyaA_{908\text{-}1008}$, $CyaA_{908\text{-}1008}$-D915L+D917L+D918L and $CyaA_{908\text{-}1008}$-G931L+G932L+G934L polypeptides. In contrast, $CyaA_{908\text{-}1008}$-N936L did not fold in the presence of calcium ions, indicating that the binding of calcium ions is completely abolished by the single mutation.

Despite the availability and worldwide use of pertussis vaccines, whooping cough remains the least-controlled vaccine-preventable disease, even in countries with high immunization rates that have experienced a rise in pertussis cases in the past years. The findings of this study represent an important contribution to understand the biological mechanism of action of CyaA produced by *B. pertussis*. This could be useful for the development of more effective pertussis vaccines, namely that can interrupt the vicious cycle of colonization and transmission of the bacterium, something that the current aP vaccines fail to achieve.

Futures perspectives would involve the development of a more efficient system/method for the expression of $CyaA_{908\text{-}1008}$ and its mutant variants that would allow obtaining higher amounts of these polypeptides for NMR spectroscopy and X-ray crystallography, enabling to solve their three-dimensional structures. Moreover, it would be interesting to experimentally determine whether other related RTX toxins also possess two calcium-binding sites located in the corresponding acylated regions of the toxin molecules. Indeed, a previous study have shown that similarly to CyaA of *B. pertussis*, the α-hemolysin of *E. coli* exhibited a calcium-independent hemolytic activity after being previously exposed to calcium ions. The activation of HlyA by calcium ions and subsequent activity, even in the presence of EGTA, strongly suggested that the toxin binds calcium ions to high-affinity calcium-binding sites [258].

7. REFERENCES

1. Kilgore, P.E.; Salim, A.M.; Zervos, M.J.; Schmitt, H.J. Pertussis: Microbiology, Disease, Treatment, and Prevention. *Clinical microbiology reviews* **2016**, *29*, 449-486.
2. Mattoo, S.; Cherry, J.D. Molecular pathogenesis, epidemiology, and clinical manifestations of respiratory infections due to *Bordetella pertussis* and other *Bordetella* subspecies. *Clinical microbiology reviews* **2005**, *18*, 326-382.
3. Kline, J.M.; Lewis, W.D.; Smith, E.A.; Tracy, L.R.; Moerschel, S.K. Pertussis: a reemerging infection. *American family physician* **2013**, *88*, 507-514.
4. Nieves, D.J.; Heininger, U. *Bordetella pertussis*. *Microbiology spectrum* **2016**, *4*.
5. Centers for Disease Control and Prevention. Pertussis in Other Countries. Availabe online: https://www.cdc.gov/pertussis/countries/index.html.
6. Pinto, M.V.; Merkel, T.J. Pertussis disease and transmission and host responses: insights from the baboon model of pertussis. *The Journal of infection* **2017**, *74 Suppl 1*, S114-s119.
7. Trainor, E.A.; Nicholson, T.L.; Merkel, T.J. *Bordetella pertussis* transmission. *Pathogens and disease* **2015**, *73*, ftv068.
8. Melvin, J.A.; Scheller, E.V.; Miller, J.F.; Cotter, P.A. *Bordetella pertussis* pathogenesis: current and future challenges. *Nature reviews. Microbiology* **2014**, *12*, 274-288.
9. Hasan, S.; Kulkarni, N.N.; Asbjarnarson, A.; Linhartova, I.; Osicka, R.; Sebo, P.; Gudmundsson, G.H. *Bordetella pertussis* Adenylate Cyclase Toxin Disrupts Functional Integrity of Bronchial Epithelial Layers. *Infection and immunity* **2018**, *86*.
10. Rocha, G.; Soares, P.; Soares, H.; Pissarra, S.; Guimarães, H. Pertussis in the newborn: certainties and uncertainties in 2014. *Paediatric respiratory reviews* **2015**, *16*, 112-118.
11. Kowalzik, F.; Barbosa, A.P.; Fernandes, V.R.; Carvalho, P.R.; Avila-Aguero, M.L.; Goh, D.Y.; Goh, A.; de Miguel, J.G.; Moraga, F.; Roca, J., et al. Prospective multinational study of pertussis infection in hospitalized infants and their household contacts. *The Pediatric infectious disease journal* **2007**, *26*, 238-242.
12. Wendelboe, A.M.; Njamkepo, E.; Bourillon, A.; Floret, D.D.; Gaudelus, J.; Gerber, M.; Grimprel, E.; Greenberg, D.; Halperin, S.; Liese, J., et al. Transmission of *Bordetella pertussis* to young infants. *The Pediatric infectious disease journal* **2007**, *26*, 293-299.
13. de Greeff, S.C.; Mooi, F.R.; Westerhof, A.; Verbakel, J.M.; Peeters, M.F.; Heuvelman, C.J.; Notermans, D.W.; Elvers, L.H.; Schellekens, J.F.; de Melker, H.E. Pertussis disease burden in the household: how to protect young infants. *Clinical infectious diseases : an official publication of the Infectious Diseases Society of America* **2010**, *50*, 1339-1345.
14. Craig, R.; Kunkel, E.; Crowcroft, N.S.; Fitzpatrick, M.C.; de Melker, H.; Althouse, B.M.; Merkel, T.; Scarpino, S.V.; Koelle, K.; Friedman, L., et al. Asymptomatic Infection and Transmission of Pertussis in Households: A Systematic Review. *Clinical infectious diseases : an official publication of the Infectious Diseases Society of America* **2020**, *70*, 152-161.
15. Crowcroft, N.S.; Pebody, R.G. Recent developments in pertussis. *Lancet (London, England)* **2006**, *367*, 1926-1936.
16. Kent, A.; Heath, P.T. Pertussis. *Medicine* **2013**, *42*, 8-10.

17. Burgos-Rivera, B.; Lee, A.D.; Bowden, K.E.; Faulkner, A.E.; Seaton, B.L.; Lembke, B.D.; Cartwright, C.P.; Martin, S.W.; Tondella, M.L. Evaluation of Level of Agreement in *Bordetella* Species Identification in Three U.S. Laboratories during a Period of Increased Pertussis. *Journal of clinical microbiology* **2015**, *53*, 1842-1847.
18. Loeffelholz, M.J.; Thompson, C.J.; Long, K.S.; Gilchrist, M.J. Comparison of PCR, culture, and direct fluorescent-antibody testing for detection of *Bordetella pertussis*. *Journal of clinical microbiology* **1999**, *37*, 2872-2876.
19. Bettiol, S.; Thompson, M.J.; Roberts, N.W.; Perera, R.; Heneghan, C.J.; Harnden, A. Symptomatic treatment of the cough in whooping cough. *The Cochrane database of systematic reviews* **2010**, 10.1002/14651858.CD003257.pub3, Cd003257.
20. Pillay, V.; Swingler, G. Symptomatic treatment of the cough in whooping cough. *The Cochrane database of systematic reviews* **2003**, 10.1002/14651858.cd003257, Cd003257.
21. Martinez, M.; Rochat, I.; Corbelli, R.; Tissières, P.; Rimensberger, P.C.; Barazzone-Argiroffo, C. Early blood exchange transfusion in malignant pertussis: a case report. *Pediatric critical care medicine : a journal of the Society of Critical Care Medicine and the World Federation of Pediatric Intensive and Critical Care Societies* **2011**, *12*, e107-109.
22. Tozzi, A.E.; Celentano, L.P.; Ciofi degli Atti, M.L.; Salmaso, S. Diagnosis and management of pertussis. *CMAJ : Canadian Medical Association journal = journal de l'Association medicale canadienne* **2005**, *172*, 509-515.
23. Tiwari, T.; Murphy, T.V.; Moran, J. Recommended antimicrobial agents for the treatment and postexposure prophylaxis of pertussis: 2005 CDC Guidelines. *MMWR. Recommendations and reports : Morbidity and mortality weekly report. Recommendations and reports* **2005**, *54*, 1-16.
24. Lozada, L.E.; Royall, M.J.; Nylund, C.M.; Eberly, M.D. Development of pyloric stenosis after a 4-day course of oral erythromycin. *Pediatric emergency care* **2013**, *29*, 498-499.
25. Watkins, V.S.; Polk, R.E.; Stotka, J.L. Drug interactions of macrolides: emphasis on dirithromycin. *The Annals of pharmacotherapy* **1997**, *31*, 349-356.
26. World Health Organization. Immunization, Vaccines and Biologicals. Availabe online: https://www.who.int/immunization/monitoring_surveillance/en/.
27. Locht, C.; Mielcarek, N. New pertussis vaccination approaches: en route to protect newborns? *FEMS immunology and medical microbiology* **2012**, *66*, 121-133.
28. Pertussis vaccination: use of acellular pertussis vaccines among infants and young children. Recommendations of the Advisory Committee on Immunization Practices (ACIP). *MMWR. Recommendations and reports : Morbidity and mortality weekly report. Recommendations and reports* **1997**, *46*, 1-25.
29. Pertussis vaccines: WHO position paper, August 2015-Recommendations. *Vaccine* **2016**, *34*, 1423-1425.
30. Liang, J.L.; Tiwari, T.; Moro, P.; Messonnier, N.E.; Reingold, A.; Sawyer, M.; Clark, T.A. Prevention of Pertussis, Tetanus, and Diphtheria with Vaccines in the United States: Recommendations of the Advisory Committee on Immunization Practices (ACIP). *MMWR. Recommendations and reports : Morbidity and mortality weekly report. Recommendations and reports* **2018**, *67*, 1-44.
31. Ausiello, C.M.; Urbani, F.; la Sala, A.; Lande, R.; Cassone, A. Vaccine- and antigen-dependent type 1 and type 2 cytokine induction after primary vaccination

of infants with whole-cell or acellular pertussis vaccines. *Infection and immunity* **1997**, *65*, 2168-2174.
32. Ryan, M.; Murphy, G.; Gothefors, L.; Nilsson, L.; Storsaeter, J.; Mills, K.H. *Bordetella pertussis* respiratory infection in children is associated with preferential activation of type 1 T helper cells. *The Journal of infectious diseases* **1997**, *175*, 1246-1250.
33. Warfel, J.M.; Zimmerman, L.I.; Merkel, T.J. Acellular pertussis vaccines protect against disease but fail to prevent infection and transmission in a nonhuman primate model. *Proc Natl Acad Sci U S A* **2014**, *111*, 787-792.
34. Greco, D.; Salmaso, S.; Mastrantonio, P.; Giuliano, M.; Tozzi, A.E.; Anemona, A.; Ciofi degli Atti, M.L.; Giammanco, A.; Panei, P.; Blackwelder, W.C., et al. A controlled trial of two acellular vaccines and one whole-cell vaccine against pertussis. Progetto Pertosse Working Group. *The New England journal of medicine* **1996**, *334*, 341-348.
35. Gustafsson, L.; Hallander, H.O.; Olin, P.; Reizenstein, E.; Storsaeter, J. A controlled trial of a two-component acellular, a five-component acellular, and a whole-cell pertussis vaccine. *The New England journal of medicine* **1996**, *334*, 349-355.
36. Winter, K.; Harriman, K.; Zipprich, J.; Schechter, R.; Talarico, J.; Watt, J.; Chavez, G. California pertussis epidemic, 2010. *The Journal of pediatrics* **2012**, *161*, 1091-1096.
37. Cherry, J.D. Epidemic pertussis in 2012-the resurgence of a vaccine-preventable disease. *The New England journal of medicine* **2012**, *367*, 785-787.
38. Acosta, A.M.; DeBolt, C.; Tasslimi, A.; Lewis, M.; Stewart, L.K.; Misegades, L.K.; Messonnier, N.E.; Clark, T.A.; Martin, S.W.; Patel, M. Tdap vaccine effectiveness in adolescents during the 2012 Washington State pertussis epidemic. *Pediatrics* **2015**, *135*, 981-989.
39. Koepke, R.; Eickhoff, J.C.; Ayele, R.A.; Petit, A.B.; Schauer, S.L.; Hopfensperger, D.J.; Conway, J.H.; Davis, J.P. Estimating the effectiveness of tetanus-diphtheria-acellular pertussis vaccine (Tdap) for preventing pertussis: evidence of rapidly waning immunity and difference in effectiveness by Tdap brand. *The Journal of infectious diseases* **2014**, *210*, 942-953.
40. Witt, M.A.; Katz, P.H.; Witt, D.J. Unexpectedly limited durability of immunity following acellular pertussis vaccination in preadolescents in a North American outbreak. *Clinical infectious diseases : an official publication of the Infectious Diseases Society of America* **2012**, *54*, 1730-1735.
41. Witt, M.A.; Arias, L.; Katz, P.H.; Truong, E.T.; Witt, D.J. Reduced risk of pertussis among persons ever vaccinated with whole cell pertussis vaccine compared to recipients of acellular pertussis vaccines in a large US cohort. *Clinical infectious diseases : an official publication of the Infectious Diseases Society of America* **2013**, *56*, 1248-1254.
42. Broder, K.R.; Cortese, M.M.; Iskander, J.K.; Kretsinger, K.; Slade, B.A.; Brown, K.H.; Mijalski, C.M.; Tiwari, T.; Weston, E.J.; Cohn, A.C., et al. Preventing tetanus, diphtheria, and pertussis among adolescents: use of tetanus toxoid, reduced diphtheria toxoid and acellular pertussis vaccines recommendations of the Advisory Committee on Immunization Practices (ACIP). *MMWR. Recommendations and reports : Morbidity and mortality weekly report. Recommendations and reports* **2006**, *55*, 1-34.
43. Shakib, J.H.; Ralston, S.; Raissy, H.H.; Stoddard, G.J.; Edwards, K.M.; Byington, C.L. Pertussis antibodies in postpartum women and their newborns. *Journal of*

perinatology : official journal of the California Perinatal Association **2010**, *30*, 93-97.
44. Healy, C.M.; Munoz, F.M.; Rench, M.A.; Halasa, N.B.; Edwards, K.M.; Baker, C.J. Prevalence of pertussis antibodies in maternal delivery, cord, and infant serum. *The Journal of infectious diseases* **2004**, *190*, 335-340.
45. Updated recommendations for use of tetanus toxoid, reduced diphtheria toxoid, and acellular pertussis vaccine (Tdap) in pregnant women-Advisory Committee on Immunization Practices (ACIP), 2012. *MMWR. Morbidity and mortality weekly report* **2013**, *62*, 131-135.
46. Gerlach, G.; von Wintzingerode, F.; Middendorf, B.; Gross, R. Evolutionary trends in the genus *Bordetella*. *Microbes and infection* **2001**, *3*, 61-72.
47. Hamidou Soumana, I.; Linz, B.; Harvill, E.T. Environmental Origin of the Genus *Bordetella*. *Frontiers in microbiology* **2017**, *8*, 28.
48. Diavatopoulos, D.A.; Cummings, C.A.; Schouls, L.M.; Brinig, M.M.; Relman, D.A.; Mooi, F.R. *Bordetella pertussis*, the causative agent of whooping cough, evolved from a distinct, human-associated lineage of *B. bronchiseptica*. *PLoS pathogens* **2005**, *1*, e45.
49. Parkhill, J.; Sebaihia, M.; Preston, A.; Murphy, L.D.; Thomson, N.; Harris, D.E.; Holden, M.T.; Churcher, C.M.; Bentley, S.D.; Mungall, K.L., et al. Comparative analysis of the genome sequences of *Bordetella pertussis*, *Bordetella parapertussis* and *Bordetella bronchiseptica*. *Nature genetics* **2003**, *35*, 32-40.
50. Cummings, C.A.; Brinig, M.M.; Lepp, P.W.; van de Pas, S.; Relman, D.A. *Bordetella* species are distinguished by patterns of substantial gene loss and host adaptation. *Journal of bacteriology* **2004**, *186*, 1484-1492.
51. Parkhill, J.; Dougan, G.; James, K.D.; Thomson, N.R.; Pickard, D.; Wain, J.; Churcher, C.; Mungall, K.L.; Bentley, S.D.; Holden, M.T., et al. Complete genome sequence of a multiple drug resistant *Salmonella enterica* serovar Typhi CT18. *Nature* **2001**, *413*, 848-852.
52. Ring, N.; Abrahams, J.S.; Bagby, S.; Preston, A.; MacArthur, I. How Genomics Is Changing What We Know About the Evolution and Genome of *Bordetella pertussis*. *Advances in experimental medicine and biology* **2019**, *1183*, 1-17.
53. Coote, J.G. Antigenic switching and pathogenicity: environmental effects on virulence gene expression in *Bordetella pertussis*. *J Gen Microbiol* **1991**, *137*, 2493-2503.
54. Dorman, C.J. 1995 Flemming Lecture. DNA topology and the global control of bacterial gene expression: implications for the regulation of virulence gene expression. *Microbiology (Reading, England)* **1995**, *141 (Pt 6)*, 1271-1280.
55. Gross, R. Signal transduction and virulence regulation in human and animal pathogens. *FEMS Microbiol Rev* **1993**, *10*, 301-326.
56. Merkel, T.J.; Stibitz, S.; Keith, J.M.; Leef, M.; Shahin, R. Contribution of regulation by the *bvg* locus to respiratory infection of mice by *Bordetella pertussis*. *Infection and immunity* **1998**, *66*, 4367-4373.
57. Aricó, B.; Miller, J.F.; Roy, C.; Stibitz, S.; Monack, D.; Falkow, S.; Gross, R.; Rappuoli, R. Sequences required for expression of *Bordetella pertussis* virulence factors share homology with prokaryotic signal transduction proteins. *Proc Natl Acad Sci U S A* **1989**, *86*, 6671-6675.
58. Cotter, P.A.; Jones, A.M. Phosphorelay control of virulence gene expression in *Bordetella*. *Trends in microbiology* **2003**, *11*, 367-373.

59. Decker, K.B.; James, T.D.; Stibitz, S.; Hinton, D.M. The *Bordetella pertussis* model of exquisite gene control by the global transcription factor BvgA. *Microbiology (Reading, England)* **2012**, *158*, 1665-1676.
60. Preston, A.; Parkhill, J.; Maskell, D.J. The bordetellae: lessons from genomics. *Nature reviews. Microbiology* **2004**, *2*, 379-390.
61. Brickman, T.J.; Cummings, C.A.; Liew, S.Y.; Relman, D.A.; Armstrong, S.K. Transcriptional profiling of the iron starvation response in *Bordetella pertussis* provides new insights into siderophore utilization and virulence gene expression. *Journal of bacteriology* **2011**, *193*, 4798-4812.
62. Hester, S.E.; Lui, M.; Nicholson, T.; Nowacki, D.; Harvill, E.T. Identification of a CO2 responsive regulon in *Bordetella*. *PloS one* **2012**, *7*, e47635.
63. Luu, L.D.W.; Octavia, S.; Zhong, L.; Raftery, M.; Sintchenko, V.; Lan, R. Characterisation of the *Bordetella pertussis* secretome under different media. *Journal of proteomics* **2017**, *158*, 43-51.
64. Locht, C.; Antoine, R.; Jacob-Dubuisson, F. *Bordetella pertussis*, molecular pathogenesis under multiple aspects. *Current opinion in microbiology* **2001**, *4*, 82-89.
65. Mazar, J.; Cotter, P.A. Topology and maturation of filamentous haemagglutinin suggest a new model for two-partner secretion. *Molecular microbiology* **2006**, *62*, 641-654.
66. Julio, S.M.; Inatsuka, C.S.; Mazar, J.; Dieterich, C.; Relman, D.A.; Cotter, P.A. Natural-host animal models indicate functional interchangeability between the filamentous haemagglutinins of *Bordetella pertussis* and *Bordetella bronchiseptica* and reveal a role for the mature C-terminal domain, but not the RGD motif, during infection. *Molecular microbiology* **2009**, *71*, 1574-1590.
67. Alonso, S.; Pethe, K.; Mielcarek, N.; Raze, D.; Locht, C. Role of ADP-ribosyltransferase activity of pertussis toxin in toxin-adhesin redundancy with filamentous hemagglutinin during *Bordetella pertussis* infection. *Infection and immunity* **2001**, *69*, 6038-6043.
68. Inatsuka, C.S.; Julio, S.M.; Cotter, P.A. *Bordetella* filamentous hemagglutinin plays a critical role in immunomodulation, suggesting a mechanism for host specificity. *Proc Natl Acad Sci U S A* **2005**, *102*, 18578-18583.
69. Van Strijp, J.A.; Russell, D.G.; Tuomanen, E.; Brown, E.J.; Wright, S.D. Ligand specificity of purified complement receptor type three (CD11b/CD18, alpha m beta 2, Mac-1). Indirect effects of an Arg-Gly-Asp (RGD) sequence. *Journal of immunology* **1993**, *151*, 3324-3336.
70. Relman, D.; Tuomanen, E.; Falkow, S.; Golenbock, D.T.; Saukkonen, K.; Wright, S.D. Recognition of a bacterial adhesion by an integrin: macrophage CR3 (alpha M beta 2, CD11b/CD18) binds filamentous hemagglutinin of *Bordetella pertussis*. *Cell* **1990**, *61*, 1375-1382.
71. Ishibashi, Y.; Relman, D.A.; Nishikawa, A. Invasion of human respiratory epithelial cells by *Bordetella pertussis*: possible role for a filamentous hemagglutinin Arg-Gly-Asp sequence and alpha5beta1 integrin. *Microbial pathogenesis* **2001**, *30*, 279-288.
72. Ishibashi, Y.; Claus, S.; Relman, D.A. *Bordetella pertussis* filamentous hemagglutinin interacts with a leukocyte signal transduction complex and stimulates bacterial adherence to monocyte CR3 (CD11b/CD18). *The Journal of experimental medicine* **1994**, *180*, 1225-1233.
73. de Gouw, D.; Diavatopoulos, D.A.; Bootsma, H.J.; Hermans, P.W.; Mooi, F.R. Pertussis: a matter of immune modulation. *FEMS Microbiol Rev* **2011**, *35*, 441-474.

74. Nicholson, T.L.; Brockmeier, S.L.; Loving, C.L. Contribution of *Bordetella bronchiseptica* filamentous hemagglutinin and pertactin to respiratory disease in swine. *Infection and immunity* **2009**, *77*, 2136-2146.
75. Locht, C.; Bertin, P.; Menozzi, F.D.; Renauld, G. The filamentous haemagglutinin, a multifaceted adhesion produced by virulent *Bordetella* spp. *Molecular microbiology* **1993**, *9*, 653-660.
76. Mobberley-Schuman, P.S.; Connelly, B.; Weiss, A.A. Phagocytosis of *Bordetella pertussis* incubated with convalescent serum. *The Journal of infectious diseases* **2003**, *187*, 1646-1653.
77. McGuirk, P.; McCann, C.; Mills, K.H. Pathogen-specific T regulatory 1 cells induced in the respiratory tract by a bacterial molecule that stimulates interleukin 10 production by dendritic cells: a novel strategy for evasion of protective T helper type 1 responses by *Bordetella pertussis*. *The Journal of experimental medicine* **2002**, *195*, 221-231.
78. McGuirk, P.; Mills, K.H. Direct anti-inflammatory effect of a bacterial virulence factor: IL-10-dependent suppression of IL-12 production by filamentous hemagglutinin from *Bordetella pertussis*. *European journal of immunology* **2000**, *30*, 415-422.
79. Zaretzky, F.R.; Gray, M.C.; Hewlett, E.L. Mechanism of association of adenylate cyclase toxin with the surface of *Bordetella pertussis*: a role for toxin-filamentous haemagglutinin interaction. *Molecular microbiology* **2002**, *45*, 1589-1598.
80. Irie, Y.; Mattoo, S.; Yuk, M.H. The Bvg virulence control system regulates biofilm formation in *Bordetella bronchiseptica*. *Journal of bacteriology* **2004**, *186*, 5692-5698.
81. Ashworth, L.A.; Irons, L.I.; Dowsett, A.B. Antigenic relationship between serotype-specific agglutinogen and fimbriae of *Bordetella pertussis*. *Infection and immunity* **1982**, *37*, 1278-1281.
82. Willems, R.; Paul, A.; van der Heide, H.G.; ter Avest, A.R.; Mooi, F.R. Fimbrial phase variation in *Bordetella pertussis*: a novel mechanism for transcriptional regulation. *The EMBO journal* **1990**, *9*, 2803-2809.
83. De Graaf, F.K.; Mooi, F.R. The fimbrial adhesins of *Escherichia coli*. *Advances in microbial physiology* **1986**, *28*, 65-143.
84. Willems, R.J.; van der Heide, H.G.; Mooi, F.R. Characterization of a B*ordetella pertussis* fimbrial gene cluster which is located directly downstream of the filamentous haemagglutinin gene. *Molecular microbiology* **1992**, *6*, 2661-2671.
85. Kania, S.A.; Rajeev, S.; Burns, E.H., Jr.; Odom, T.F.; Holloway, S.M.; Bemis, D.A. Characterization of fimN, a new *Bordetella bronchiseptica* major fimbrial subunit gene. *Gene* **2000**, *256*, 149-155.
86. Pedroni, P.; Riboli, B.; de Ferra, F.; Grandi, G.; Toma, S.; Aricò, B.; Rappuoli, R. Cloning of a novel pilin-like gene from *Bordetella pertussis*: homology to the *fim2* gene. *Molecular microbiology* **1988**, *2*, 539-543.
87. Boschwitz, J.S.; van der Heide, H.G.; Mooi, F.R.; Relman, D.A. *Bordetella bronchiseptica* expresses the fimbrial structural subunit gene *fimA*. *Journal of bacteriology* **1997**, *179*, 7882-7885.
88. Hazenbos, W.L.; Geuijen, C.A.; van den Berg, B.M.; Mooi, F.R.; van Furth, R. *Bordetella pertussis* fimbriae bind to human monocytes via the minor fimbrial subunit FimD. *The Journal of infectious diseases* **1995**, *171*, 924-929.
89. Mattoo, S.; Miller, J.F.; Cotter, P.A. Role of *Bordetella bronchiseptica* fimbriae in tracheal colonization and development of a humoral immune response. *Infection and immunity* **2000**, *68*, 2024-2033.

90. Geuijen, C.A.; Willems, R.J.; Bongaerts, M.; Top, J.; Gielen, H.; Mooi, F.R. Role of the *Bordetella pertussis* minor fimbrial subunit, FimD, in colonization of the mouse respiratory tract. *Infection and immunity* **1997**, *65*, 4222-4228.
91. Vandebriel, R.J.; Hellwig, S.M.; Vermeulen, J.P.; Hoekman, J.H.; Dormans, J.A.; Roholl, P.J.; Mooi, F.R. Association of *Bordetella pertussis* with host immune cells in the mouse lung. *Microbial pathogenesis* **2003**, *35*, 19-29.
92. Inatsuka, C.S.; Xu, Q.; Vujkovic-Cvijin, I.; Wong, S.; Stibitz, S.; Miller, J.F.; Cotter, P.A. Pertactin is required for *Bordetella* species to resist neutrophil-mediated clearance. *Infection and immunity* **2010**, *78*, 2901-2909.
93. Henderson, I.R.; Navarro-Garcia, F.; Desvaux, M.; Fernandez, R.C.; Ala'Aldeen, D. Type V protein secretion pathway: the autotransporter story. *Microbiology and molecular biology reviews : MMBR* **2004**, *68*, 692-744.
94. Charles, I.G.; Dougan, G.; Pickard, D.; Chatfield, S.; Smith, M.; Novotny, P.; Morrissey, P.; Fairweather, N.F. Molecular cloning and characterization of protective outer membrane protein P.69 from *Bordetella pertussis*. *Proc Natl Acad Sci U S A* **1989**, *86*, 3554-3558.
95. Everest, P.; Li, J.; Douce, G.; Charles, I.; De Azavedo, J.; Chatfield, S.; Dougan, G.; Roberts, M. Role of the *Bordetella pertussis* P.69/pertactin protein and the P.69/pertactin RGD motif in the adherence to and invasion of mammalian cells. *Microbiology (Reading, England)* **1996**, *142 (Pt 11)*, 3261-3268.
96. Edwards, J.A.; Groathouse, N.A.; Boitano, S. *Bordetella bronchiseptica* adherence to cilia is mediated by multiple adhesin factors and blocked by surfactant protein A. *Infection and immunity* **2005**, *73*, 3618-3626.
97. Khelef, N.; Bachelet, C.M.; Vargaftig, B.B.; Guiso, N. Characterization of murine lung inflammation after infection with parental *Bordetella pertussis* and mutants deficient in adhesins or toxins. *Infection and immunity* **1994**, *62*, 2893-2900.
98. Novotny, P.; Chubb, A.P.; Cownley, K.; Charles, I.G. Biologic and protective properties of the 69-kDa outer membrane protein of *Bordetella pertussis*: a novel formulation for an acellular pertussis vaccine. *The Journal of infectious diseases* **1991**, *164*, 114-122.
99. Mooi, F.R.; van Loo, I.H.; King, A.J. Adaptation of *Bordetella pertussis* to vaccination: a cause for its reemergence? *Emerging infectious diseases* **2001**, *7*, 526-528.
100. Preston, A.; Allen, A.G.; Cadisch, J.; Thomas, R.; Stevens, K.; Churcher, C.M.; Badcock, K.L.; Parkhill, J.; Barrell, B.; Maskell, D.J. Genetic basis for lipopolysaccharide O-antigen biosynthesis in bordetellae. *Infection and immunity* **1999**, *67*, 3763-3767.
101. Kawai, T.; Akira, S. The role of pattern-recognition receptors in innate immunity: update on Toll-like receptors. *Nature immunology* **2010**, *11*, 373-384.
102. Hajjar, A.M.; Ernst, R.K.; Tsai, J.H.; Wilson, C.B.; Miller, S.I. Human Toll-like receptor 4 recognizes host-specific LPS modifications. *Nature immunology* **2002**, *3*, 354-359.
103. Marr, N.; Hajjar, A.M.; Shah, N.R.; Novikov, A.; Yam, C.S.; Caroff, M.; Fernandez, R.C. Substitution of the *Bordetella pertussis* lipid A phosphate groups with glucosamine is required for robust NF-kappaB activation and release of proinflammatory cytokines in cells expressing human but not murine Toll-like receptor 4-MD-2-CD14. *Infection and immunity* **2010**, *78*, 2060-2069.
104. Marr, N.; Novikov, A.; Hajjar, A.M.; Caroff, M.; Fernandez, R.C. Variability in the lipooligosaccharide structure and endotoxicity among *Bordetella pertussis* strains. *The Journal of infectious diseases* **2010**, *202*, 1897-1906.

105. Marr, N.; Tirsoaga, A.; Blanot, D.; Fernandez, R.; Caroff, M. Glucosamine found as a substituent of both phosphate groups in *Bordetella* lipid A backbones: role of a BvgAS-activated ArnT ortholog. *Journal of bacteriology* **2008**, *190*, 4281-4290.
106. Higgins, S.C.; Lavelle, E.C.; McCann, C.; Keogh, B.; McNeela, E.; Byrne, P.; O'Gorman, B.; Jarnicki, A.; McGuirk, P.; Mills, K.H. Toll-like receptor 4-mediated innate IL-10 activates antigen-specific regulatory T cells and confers resistance to *Bordetella pertussis* by inhibiting inflammatory pathology. *Journal of immunology* **2003**, *171*, 3119-3127.
107. Mann, P.B.; Wolfe, D.; Latz, E.; Golenbock, D.; Preston, A.; Harvill, E.T. Comparative toll-like receptor 4-mediated innate host defense to *Bordetella* infection. *Infection and immunity* **2005**, *73*, 8144-8152.
108. Banus, H.A.; Vandebriel, R.J.; de Ruiter, H.; Dormans, J.A.; Nagelkerke, N.J.; Mooi, F.R.; Hoebee, B.; van Kranen, H.J.; Kimman, T.G. Host genetics of *Bordetella pertussis* infection in mice: significance of Toll-like receptor 4 in genetic susceptibility and pathobiology. *Infection and immunity* **2006**, *74*, 2596-2605.
109. Stein, P.E.; Boodhoo, A.; Armstrong, G.D.; Cockle, S.A.; Klein, M.H.; Read, R.J. The crystal structure of pertussis toxin. *Structure (London, England : 1993)* **1994**, *2*, 45-57.
110. Kotob, S.I.; Hausman, S.Z.; Burns, D.L. Localization of the promoter for the *ptl* genes of *Bordetella pertussis*, which encode proteins essential for secretion of pertussis toxin. *Infection and immunity* **1995**, *63*, 3227-3230.
111. Stein, P.E.; Boodhoo, A.; Armstrong, G.D.; Heerze, L.D.; Cockle, S.A.; Klein, M.H.; Read, R.J. Structure of a pertussis toxin-sugar complex as a model for receptor binding. *Nature structural biology* **1994**, *1*, 591-596.
112. Locht, C.; Coutte, L.; Mielcarek, N. The ins and outs of pertussis toxin. *The FEBS journal* **2011**, *278*, 4668-4682.
113. el Bayâ, A.; Brückener, K.; Schmidt, M.A. Nonrestricted differential intoxication of cells by pertussis toxin. *Infection and immunity* **1999**, *67*, 433-435.
114. Worthington, Z.E.; Carbonetti, N.H. Evading the proteasome: absence of lysine residues contributes to pertussis toxin activity by evasion of proteasome degradation. *Infection and immunity* **2007**, *75*, 2946-2953.
115. Carbonetti, N.H.; Artamonova, G.V.; Van Rooijen, N.; Ayala, V.I. Pertussis toxin targets airway macrophages to promote *Bordetella pertussis* infection of the respiratory tract. *Infection and immunity* **2007**, *75*, 1713-1720.
116. Spangrude, G.J.; Sacchi, F.; Hill, H.R.; Van Epps, D.E.; Daynes, R.A. Inhibition of lymphocyte and neutrophil chemotaxis by pertussis toxin. *Journal of immunology* **1985**, *135*, 4135-4143.
117. Andreasen, C.; Carbonetti, N.H. Pertussis toxin inhibits early chemokine production to delay neutrophil recruitment in response to *Bordetella pertussis* respiratory tract infection in mice. *Infection and immunity* **2008**, *76*, 5139-5148.
118. Kirimanjeswara, G.S.; Agosto, L.M.; Kennett, M.J.; Bjornstad, O.N.; Harvill, E.T. Pertussis toxin inhibits neutrophil recruitment to delay antibody-mediated clearance of *Bordetella pertussis*. *The Journal of clinical investigation* **2005**, *115*, 3594-3601.
119. Connelly, C.E.; Sun, Y.; Carbonetti, N.H. Pertussis toxin exacerbates and prolongs airway inflammatory responses during *Bordetella pertussis* infection. *Infection and immunity* **2012**, *80*, 4317-4332.
120. Mu, H.H.; Cooley, M.A.; Sewell, W.A. Studies on the lymphocytosis induced by pertussis toxin. *Immunology and cell biology* **1994**, *72*, 267-270.
121. Paddock, C.D.; Sanden, G.N.; Cherry, J.D.; Gal, A.A.; Langston, C.; Tatti, K.M.; Wu, K.H.; Goldsmith, C.S.; Greer, P.W.; Montague, J.L., et al. Pathology and

pathogenesis of fatal *Bordetella pertussis* infection in infants. *Clinical infectious diseases : an official publication of the Infectious Diseases Society of America* **2008**, *47*, 328-338.
122. Bruss, J.B.; Malley, R.; Halperin, S.; Dobson, S.; Dhalla, M.; McIver, J.; Siber, G.R. Treatment of severe pertussis: a study of the safety and pharmacology of intravenous pertussis immunoglobulin. *The Pediatric infectious disease journal* **1999**, *18*, 505-511.
123. Cherry, J.D.; Paddock, C.D. Pathogenesis and histopathology of pertussis: implications for immunization. *Expert review of vaccines* **2014**, *13*, 1115-1123.
124. Horiguchi, Y.; Senda, T.; Sugimoto, N.; Katahira, J.; Matsuda, M. *Bordetella bronchiseptica* dermonecrotizing toxin stimulates assembly of actin stress fibers and focal adhesions by modifying the small GTP-binding protein rho. *Journal of cell science* **1995**, *108 (Pt 10)*, 3243-3251.
125. Schmidt, G.; Goehring, U.M.; Schirmer, J.; Lerm, M.; Aktories, K. Identification of the C-terminal part of *Bordetella* dermonecrotic toxin as a transglutaminase for rho GTPases. *The Journal of biological chemistry* **1999**, *274*, 31875-31881.
126. Horiguchi, Y.; Nakai, T.; Kume, K. Effects of *Bordetella bronchiseptica* dermonecrotic toxin on the structure and function of osteoblastic clone MC3T3-e1 cells. *Infection and immunity* **1991**, *59*, 1112-1116.
127. Cowell, J.L.; Hewlett, E.L.; Manclark, C.R. Intracellular localization of the dermonecrotic toxin of *Bordetella pertussis*. *Infection and immunity* **1979**, *25*, 896-901.
128. Nakai, T.; Sawata, A.; Kume, K. Intracellular locations of dermonecrotic toxins in *Pasteurella multocida* and in *Bordetella bronchiseptica*. *American journal of veterinary research* **1985**, *46*, 870-874.
129. Teruya, S.; Hiramatsu, Y. *Bordetella* Dermonecrotic Toxin Is a Neurotropic Virulence Factor That Uses Ca(V)3.1 as the Cell Surface Receptor. **2020**, *11*.
130. Cookson, B.T.; Tyler, A.N.; Goldman, W.E. Primary structure of the peptidoglycan-derived tracheal cytotoxin of *Bordetella pertussis*. *Biochemistry* **1989**, *28*, 1744-1749.
131. Flak, T.A.; Goldman, W.E. Signalling and cellular specificity of airway nitric oxide production in pertussis. *Cellular microbiology* **1999**, *1*, 51-60.
132. Heiss, L.N.; Moser, S.A.; Unanue, E.R.; Goldman, W.E. Interleukin-1 is linked to the respiratory epithelial cytopathology of pertussis. *Infection and immunity* **1993**, *61*, 3123-3128.
133. Cookson, B.T.; Cho, H.L.; Herwaldt, L.A.; Goldman, W.E. Biological activities and chemical composition of purified tracheal cytotoxin of *Bordetella pertussis*. *Infection and immunity* **1989**, *57*, 2223-2229.
134. Magalhaes, J.G.; Philpott, D.J.; Nahori, M.A.; Jéhanno, M.; Fritz, J.; Le Bourhis, L.; Viala, J.; Hugot, J.P.; Giovannini, M.; Bertin, J., et al. Murine Nod1 but not its human orthologue mediates innate immune detection of tracheal cytotoxin. *EMBO reports* **2005**, *6*, 1201-1207.
135. Coburn, B.; Sekirov, I.; Finlay, B.B. Type III secretion systems and disease. *Clinical microbiology reviews* **2007**, *20*, 535-549.
136. Galán, J.E.; Wolf-Watz, H. Protein delivery into eukaryotic cells by type III secretion machines. *Nature* **2006**, *444*, 567-573.
137. Ghosh, P. Process of protein transport by the type III secretion system. *Microbiology and molecular biology reviews : MMBR* **2004**, *68*, 771-795.
138. Mueller, C.A.; Broz, P.; Cornelis, G.R. The type III secretion system tip complex and translocon. *Molecular microbiology* **2008**, *68*, 1085-1095.

139. Kozak, N.A.; Mattoo, S.; Foreman-Wykert, A.K.; Whitelegge, J.P.; Miller, J.F. Interactions between partner switcher orthologs BtrW and BtrV regulate type III secretion in *Bordetella*. *Journal of bacteriology* **2005**, *187*, 5665-5676.
140. Yuk, M.H.; Harvill, E.T.; Miller, J.F. The BvgAS virulence control system regulates type III secretion in *Bordetella bronchiseptica*. *Molecular microbiology* **1998**, *28*, 945-959.
141. Medhekar, B.; Shrivastava, R.; Mattoo, S.; Gingery, M.; Miller, J.F. *Bordetella* Bsp22 forms a filamentous type III secretion system tip complex and is immunoprotective *in vitro* and *in vivo*. *Molecular microbiology* **2009**, *71*, 492-504.
142. Ahuja, U.; Shokeen, B.; Cheng, N.; Cho, Y.; Blum, C.; Coppola, G.; Miller, J.F. Differential regulation of type III secretion and virulence genes in *Bordetella pertussis* and *Bordetella bronchiseptica* by a secreted anti-σ factor. *Proc Natl Acad Sci U S A* **2016**, *113*, 2341-2348.
143. Panina, E.M.; Mattoo, S.; Griffith, N.; Kozak, N.A.; Yuk, M.H.; Miller, J.F. A genome-wide screen identifies a *Bordetella* type III secretion effector and candidate effectors in other species. *Molecular microbiology* **2005**, *58*, 267-279.
144. Kuwae, A.; Matsuzawa, T.; Ishikawa, N.; Abe, H.; Nonaka, T.; Fukuda, H.; Imajoh-Ohmi, S.; Abe, A. BopC is a novel type III effector secreted by *Bordetella bronchiseptica* and has a critical role in type III-dependent necrotic cell death. *The Journal of biological chemistry* **2006**, *281*, 6589-6600.
145. Stockbauer, K.E.; Foreman-Wykert, A.K.; Miller, J.F. *Bordetella* type III secretion induces caspase 1-independent necrosis. *Cellular microbiology* **2003**, *5*, 123-132.
146. Yuk, M.H.; Harvill, E.T.; Cotter, P.A.; Miller, J.F. Modulation of host immune responses, induction of apoptosis and inhibition of NF-kappaB activation by the *Bordetella* type III secretion system. *Molecular microbiology* **2000**, *35*, 991-1004.
147. Skinner, J.A.; Pilione, M.R.; Shen, H.; Harvill, E.T.; Yuk, M.H. *Bordetella* type III secretion modulates dendritic cell migration resulting in immunosuppression and bacterial persistence. *Journal of immunology* **2005**, *175*, 4647-4652.
148. French, C.T.; Panina, E.M.; Yeh, S.H.; Griffith, N.; Arambula, D.G.; Miller, J.F. The *Bordetella* type III secretion system effector BteA contains a conserved N-terminal motif that guides bacterial virulence factors to lipid rafts. *Cellular microbiology* **2009**, *11*, 1735-1749.
149. Mattoo, S.; Yuk, M.H.; Huang, L.L.; Miller, J.F. Regulation of type III secretion in *Bordetella*. *Molecular microbiology* **2004**, *52*, 1201-1214.
150. Fennelly, N.K.; Sisti, F.; Higgins, S.C.; Ross, P.J.; van der Heide, H.; Mooi, F.R.; Boyd, A.; Mills, K.H. *Bordetella pertussis* expresses a functional type III secretion system that subverts protective innate and adaptive immune responses. *Infection and immunity* **2008**, *76*, 1257-1266.
151. Han, H.J.; Kuwae, A.; Abe, A.; Arakawa, Y.; Kamachi, K. Differential expression of type III effector BteA protein due to IS481 insertion in *Bordetella pertussis*. *PloS one* **2011**, *6*, e17797.
152. Gaillard, M.E.; Bottero, D.; Castuma, C.E.; Basile, L.A.; Hozbor, D. Laboratory adaptation of *Bordetella pertussis* is associated with the loss of type three secretion system functionality. *Infection and immunity* **2011**, *79*, 3677-3682.
153. Hanawa, T.; Kamachi, K.; Yonezawa, H.; Fukutomi, T.; Kawakami, H.; Kamiya, S. Glutamate Limitation, BvgAS Activation, and (p)ppGpp Regulate the Expression of the *Bordetella pertussis* Type 3 Secretion System. *Journal of bacteriology* **2016**, *198*, 343-351.
154. Hewlett, E.L.; Urban, M.A.; Manclark, C.R.; Wolff, J. Extracytoplasmic adenylate cyclase of *Bordetella pertussis*. *Proc Natl Acad Sci U S A* **1976**, *73*, 1926-1930.

155. Park, J.; Zhang, Y.; Buboltz, A.M.; Zhang, X.; Schuster, S.C.; Ahuja, U.; Liu, M.; Miller, J.F.; Sebaihia, M.; Bentley, S.D., et al. Comparative genomics of the classical *Bordetella* subspecies: the evolution and exchange of virulence-associated diversity amongst closely related pathogens. *BMC genomics* **2012**, *13*, 545.
156. Glaser, P.; Danchin, A.; Ladant, D.; Barzu, O.; Ullmann, A. *Bordetella pertussis* adenylate cyclase: the gene and the protein. *The Tokai journal of experimental and clinical medicine* **1988**, *13 Suppl*, 239-252.
157. Hackett, M.; Guo, L.; Shabanowitz, J.; Hunt, D.F.; Hewlett, E.L. Internal lysine palmitoylation in adenylate cyclase toxin from *Bordetella pertussis*. *Science* **1994**, *266*, 433-435.
158. Ladant, D.; Michelson, S.; Sarfati, R.; Gilles, A.M.; Predeleanu, R.; Bârzu, O. Characterization of the calmodulin-binding and of the catalytic domains of *Bordetella pertussis* adenylate cyclase. *The Journal of biological chemistry* **1989**, *264*, 4015-4020.
159. Glaser, P.; Elmaoglou-Lazaridou, A.; Krin, E.; Ladant, D.; Bârzu, O.; Danchin, A. Identification of residues essential for catalysis and binding of calmodulin in *Bordetella pertussis* adenylate cyclase by site-directed mutagenesis. *The EMBO journal* **1989**, *8*, 967-972.
160. El-Azami-El-Idrissi, M.; Bauche, C.; Loucka, J.; Osicka, R.; Sebo, P.; Ladant, D.; Leclerc, C. Interaction of *Bordetella pertussis* adenylate cyclase with CD11b/CD18: Role of toxin acylation and identification of the main integrin interaction domain. *The Journal of biological chemistry* **2003**, *278*, 38514-38521.
161. Sakamoto, H.; Bellalou, J.; Sebo, P.; Ladant, D. *Bordetella pertussis* adenylate cyclase toxin. Structural and functional independence of the catalytic and hemolytic activities. *The Journal of biological chemistry* **1992**, *267*, 13598-13602.
162. Guermonprez, P.; Khelef, N.; Blouin, E.; Rieu, P.; Ricciardi-Castagnoli, P.; Guiso, N.; Ladant, D.; Leclerc, C. The adenylate cyclase toxin of *Bordetella pertussis* binds to target cells via the alpha(M)beta(2) integrin (CD11b/CD18). *The Journal of experimental medicine* **2001**, *193*, 1035-1044.
163. Kamanova, J.; Kofronova, O.; Masin, J.; Genth, H.; Vojtova, J.; Linhartova, I.; Benada, O.; Just, I.; Sebo, P. Adenylate cyclase toxin subverts phagocyte function by RhoA inhibition and unproductive ruffling. *Journal of immunology* **2008**, *181*, 5587-5597.
164. Paccani, S.R.; Dal Molin, F.; Benagiano, M.; Ladant, D.; D'Elios, M.M.; Montecucco, C.; Baldari, C.T. Suppression of T-lymphocyte activation and chemotaxis by the adenylate cyclase toxin of *Bordetella pertussis*. *Infection and immunity* **2008**, *76*, 2822-2832.
165. Confer, D.L.; Eaton, J.W. Phagocyte impotence caused by an invasive bacterial adenylate cyclase. *Science* **1982**, *217*, 948-950.
166. Harvill, E.T.; Cotter, P.A.; Yuk, M.H.; Miller, J.F. Probing the function of *Bordetella bronchiseptica* adenylate cyclase toxin by manipulating host immunity. *Infection and immunity* **1999**, *67*, 1493-1500.
167. Henderson, M.W.; Inatsuka, C.S.; Sheets, A.J.; Williams, C.L.; Benaron, D.J.; Donato, G.M.; Gray, M.C.; Hewlett, E.L.; Cotter, P.A. Contribution of *Bordetella* filamentous hemagglutinin and adenylate cyclase toxin to suppression and evasion of interleukin-17-mediated inflammation. *Infection and immunity* **2012**, *80*, 2061-2075.
168. Eby, J.C.; Gray, M.C.; Warfel, J.M.; Paddock, C.D.; Jones, T.F.; Day, S.R.; Bowden, J.; Poulter, M.D.; Donato, G.M.; Merkel, T.J., et al. Quantification of the

adenylate cyclase toxin of *Bordetella pertussis* in vitro and during respiratory infection. *Infection and immunity* **2013**, *81*, 1390-1398.
169. Adkins, I.; Kamanova, J.; Kocourkova, A.; Svedova, M.; Tomala, J.; Janova, H.; Masin, J.; Chladkova, B.; Bumba, L.; Kovar, M., et al. *Bordetella* adenylate cyclase toxin differentially modulates toll-like receptor-stimulated activation, migration and T cell stimulatory capacity of dendritic cells. *PloS one* **2014**, *9*, e104064.
170. Bagley, K.C.; Abdelwahab, S.F.; Tuskan, R.G.; Fouts, T.R.; Lewis, G.K. Pertussis toxin and the adenylate cyclase toxin from *Bordetella pertussis* activate human monocyte-derived dendritic cells and dominantly inhibit cytokine production through a cAMP-dependent pathway. *Journal of leukocyte biology* **2002**, *72*, 962-969.
171. Boschwitz, J.S.; Batanghari, J.W.; Kedem, H.; Relman, D.A. *Bordetella pertussis* infection of human monocytes inhibits antigen-dependent CD4 T cell proliferation. *The Journal of infectious diseases* **1997**, *176*, 678-686.
172. Njamkepo, E.; Pinot, F.; François, D.; Guiso, N.; Polla, B.S.; Bachelet, M. Adaptive responses of human monocytes infected by *Bordetella pertussis*: the role of adenylate cyclase hemolysin. *Journal of cellular physiology* **2000**, *183*, 91-99.
173. Ross, P.J.; Lavelle, E.C.; Mills, K.H.; Boyd, A.P. Adenylate cyclase toxin from *Bordetella pertussis* synergizes with lipopolysaccharide to promote innate interleukin-10 production and enhances the induction of Th2 and regulatory T cells. *Infection and immunity* **2004**, *72*, 1568-1579.
174. Spensieri, F.; Fedele, G.; Fazio, C.; Nasso, M.; Stefanelli, P.; Mastrantonio, P.; Ausiello, C.M. *Bordetella pertussis* inhibition of interleukin-12 (IL-12) p70 in human monocyte-derived dendritic cells blocks IL-12 p35 through adenylate cyclase toxin-dependent cyclic AMP induction. *Infection and immunity* **2006**, *74*, 2831-2838.
175. Sebo, P.; Osicka, R.; Masin, J. Adenylate cyclase toxin-hemolysin relevance for pertussis vaccines. *Expert review of vaccines* **2014**, *13*, 1215-1227.
176. Glaser, P.; Sakamoto, H.; Bellalou, J.; Ullmann, A.; Danchin, A. Secretion of cyclolysin, the calmodulin-sensitive adenylate cyclase-haemolysin bifunctional protein of *Bordetella pertussis*. *The EMBO journal* **1988**, *7*, 3997-4004.
177. Barry, E.M.; Weiss, A.A.; Ehrmann, I.E.; Gray, M.C.; Hewlett, E.L.; Goodwin, M.S. *Bordetella pertussis* adenylate cyclase toxin and hemolytic activities require a second gene, *cyaC*, for activation. *Journal of bacteriology* **1991**, *173*, 720-726.
178. Laoide, B.M.; Ullmann, A. Virulence dependent and independent regulation of the *Bordetella pertussis* cya operon. *The EMBO journal* **1990**, *9*, 999-1005.
179. Bibova, I.; Skopova, K.; Masin, J.; Cerny, O.; Hot, D.; Sebo, P.; Vecerek, B. The RNA chaperone Hfq is required for virulence of *Bordetella pertussis*. *Infection and immunity* **2013**, *81*, 4081-4090.
180. Thomas, S.; Holland, I.B.; Schmitt, L. The Type 1 secretion pathway - the hemolysin system and beyond. *Biochimica et biophysica acta* **2014**, *1843*, 1629-1641.
181. Holland, I.B.; Schmitt, L.; Young, J. Type 1 protein secretion in bacteria, the ABC-transporter dependent pathway (review). *Molecular membrane biology* **2005**, *22*, 29-39.
182. Koronakis, V.; Eswaran, J.; Hughes, C. Structure and function of TolC: the bacterial exit duct for proteins and drugs. *Annual review of biochemistry* **2004**, *73*, 467-489.
183. Sebo, P.; Ladant, D. Repeat sequences in the *Bordetella pertussis* adenylate cyclase toxin can be recognized as alternative carboxy-proximal secretion signals by the

Escherichia coli alpha-haemolysin translocator. *Molecular microbiology* **1993**, *9*, 999-1009.
184. Bumba, L.; Masin, J.; Macek, P.; Wald, T.; Motlova, L.; Bibova, I.; Klimova, N.; Bednarova, L.; Veverka, V.; Kachala, M., et al. Calcium-Driven Folding of RTX Domain β-Rolls Ratchets Translocation of RTX Proteins through Type I Secretion Ducts. *Molecular cell* **2016**, *62*, 47-62.
185. Linhartová, I.; Bumba, L.; Mašín, J.; Basler, M.; Osička, R.; Kamanová, J.; Procházková, K.; Adkins, I.; Hejnová-Holubová, J.; Sadílková, L., et al. RTX proteins: a highly diverse family secreted by a common mechanism. *FEMS Microbiol Rev* **2010**, *34*, 1076-1112.
186. Benz, R.; Maier, E.; Ladant, D.; Ullmann, A.; Sebo, P. Adenylate cyclase toxin (CyaA) of *Bordetella pertussis*. Evidence for the formation of small ion-permeable channels and comparison with HlyA of *Escherichia coli*. *The Journal of biological chemistry* **1994**, *269*, 27231-27239.
187. Hackett, M.; Walker, C.B.; Guo, L.; Gray, M.C.; Van Cuyk, S.; Ullmann, A.; Shabanowitz, J.; Hunt, D.F.; Hewlett, E.L.; Sebo, P. Hemolytic, but not cell-invasive activity, of adenylate cyclase toxin is selectively affected by differential fatty-acylation in *Escherichia coli*. *The Journal of biological chemistry* **1995**, *270*, 20250-20253.
188. Osicka, R.; Osicková, A.; Basar, T.; Guermonprez, P.; Rojas, M.; Leclerc, C.; Sebo, P. Delivery of CD8(+) T-cell epitopes into major histocompatibility complex class I antigen presentation pathway by *Bordetella pertussis* adenylate cyclase: delineation of cell invasive structures and permissive insertion sites. *Infection and immunity* **2000**, *68*, 247-256.
189. Rose, T.; Sebo, P.; Bellalou, J.; Ladant, D. Interaction of calcium with *Bordetella pertussis* adenylate cyclase toxin. Characterization of multiple calcium-binding sites and calcium-induced conformational changes. *The Journal of biological chemistry* **1995**, *270*, 26370-26376.
190. Novak, J.; Cerny, O.; Osickova, A.; Linhartova, I.; Masin, J.; Bumba, L.; Sebo, P.; Osicka, R. Structure-Function Relationships Underlying the Capacity of *Bordetella* Adenylate Cyclase Toxin to Disarm Host Phagocytes. *Toxins* **2017**, *9*.
191. Goyard, S.; Sebo, P.; D'Andria, O.; Ladant, D.; Ullmann, A. *Bordetella pertussis* adenylate cyclase: a toxin with multiple talents. *Zentralblatt fur Bakteriologie : international journal of medical microbiology* **1993**, *278*, 326-333.
192. Vojtova, J.; Kamanova, J.; Sebo, P. *Bordetella* adenylate cyclase toxin: a swift saboteur of host defense. *Current opinion in microbiology* **2006**, *9*, 69-75.
193. Wolff, J.; Cook, G.H.; Goldhammer, A.R.; Berkowitz, S.A. Calmodulin activates prokaryotic adenylate cyclase. *Proc Natl Acad Sci U S A* **1980**, *77*, 3841-3844.
194. Ladant, D. Interaction of *Bordetella pertussis* adenylate cyclase with calmodulin. Identification of two separated calmodulin-binding domains. *The Journal of biological chemistry* **1988**, *263*, 2612-2618.
195. Guo, Q.; Shen, Y.; Lee, Y.S.; Gibbs, C.S.; Mrksich, M.; Tang, W.J. Structural basis for the interaction of *Bordetella pertussis* adenylyl cyclase toxin with calmodulin. *The EMBO journal* **2005**, *24*, 3190-3201.
196. Bouhss, A.; Krin, E.; Munier, H.; Gilles, A.M.; Danchin, A.; Glaser, P.; Bârzu, O. Cooperative phenomena in binding and activation of *Bordetella pertussis* adenylate cyclase by calmodulin. *The Journal of biological chemistry* **1993**, *268*, 1690-1694.
197. Munier, H.; Bouhss, A.; Krin, E.; Danchin, A.; Gilles, A.M.; Glaser, P.; Bârzu, O. The role of histidine 63 in the catalytic mechanism of *Bordetella pertussis* adenylate cyclase. *The Journal of biological chemistry* **1992**, *267*, 9816-9820.

198. Göttle, M.; Dove, S.; Kees, F.; Schlossmann, J.; Geduhn, J.; König, B.; Shen, Y.; Tang, W.J.; Kaever, V.; Seifert, R. Cytidylyl and uridylyl cyclase activity of bacillus anthracis edema factor and *Bordetella pertussis* CyaA. *Biochemistry* **2010**, *49*, 5494-5503.
199. Anderson, T.R. Cyclic cytidine 3',5'-monophosphate (cCMP) in cell regulation. *Molecular and cellular endocrinology* **1982**, *28*, 373-385.
200. Karst, J.C.; Barker, R.; Devi, U.; Swann, M.J.; Davi, M.; Roser, S.J.; Ladant, D.; Chenal, A. Identification of a region that assists membrane insertion and translocation of the catalytic domain of *Bordetella pertussis* CyaA toxin. *The Journal of biological chemistry* **2012**, *287*, 9200-9212.
201. Subrini, O.; Sotomayor-Perez, A.C.; Hessel, A.; Spiaczka-Karst, J.; Selwa, E.; Sapay, N.; Veneziano, R.; Pansieri, J.; Chopineau, J.; Ladant, D., et al. Characterization of a membrane-active peptide from the *Bordetella pertussis* CyaA toxin. *The Journal of biological chemistry* **2013**, *288*, 32585-32598.
202. Masin, J.; Osickova, A.; Sukova, A.; Fiser, R.; Halada, P.; Bumba, L.; Linhartova, I.; Osicka, R.; Sebo, P. Negatively charged residues of the segment linking the enzyme and cytolysin moieties restrict the membrane-permeabilizing capacity of adenylate cyclase toxin. *Sci Rep* **2016**, *6*, 29137.
203. Basler, M.; Knapp, O.; Masin, J.; Fiser, R.; Maier, E.; Benz, R.; Sebo, P.; Osicka, R. Segments crucial for membrane translocation and pore-forming activity of *Bordetella* adenylate cyclase toxin. *The Journal of biological chemistry* **2007**, *282*, 12419-12429.
204. Bellalou, J.; Sakamoto, H.; Ladant, D.; Geoffroy, C.; Ullmann, A. Deletions affecting hemolytic and toxin activities of *Bordetella pertussis* adenylate cyclase. *Infection and immunity* **1990**, *58*, 3242-3247.
205. Osicková, A.; Osicka, R.; Maier, E.; Benz, R.; Sebo, P. An amphipathic alpha-helix including glutamates 509 and 516 is crucial for membrane translocation of adenylate cyclase toxin and modulates formation and cation selectivity of its membrane channels. *The Journal of biological chemistry* **1999**, *274*, 37644-37650.
206. Ehrmann, I.E.; Gray, M.C.; Gordon, V.M.; Gray, L.S.; Hewlett, E.L. Hemolytic activity of adenylate cyclase toxin from *Bordetella pertussis*. *FEBS letters* **1991**, *278*, 79-83.
207. Gray, M.; Szabo, G.; Otero, A.S.; Gray, L.; Hewlett, E. Distinct mechanisms for K^+ efflux, intoxication, and hemolysis by *Bordetella pertussis* AC toxin. *The Journal of biological chemistry* **1998**, *273*, 18260-18267.
208. Weiss, A.A.; Hewlett, E.L.; Myers, G.A.; Falkow, S. Pertussis toxin and extracytoplasmic adenylate cyclase as virulence factors of *Bordetella pertussis*. *The Journal of infectious diseases* **1984**, *150*, 219-222.
209. Masin, J.; Fiser, R.; Linhartova, I.; Osicka, R.; Bumba, L.; Hewlett, E.L.; Benz, R.; Sebo, P. Differences in purinergic amplification of osmotic cell lysis by the pore-forming RTX toxins *Bordetella pertussis* CyaA and *Actinobacillus pleuropneumoniae* ApxIA: the role of pore size. *Infection and immunity* **2013**, *81*, 4571-4582.
210. Knapp, O.; Maier, E.; Polleichtner, G.; Masín, J.; Sebo, P.; Benz, R. Channel formation in model membranes by the adenylate cyclase toxin of *Bordetella pertussis*: effect of calcium. *Biochemistry* **2003**, *42*, 8077-8084.
211. Knapp, O.; Maier, E.; Masín, J.; Sebo, P.; Benz, R. Pore formation by the *Bordetella* adenylate cyclase toxin in lipid bilayer membranes: role of voltage and pH. *Biochimica et biophysica acta* **2008**, *1778*, 260-269.

212. Gray, M.C.; Lee, S.J.; Gray, L.S.; Zaretzky, F.R.; Otero, A.S.; Szabo, G.; Hewlett, E.L. Translocation-specific conformation of adenylate cyclase toxin from *Bordetella pertussis* inhibits toxin-mediated hemolysis. *Journal of bacteriology* **2001**, *183*, 5904-5910.
213. Dunne, A.; Ross, P.J.; Pospisilova, E.; Masin, J.; Meaney, A.; Sutton, C.E.; Iwakura, Y.; Tschopp, J.; Sebo, P.; Mills, K.H. Inflammasome activation by adenylate cyclase toxin directs Th17 responses and protection against *Bordetella pertussis*. *Journal of immunology* **2010**, *185*, 1711-1719.
214. Osickova, A.; Masin, J.; Fayolle, C.; Krusek, J.; Basler, M.; Pospisilova, E.; Leclerc, C.; Osicka, R.; Sebo, P. Adenylate cyclase toxin translocates across target cell membrane without forming a pore. *Molecular microbiology* **2010**, *75*, 1550-1562.
215. Basler, M.; Masin, J.; Osicka, R.; Sebo, P. Pore-forming and enzymatic activities of *Bordetella pertussis* adenylate cyclase toxin synergize in promoting lysis of monocytes. *Infection and immunity* **2006**, *74*, 2207-2214.
216. Karst, J.C.; Ntsogo Enguéné, V.Y.; Cannella, S.E.; Subrini, O.; Hessel, A.; Debard, S.; Ladant, D.; Chenal, A. Calcium, acylation, and molecular confinement favor folding of *Bordetella pertussis* adenylate cyclase CyaA toxin into a monomeric and cytotoxic form. *The Journal of biological chemistry* **2014**, *289*, 30702-30716.
217. Basar, T.; Havlícek, V.; Bezousková, S.; Hackett, M.; Sebo, P. Acylation of lysine 983 is sufficient for toxin activity of *Bordetella pertussis* adenylate cyclase. Substitutions of alanine 140 modulate acylation site selectivity of the toxin acyltransferase CyaC. *The Journal of biological chemistry* **2001**, *276*, 348-354.
218. Basar, T.; Havlícek, V.; Bezousková, S.; Halada, P.; Hackett, M.; Sebo, P. The conserved lysine 860 in the additional fatty-acylation site of *Bordetella pertussis* adenylate cyclase is crucial for toxin function independently of its acylation status. *The Journal of biological chemistry* **1999**, *274*, 10777-10783.
219. Masin, J.; Basler, M.; Knapp, O.; El-Azami-El-Idrissi, M.; Maier, E.; Konopasek, I.; Benz, R.; Leclerc, C.; Sebo, P. Acylation of lysine 860 allows tight binding and cytotoxicity of *Bordetella* adenylate cyclase on CD11b-expressing cells. *Biochemistry* **2005**, *44*, 12759-12766.
220. Masín, J.; Konopásek, I.; Svobodová, J.; Sebo, P. Different structural requirements for adenylate cyclase toxin interactions with erythrocyte and liposome membranes. *Biochimica et biophysica acta* **2004**, *1660*, 144-154.
221. Baumann, U. Crystal structure of the 50 kDa metallo protease from *Serratia marcescens*. *Journal of molecular biology* **1994**, *242*, 244-251.
222. Baumann, U.; Wu, S.; Flaherty, K.M.; McKay, D.B. Three-dimensional structure of the alkaline protease of *Pseudomonas aeruginosa*: a two-domain protein with a calcium binding parallel beta roll motif. *The EMBO journal* **1993**, *12*, 3357-3364.
223. Meier, R.; Drepper, T.; Svensson, V.; Jaeger, K.E.; Baumann, U. A calcium-gated lid and a large beta-roll sandwich are revealed by the crystal structure of extracellular lipase from *Serratia marcescens*. *The Journal of biological chemistry* **2007**, *282*, 31477-31483.
224. Wang, X.; Gray, M.C.; Hewlett, E.L.; Maynard, J.A. The *Bordetella* adenylate cyclase repeat-in-toxin (RTX) domain is immunodominant and elicits neutralizing antibodies. *The Journal of biological chemistry* **2015**, *290*, 3576-3591.
225. Bejerano, M.; Nisan, I.; Ludwig, A.; Goebel, W.; Hanski, E. Characterization of the C-terminal domain essential for toxic activity of adenylate cyclase toxin. *Molecular microbiology* **1999**, *31*, 381-392.

226. Iwaki, M.; Ullmann, A.; Sebo, P. Identification by *in vitro* complementation of regions required for cell-invasive activity of *Bordetella pertussis* adenylate cyclase toxin. *Molecular microbiology* **1995**, *17*, 1015-1024.
227. Chenal, A.; Guijarro, J.I.; Raynal, B.; Delepierre, M.; Ladant, D. RTX calcium binding motifs are intrinsically disordered in the absence of calcium: implication for protein secretion. *The Journal of biological chemistry* **2009**, *284*, 1781-1789.
228. O'Brien, D.P.; Hernandez, B.; Durand, D.; Hourdel, V.; Sotomayor-Pérez, A.C.; Vachette, P.; Ghomi, M.; Chamot-Rooke, J.; Ladant, D.; Brier, S., et al. Structural models of intrinsically disordered and calcium-bound folded states of a protein adapted for secretion. *Sci Rep* **2015**, *5*, 14223.
229. Sotomayor-Pérez, A.C.; Ladant, D.; Chenal, A. Disorder-to-order transition in the CyaA toxin RTX domain: implications for toxin secretion. *Toxins* **2014**, *7*, 1-20.
230. Szilvay, G.R.; Blenner, M.A.; Shur, O.; Cropek, D.M.; Banta, S. A FRET-based method for probing the conformational behavior of an intrinsically disordered repeat domain from *Bordetella pertussis* adenylate cyclase. *Biochemistry* **2009**, *48*, 11273-11282.
231. Sotomayor-Pérez, A.C.; Ladant, D.; Chenal, A. Calcium-induced folding of intrinsically disordered repeat-in-toxin (RTX) motifs via changes of protein charges and oligomerization states. *The Journal of biological chemistry* **2011**, *286*, 16997-17004.
232. O'Brien, D.P.; Perez, A.C.S.; Karst, J.; Cannella, S.E.; Enguéné, V.Y.N.; Hessel, A.; Raoux-Barbot, D.; Voegele, A.; Subrini, O.; Davi, M., et al. Calcium-dependent disorder-to-order transitions are central to the secretion and folding of the CyaA toxin of *Bordetella pertussis*, the causative agent of whooping cough. *Toxicon : official journal of the International Society on Toxinology* **2018**, *149*, 37-44.
233. Gray, M.C.; Ross, W.; Kim, K.; Hewlett, E.L. Characterization of binding of adenylate cyclase toxin to target cells by flow cytometry. *Infection and immunity* **1999**, *67*, 4393-4399.
234. Gordon, V.M.; Young, W.W., Jr.; Lechler, S.M.; Gray, M.C.; Leppla, S.H.; Hewlett, E.L. Adenylate cyclase toxins from *Bacillus anthracis* and *Bordetella pertussis*. Different processes for interaction with and entry into target cells. *The Journal of biological chemistry* **1989**, *264*, 14792-14796.
235. Hanski, E. Invasive adenylate cyclase toxin of *Bordetella pertussis*. *Trends in biochemical sciences* **1989**, *14*, 459-463.
236. Morova, J.; Osicka, R.; Masin, J.; Sebo, P. RTX cytotoxins recognize beta2 integrin receptors through N-linked oligosaccharides. *Proc Natl Acad Sci U S A* **2008**, *105*, 5355-5360.
237. Osicka, R.; Osickova, A.; Hasan, S.; Bumba, L.; Cerny, J.; Sebo, P. *Bordetella* adenylate cyclase toxin is a unique ligand of the integrin complement receptor 3. *eLife* **2015**, *4*, e10766.
238. Hasan, S.; Osickova, A.; Bumba, L.; Novák, P.; Sebo, P.; Osicka, R. Interaction of *Bordetella* adenylate cyclase toxin with complement receptor 3 involves multivalent glycan binding. *FEBS letters* **2015**, *589*, 374-379.
239. Masin, J.; Osicka, R.; Bumba, L.; Sebo, P. *Bordetella* adenylate cyclase toxin: a unique combination of a pore-forming moiety with a cell-invading adenylate cyclase enzyme. *Pathogens and disease* **2015**, *73*, ftv075.
240. Cerny, O.; Kamanova, J.; Masin, J.; Bibova, I.; Skopova, K.; Sebo, P. *Bordetella pertussis* Adenylate Cyclase Toxin Blocks Induction of Bactericidal Nitric Oxide in Macrophages through cAMP-Dependent Activation of the SHP-1 Phosphatase. *Journal of immunology* **2015**, *194*, 4901-4913.

241. Pearson, R.D.; Symes, P.; Conboy, M.; Weiss, A.A.; Hewlett, E.L. Inhibition of monocyte oxidative responses by *Bordetella pertussis* adenylate cyclase toxin. *Journal of immunology* **1987**, *139*, 2749-2754.
242. Fiser, R.; Masin, J.; Bumba, L.; Pospisilova, E.; Fayolle, C.; Basler, M.; Sadilkova, L.; Adkins, I.; Kamanova, J.; Cerny, J., et al. Calcium influx rescues adenylate cyclase-hemolysin from rapid cell membrane removal and enables phagocyte permeabilization by toxin pores. *PLoS pathogens* **2012**, *8*, e1002580.
243. Wald, T.; Petry-Podgorska, I.; Fiser, R.; Matousek, T.; Dedina, J.; Osicka, R.; Sebo, P.; Masin, J. Quantification of potassium levels in cells treated with *Bordetella* adenylate cyclase toxin. *Analytical biochemistry* **2014**, *450*, 57-62.
244. Khelef, N.; Guiso, N. Induction of macrophage apoptosis by *Bordetella pertussis* adenylate cyclase-hemolysin. *FEMS microbiology letters* **1995**, *134*, 27-32.
245. Bachelet, M.; Richard, M.J.; François, D.; Polla, B.S. Mitochondrial alterations precede *Bordetella* pertussis-induced apoptosis. *FEMS immunology and medical microbiology* **2002**, *32*, 125-131.
246. Hewlett, E.L.; Donato, G.M.; Gray, M.C. Macrophage cytotoxicity produced by adenylate cyclase toxin from *Bordetella pertussis*: more than just making cyclic AMP! *Molecular microbiology* **2006**, *59*, 447-459.
247. Bumba, L.; Masin, J.; Fiser, R.; Sebo, P. *Bordetella* adenylate cyclase toxin mobilizes its beta2 integrin receptor into lipid rafts to accomplish translocation across target cell membrane in two steps. *PLoS pathogens* **2010**, *6*, e1000901.
248. Otero, A.S.; Yi, X.B.; Gray, M.C.; Szabo, G.; Hewlett, E.L. Membrane depolarization prevents cell invasion by *Bordetella pertussis* adenylate cyclase toxin. *The Journal of biological chemistry* **1995**, *270*, 9695-9697.
249. Rogel, A.; Hanski, E. Distinct steps in the penetration of adenylate cyclase toxin of *Bordetella pertussis* into sheep erythrocytes. Translocation of the toxin across the membrane. *The Journal of biological chemistry* **1992**, *267*, 22599-22605.
250. Masin, J.; Osickova, A.; Jurnecka, D. Retargeting from the CR3 to the LFA-1 receptor uncovers the adenylyl cyclase enzyme-translocating segment of *Bordetella* adenylate cyclase toxin. **2020**, *295*, 9349-9365.
251. Geourjon, C.; Deléage, G. SOPMA: significant improvements in protein secondary structure prediction by consensus prediction from multiple alignments. *Computer applications in the biosciences : CABIOS* **1995**, *11*, 681-684.
252. Lavina, M.; Pugsley, A.P.; Moreno, F. Identification, mapping, cloning and characterization of a gene (*sbmA*) required for microcin B17 action on *Escherichia coli* K12. *J Gen Microbiol* **1986**, *132*, 1685-1693.
253. Sebo, P.; Glaser, P.; Sakamoto, H.; Ullmann, A. High-level synthesis of active adenylate cyclase toxin of *Bordetella pertussis* in a reconstructed *Escherichia coli* system. *Gene* **1991**, *104*, 19-24.
254. Greenfield, N.J. Using circular dichroism spectra to estimate protein secondary structure. *Nature protocols* **2006**, *1*, 2876-2890.
255. Benz, R. Channel formation by RTX-toxins of pathogenic bacteria: Basis of their biological activity. *Biochimica et biophysica acta* **2016**, *1858*, 526-537.
256. Szabo, G.; Gray, M.C.; Hewlett, E.L. Adenylate cyclase toxin from *Bordetella pertussis* produces ion conductance across artificial lipid bilayers in a calcium- and polarity-dependent manner. *The Journal of biological chemistry* **1994**, *269*, 22496-22499.
257. Vojtova-Vodolanova, J.; Basler, M.; Osicka, R.; Knapp, O.; Maier, E.; Cerny, J.; Benada, O.; Benz, R.; Sebo, P. Oligomerization is involved in pore formation by

Bordetella adenylate cyclase toxin. *FASEB journal : official publication of the Federation of American Societies for Experimental Biology* **2009**, *23*, 2831-2843.
258. Boehm, D.F.; Welch, R.A.; Snyder, I.S. Calcium is required for binding of *Escherichia coli* hemolysin (HlyA) to erythrocyte membranes. *Infection and immunity* **1990**, *58*, 1951-1958.
259. University of Waterloo. WatCut: An on-line tool for restriction analysis, silent mutation scanning, and SNP-RFLP analysis. Availabe online: http://watcut.uwaterloo.ca/template.php?act=silent_new.

8. Appendix

Site-directed PCR mutagenesis of the *cyaA* gene

The strategy employed to introduce substitutions to the *cyaA* gene (**Figure 24**) was based on an initial analysis of unique restriction cutters (enzymes) of the pT7CACT1 plasmid closer to a site of the substitution, preferably carrying a hexanucleotide restriction site, using the bioinformatic tool WatCut, University of Waterloo [259]. A set of mutated primers was manually designed for the amplification of the initial PCR fragments (**Table 8 and Table 9**). Also, in order to join the two previously amplified fragments a second PCR reaction was carried out with two primers flanking the cloning region of the *cyaA* gene (**Table 10**).

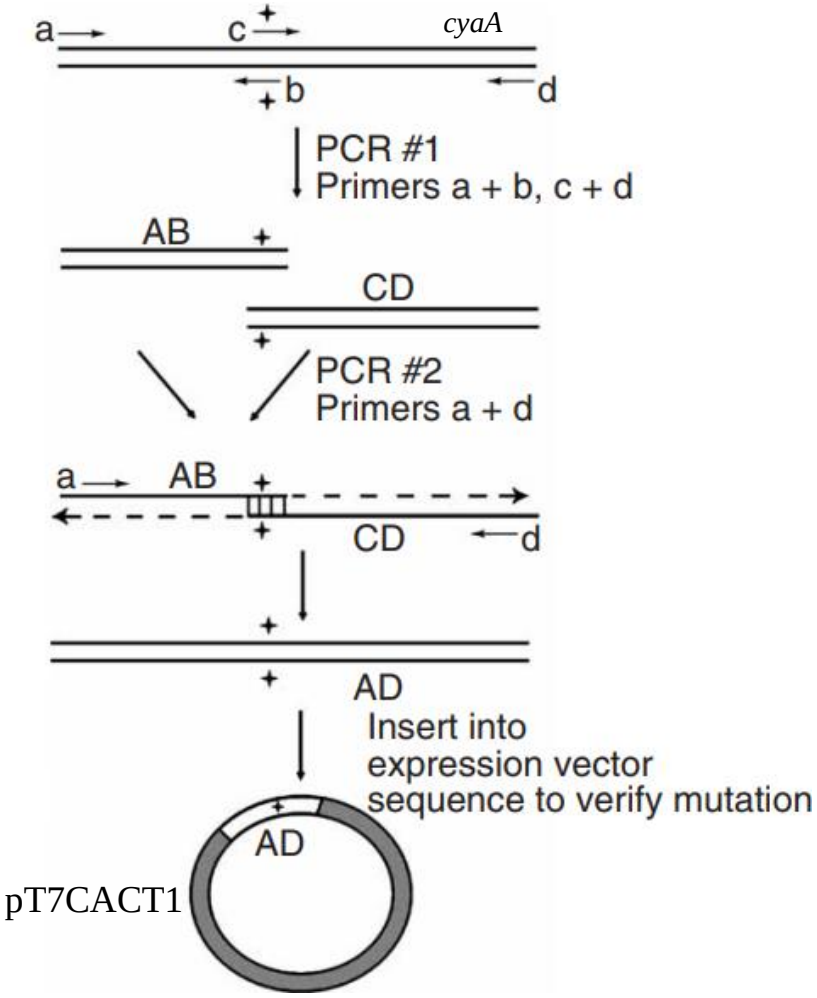

Figure 24. Schematic drawing of the site-directed PCR mutagenesis of the *cyaA* gene. Plasmid pT7CACT1 was used as the template. Two external primers (flanking the *cyaA* gene fragment) and two internal primers (each containing one or more mutated nucleotide/s) were used to generate PCR products AB and CD in separate reactions. The primers were designed to create an overlap region in the two PCR fragments. In the second PCR, purified PCR products AB and CD served as templates. The two external primers were used to amplify the full-length product (fragment AD).

An example of PCR reactions for the substitution G914L:

Table 8. Components of PCR 1A

Fragment	**1A**
Mutation	**G914L**
0.5 µl template	**pT7CACT1**
10 µl 5xQ5 Buffer HF	
10 µl GC Enhacer	
21 µl water	
5 µl 2mM dNTPs	
1.5 µl 10 µM FOR primer	**1791-SeqFor-CyaA**
1.5 µl 10 µM REV primer	**G914Lrev**
0.5 µl Q5 DNA Polymerase HF	
Σ 50 µl	
bp	**958**

Table 9. Components of PCR 1B

Fragment	**1B**
Mutation	**G914L**
0.5 µl template	**pT7CACT1**
10 µl 5xQ5 Buffer HF	
10 µl GC Enhacer	
21 µl water	
5 µl 2mM dNTPs	
1.5 µl 10 µM FOR primer	**G914Lfor**
1.5 µl 10 µM REV primer	**XhoIRev2**
0.5 µl Q5 DNA Polymerase HF	
Σ 50 µl	
bp	**303**

Cycles of PCR 1A/B:

1. 98 °C 30″
2. 98°C 10″
3. 54 °C 30″
4. 72 °C 45″
5. 30× repetition of cycles 2-4
6. 72 °C 10′
7. 4 °C keeping

Table 10. Components of PCR 2

Fragment	**1**
Mutation	**G914L**
5 µl template	**4A**
5 µl template	**4B**
10 µl 5xQ5 Buffer HF	
10 µl GC Enhacer	
11 µl water	
5 µl 2mM dNTPs	
1,5 µl 10 µM FOR primer	**1791-SeqFor-CyaA**
1,5 µl 10 µM REV primer	**XhoIRev2**
1 µl Q5 DNA Polymerase HF	
Σ 50 µl	**1240**

Cycles of PCR 2:

1. 98 °C 30″
2. 98°C 10″
3. 52 °C 30″
4. 72 °C 45″
5. 30× repetition of cycles 2-4
6. 72 °C 10′
7. 4 °C keeping